

# Reevaluation of the Classification Scheme of the Acheulian in the Levant – 50 Years Later: A Morpho-Technological Analysis of Handaxe Variability

GADI HERZLINGER\*

*Department of Physics of Complex Systems, Weizmann Institute of Science Rehovot; and, Institute of Archaeology, Mount Scopus, The Hebrew University of Jerusalem, Jerusalem, 9190501, ISRAEL; [gadi.herzlinger@weizmann.ac.il](mailto:gadi.herzlinger@weizmann.ac.il)*

ALEXANDRE VARANDA

*UNIARQ Laboratory - Centro de Arqueologia da Universidade de Lisboa Alameda da Universidade, 1600-214 Lisbon, PORTUGAL; [alexvaranda91@gmail.com](mailto:alexvaranda91@gmail.com)*

MARIANNE DESCHAMPS

*TRACES laboratory - UMR 5608, Université Toulouse - Jean Jaurès, campus of Mirail, Maison de la Recherche, 5 allée Antonio Machado 31058 Toulouse Cedex 9, FRANCE; and, UNIARQ laboratory - Centro de Arqueologia da Universidade de Lisboa Alameda da Universidade, 1600-214 Lisbon, PORTUGAL; [mardesch1690@gmail.com](mailto:mardesch1690@gmail.com)*

MICHEL BRENET

*INRAP, Domaine de Campagne, 24260 Campagne; and, UMR 5199 PACEA, Université Bordeaux, bâtiment B18, 33615, Talence, FRANCE; [michel.brenet@inrap.fr](mailto:michel.brenet@inrap.fr)*

CHRISTINA LOPEZ-TASCON

*Department of History, Universidad de Oviedo UNIOVI, Campus del Milán C/ Amparo Pedregal s/n, 33011 - Oviedo, SPAIN; [c.lopeztascon@gmail.com](mailto:c.lopeztascon@gmail.com)*

NAAMA GOREN-INBAR

*Institute of Archaeology, Mount Scopus, The Hebrew University of Jerusalem, Jerusalem, 9190501, ISRAEL; [goren@cc.huji.ac.il](mailto:goren@cc.huji.ac.il)*

\*corresponding author: Gadi Herzlinger; [gadi.herzlinger@weizmann.ac.il](mailto:gadi.herzlinger@weizmann.ac.il)

*submitted: 17 March 2021; revised: 12 July 2021; accepted: 14 July 2021*

## ABSTRACT

The chrono-cultural scheme of the Acheulian Technocomplex in the Levant, developed in the 1970's on the basis of handaxe typological variability, still serves as the main framework for the description of this cultural entity and as a benchmark for the classification of new Acheulian assemblages. It consists of a tripartite division into Early, Middle, and Late Acheulian and it postulates a development in the shapes, sizes, and refinement of handaxes, suggesting that they become rounder, smaller, and more 'finely made' over time. The following study applies new analytical approaches, a 3D geometric morphometric shape analysis, a typo-technological attribute analysis, and diacritic diagrams to a large collection of handaxes from five sites in Israel in order to test the validity of the tripartite division, and to provide a detailed characterization of the nature of diachronic changes in handaxe properties. The results suggest that the general chrono-cultural division is valid, as assemblages pertaining to each of its three phases indeed differ significantly in terms of morphology and production technologies. In addition, they indicate a complex trend of change, in which the Middle Acheulian assemblage presents higher values of morpho-technological aspects associated with craftsmanship than some of the Late Acheulian assemblages. Lastly, the quantitative and objective nature of the approach and availability of the raw data establish a foundation for future expansion of this study by additional samples from different regions and chronologies.

## INTRODUCTION

The Levantine Corridor is well-known for an exceptional abundance of archaeological sites of all periods. Within this wealth are sites situated in aquatic and water-logged environments, as well as in a variety of terrestrial environments of different periods and cultures (Enzel and

Bar-Yosef 2017; Goren-Inbar and Speth 2004). Beginning in the early 20th century, both amateurs and scholars were engaged in collecting and excavating prehistoric sites. Attempts were made to investigate the sites, classify, and assign them to known cultural and chronological records from other geographical areas. It became evident from the

1930s onwards that this particular region is extremely rich in prehistoric sites and that their typo-technological characteristics resemble those found in European and African sites (e.g., Mt. Carmel sites [Garrod and Bate 1937], Judean desert sites [Neuville 1951], Gesher Benot Ya'aqov [GBY] [Stekelis 1960], Qafzeh Cave [Neuville 1951]). The prehistoric research focused during the first 60 years of the 20th century on two major issues—the first was the excavations of caves and rock-shelters and the second was surface collections, which were primarily carried out by amateurs (e.g., Stekelis and Gilead 1966). Excavations in cave sites yielded at times very long and complex sequences (Zuttiya Cave [Turville-Petre 1927], Tabun Cave [Garrod and Bate 1937], Kebara Cave [Schick and Stekelis 1977; Stekelis 1956], Umm Qatafa Cave [Neuville 1931, 1951], Qafzeh Cave [Neuville 1951], to mention but a few). This twofold mode of gathering information and knowledge about prehistoric sites is manifested in the history of Lower Paleolithic research. Excavations of Tabun Cave revealed a cultural sequence of over 24.5m (Garrod and Bate 1937); those of Umm Qatafa yielded a sequence of ca. 12m depth (Neuville, 1951). In contrast, surface collections, and particularly those which were accidental finds, provided minimal information on the context of the artifacts (Gilead and Ronen 1977; Stekelis and Gilead 1966).

The emergence of modern intensive regional surveys in the early 1970's had a great impact on the prehistoric record of Israel. However, as far as the early cultures are concerned, and particularly that of the Acheulian Technocomplex, not much was gained. Thus, most of the Lower Paleolithic reviews note that despite the wealth of Acheulian find-spots, over 360 known localities, the number of sites that underwent well-controlled excavations with up-to-date methodologies was exceptionally meager (Bar-Yosef, 1994; Gilead 1970a; Goren 1981; Sharon 2017).

Since the onset of the 21st century, Acheulian research is marked on the one hand by small scale excavations of Acheulian sites (e.g., Zihor [Ginat et al. 2003; Grosman et al. 2011; Saragusti and Ginat 1996], Emeq Rephaim [Barzilai et al. 2006; Malinsky-Buller et al. 2016], Evron [Chazan 2013; Gilead and Ronen 1977; Ronen 1991, 2003; Shemer et al. 2019], and the cave of Milsliya [Valladas et al. 2013a; Weinstein-Evron et al. 2003; Zaidner and Weinstein-Evron 2016; Zaidner et al. 2006] to mention but a few). On the other hand, recent years are also marked by a few very large-scale open-air excavations, larger than any undertaken previously. These include the site of Revadim (Gvirtzman et al. 1999; Marder et al. 2011; Malinsky-Buller et al. 2011; Solodenko et al. 2015), Qesem (Barkai et al. 2003; Barkai et al. 2010; Blasco et al. 2014; Frumkin et al. 2009; Fornai et al. 2016; Gopher et al. 2010; Zupancich et al. 2018) and Jaljoulia (Zupancich et al. 2021).

The absence of stratigraphic context for the surface finds, the great antiquity of many of the sites, and the lack of applicable dating methods for others, leave the bulk of the Acheulian sites undated or at times with highly disputable dates (e.g., the dates obtained for the Acheulian site of Holon (Malinsky-Buller 2014). The Israeli Acheulian record

begins with the Early Acheulian site of 'Ubeidiya and terminates with the complex of the Acheulo-Yabrudian (Gopher et al. 2010; Jelinek 1982; Zaidner and Weinstein-Evron 2016). It encompasses over a million years of lithic production with only a handful of anchored dates such as those of 'Ubeidiya at ca. 1.6 Ma (Tchernov 1986), GBY at ca. 0.79 Ma (Goren-Inbar et al. 2018), Tabun Layer XIII at ca. 0.324 Ma (Mercier et al. 2000), Misliya at 0.25 Ma (Valladas et al. 2013b), and Qesem at ca. 0.2 Ma (Gopher et al. 2010; Mercier et al. 2013).

When Gilead (1970a, b) wrote his seminal synthesis of the Acheulian in the Levant, the chronological framework of this Technocomplex was even more obscure than that described above. The lack of dated Acheulian assemblages directed the focus to the tools themselves as the source for any attempt to construct a chrono-temporal framework. This was the reason for applying the widespread conventional biface morphological analyses that were centered on handaxes. This method provided a typological classification with some additional morphological indices and resulted in an elementary comparison of typological frequencies (Gilead 1970b).

However, this approach has its own difficulties, as was evident from Gilead's synthesis, which encountered several problems in attempting to classify the Acheulian record. The scarcity of Early to Middle Acheulian assemblages, in contrast with the wealth of Late Acheulian ones, caused tremendous difficulties in constructing a well-established chrono-cultural scheme. As a result, Gilead's scheme consisted of a tripartite division where 'Ubeidiya represented the Early Acheulian, GBY represented the Middle Acheulian, and all the other sites were assigned to the Late Acheulian. These sites were not ordered chronologically but were divided into four sub-groups, each somewhat different typologically. It should be noted though that Gilead made assumptions concerning the relative chronology of the four sub-groups.

The picture emerging from Gilead's observations is of a development (progress) in the Levantine Acheulian, starting with the large and crude handaxes of 'Ubeidiya and ending with the small symmetrical and refined ones that characterize some of the Late Acheulian subgroups.

Multiple factors have been suggested over the years as the main drivers underlying handaxe morphology across space and time. These include, among many others, raw material preferences and constraints, tool function, and life history (Eren et al., 2014; Kohn and Mithen 1999; McPherson 1999; O'Brien 1981; Sharon 2008). It is generally agreed, however, that all the natural and behavioral variables related to these factors are largely interconnected, and no single factor can be used as a comprehensive explanation for the entire range of known morphological variability in handaxes (Machin 2009). Some of the morphological variables mentioned by Gilead, and some additional ones, which include general shape homogeneity, symmetry, refinement, and regularity, are related to several of the above-mentioned factors. However, there is a wide consensus that all of these traits are strongly associated with 'craftsmanship'

(Apel 2008; Nonaka et al. 2010; Olausson 2017).

This term, which can also be referred to as knapping skill, reflects the ability of a knapper to maintain a mental image of his/hers desired end-product, and the specific steps required for its realization, in accordance with the physical constraints of fracture mechanics. Concurrently, it also includes the knapper's ability to successfully perform these actions in order to modify the shape of the raw material into the desired finished tool. This must also include the capacity to cope with both the changing geometrical configurations throughout the reduction sequence and with unpredicted problems that may arise from possible flaws in the raw material or unsuccessful knapping actions. Another trait characteristic of high knapping skill is the ability to plan and manifest the desired end product through different and complex technological production procedures. The acquisition of knapping skill in traditional societies is performed through training and practice in a social context, which in turn also dictates the range of acceptable forms that specific tools may receive. This notion has been formalized in several theoretical frameworks and is further corroborated through experimental studies (Bamforth and Finlay 2008; Herzlinger et al. 2017; Nonaka et al. 2010).

Handaxes serve as one of the best analytical proxies for studying the Acheulian thanks to their ubiquity and relatively constant form through time and space, facilitating their typological classification. Namely, it is a relatively symmetrical tool on two planes, possessing two main opposing flaked surfaces whose intersection results in an acute working edge continuing along all or most of the tool's circumference. Thus, an increase in craftsmanship should result in more technologically complex assemblages, containing artifacts that are more symmetrical, regular, refined, and similar to one another, as well as to the mean shape, reflecting the mental template. This is due to the fact that their morphological characteristics are directly related to the degree of control and execution quality of the knappers, or in other words, to how well the knapper controls his/her actions in order to consistently produce the same, constant, desired end product.

The description stemming from Gilead's work is in accord with the approach that views a generally linear, albeit not always consistent, evolution in these morphological attributes from the earliest to the latest Acheulian on a global scale (Bar-Yosef 1994; Clark 1966, 1975; Hodgson 2015; McNabb and Cole 2015; Stout et al. 2011). While not always explicitly stated in studies adhering to this approach, this trend is taken to reflect a general increase in the Acheulian hominins' cognitive and manual capacities, also expressed in their level of craftsmanship.

### OBJECTIVES

Gilead's contribution to the classification of the Acheulian bifaces in Levantine assemblages was, and still is today, a benchmark for understanding this cultural entity in Israel and beyond. While substantial research has been conducted since, a large number of well-excavated and dated localities have been assigned to the later part of the Tech-

nocomplex, mainly postdating 0.5 My BP. Thus, Gilead's tripartite division remains an important reference in works attempting to explain and interpret the observed patterns in terms of human behavior and evolution (Sharon and Barsky 2016). Even though Gilead's methods were very innovative for their time, relying on quantitative data, they are substantially less powerful and more subjective than currently available methods. Thus, the first objective of the current study is to assess the validity of this division using modern approaches, unavailable to Gilead.

Furthermore, while Gilead's work emphasized the development in handaxe properties over time, it did not provide any detailed description of their nature, even within the framework of the tripartite division. This too stemmed from methodological limitations with respect to the description of various properties of the tools associated with craftsmanship such as size, refinement, symmetry, and regularity. This is a crucial point both due to the fact that the non-linear nature of change was already acknowledged by Gilead himself (as evident from the four Late Acheulian subgroups), and to the importance of these processes to various arguments of hominin cognitive evolution and dispersion patterns. Thus, the second goal of this study is to provide an objective, quantitative description of changes in craftsmanship throughout the three stages.

This will be achieved through the application of novel methods such as 3D geometric morphometric shape analysis (3DGM), typo-technological attribute analysis, and diacritic diagrams. These will be used to describe the morphological and technological aspects of the handaxes, and to examine their within- and between-assemblage variability, volumes, symmetry, curvature, and regularities, as well as the shape trends that underlie their variability. Furthermore, a detailed description of the technological procedures used in their production will be provided through technological attribute-analysis and diacritic diagrams. This will allow a better understanding of the effect that each technological choice had on the various morphological aspects. Thus, results will provide a much better description of the variability that exists in various stages of the Acheulian in the Levant, as well as within the numerous manifestations that are classified to its late stage.

Lastly, as noted above, a wide variety of factors were suggested and associated with handaxe shape variability. As the current study is restricted to testing some of Gilead's insights on a specific sample of artifacts, it is clearly beyond its scope to validate these various factors. In contrast, the repeatability of the methodological procedures, objectivity, and reproducibility of the results, and full availability of the raw data and analytical tools allows it to fulfill one additional important goal. This is the establishment of a globally available infrastructure for further exploration and hypotheses testing with respect to the various factors associated with handaxe variability. The public and modular nature of the data allows other analysts (the authors included), to further expand the sample in the future with available material—and to use the exact same methodology to provide objective comparisons and better descriptions



Figure 1. A map of Israel marking the location of the sites used in this study.

of trends, patterns, and phenomena which can be derived from these data.

## MATERIALS AND METHODS

### MATERIALS

A series of samples, comprising only handaxes, were drawn from five Acheulian sites in Israel. These include 'Ubeidiya, Nahal Hesi, Holon, Ma'ayan Barukh, and GBY (Figure 1, Table 1). The samples used in this study were selected based on their relevance to the objectives and availability to the authors. Thus, they provide a good representation of Gilead's three main stages, allowing examination of

their validity and the differences in shape aspect associated with craftsmanship. All the samples originate from open air sites, and except for the sample of Ma'ayan Barukh, all derive from excavations. In addition to the above samples, we use the data generated from the analyses of the handaxe component of the Acheulian site of GBY (Goren-Inbar et al. 2018; Herzlinger and Goren-Inbar 2019, 2020). Concise details of the sample from each site are provided below and in Table 1, while a more detailed account of the sites and their history of research is available in Appendix 1. The digital 3D models in 3dl format and 2D illustrations in six views of all artifacts used in the subsequent analyses, along with a full dataset containing both their morphometric and

**TABLE 1. GENERAL DETAILS REGARDING THE DIFFERENT ASSEMBLAGES USED IN THIS STUDY.**

Site	Nature	Dates	Chrono-cultural attribution	N Bifaces	N handaxes analyzed (this study)	Reference
'Ubeidiya	Open air	1.2–1.6 Ma	Early Acheulian	272	150	Bar-Yosef and Goren-Inbar (1993)
GBY	Open air	0.750 Ma	Middle Acheulian	721	96	Goren-Inbar et al. (2018)
Nahal Hesi	Open air	0.430±35 Ma	Late Acheulian	19	19	Zaidner et al. (2018)
Holon	Open air	0.200 Ma	Late Acheulian	107	93	Malinsky-Buller (2016)
Ma'ayan Barukh	Open air	older than 0.350 Ma	Late Acheulian	6000	80	Ronen et al. (1980); Schwarcz et al. (1980); Horowitz (2001)

technological observations, are fully and freely available in a publicly accessible online repository (Herzlinger et al. 2020).

The lithic assemblages of 'Ubeidiya were viewed by Gilead (1970a) as the only Early Acheulian site in Israel, and were all assigned to the Acheulian Technocomplex, resembling some East African sites.

Of the 'Ubeidiya rich lithic inventory record, 150 LCTs derived from four assemblages excavated between 1963–1974 were sampled (see Appendix 1). These archaeological horizons include Layers K-30, K-29, I-15, and I-16 (Bar-Yosef and Goren-Inbar 1993). The selected samples include LCTs, incorporating both handaxes and trihedrals. For the purpose of the study, which consists of large-scale chronological comparisons, all four horizons and typological classes were grouped together. A finer scaled and nuanced analysis of this material is presented elsewhere (Herzlinger et al. forthcoming)

The assemblage assigned to the Middle Acheulian consists of all 96 complete handaxes (and those with slightly broken tips, see details below) from Layer II-6 Level 4 at GBY, which was excavated during the 1990s and recently published in detail (Goren-Inbar et al. 2018 and references therein). The assemblages classified to the Late Acheulian consist of Ma'ayan Barukh (MB) (see Appendix 1) from which a sample of 80 handaxes was randomly selected from the material systematically collected prior to 1970, which was originally studied by Gilead. It also consists of a sample from Holon (HOL) (see Appendix 1), which included 93 handaxes, comprising the vast majority of the material excavated during the 1960s, and that from Nahal Hesi (NH) (see Appendix 1), which includes all 19 handaxes excavated by Gilead in the 1970s and in the recent survey and excavation (Zaidner et al. 2018).

Given the high sensitivity of high-resolution 3DGM analyses and the fact that the results are intended to be interpreted in terms of human behavior, broken items should ideally be excluded from the sample to avoid bias of the morphological observations. However, to maximize sample sizes, the inclusion of artifacts with minor breakages,

which will not affect the overall morphology of the tool, was considered. To mitigate the risk of significant bias, ten morphological variables were compared in each site (excluding GBY, the sample of which does not contain any broken artifacts). Comparisons were conducted between the entire sample, including artifacts with minor breakages, and a sample consisting of exclusively complete artifacts and artifacts with slightly broken tips (Appendix 2). Artifacts with slightly broken tips are considered here as complete because their negligible effect on the morphometric results was already shown elsewhere (Goren-Inbar et al. 2018).

## METHODS

In his Ph.D. dissertation, which constituted the basis for the division of the Acheulian from Israeli sites into chrono-cultural subgroups, Gilead (1970b) systematically analyzed and studied several hundred Acheulian bifaces from a few dozen sites. In this work, he mainly employed a slightly modified version of the then innovative morphometric typological classification method developed by Bordes (1961). This was meant to provide an objective morphological analysis of the different assemblages, which would allow their classification into meaningful sub-groups.

Bordes' method for typological classification of handaxes was the first analytical method to rely heavily on quantitative morphometric indices. Despite the fact that it also incorporated more than a few subjective observations, this was the first method to allow a relatively objective classification of handaxes into sub-types based on their morphologies.

It is important to note that while Gilead (1970b) used this method extensively, his work provides neither the measurements nor the morphometric ratios obtained in the analysis (with the exception of the mean maximal length and the refinement index for some assemblages), and is exclusively restricted to the typological distribution of the assemblages. Therefore, his raw data cannot be subjected to modern multivariate statistical analyses in order to validate his results and interpretations.

In the following study we apply three different methods in order to gain new insights regarding handaxe-shape variability in Acheulian assemblages in Israel, and to assess the validity of Gilead's results and interpretations. These methods consist of 3D homologous landmarks-based geometric morphometric shape-analysis, technological attribute-analysis, and diacritic diagrams (*schema diacritique*). These are applied to handaxe assemblages sampled from five sites that were also analyzed by Gilead in his dissertation and represent his three major Acheulian chronological phases. The following is a detailed explanation regarding the principles of each of these methods.

### 3DGM

3D homologous landmarks-based geometric morphometrics is a modern quantitative and objective method for shape analysis of samples of material objects. This method was initially developed in the 1970s in the field of paleontology and has been widely used since in many biological disciplines (Bookstein et al. 1985). Since the middle of the previous decade, following the development of adequate theoretical frameworks, the method was adapted so it could also be used for the analysis of non-biological objects (MacLeod 2001), thus allowing its application to man-made archaeological artifacts such as lithic tools (Lycett et al. 2006). Since then the method has benefitted from developments in computer science and 3D digital modeling technologies and has been widely applied in prehistoric archaeology (Herzlinger and Grosman 2018).

In contrast to morphometric methods that were developed for archaeological artifacts in the 1960s and '70s (Bordes 1961; Isaac and Isaac 1977; Roe 1964), this method is not based on metrical measurements, but rather on a finite number of points, or landmarks, placed on the surface of artifacts. These landmarks, expressed by two or three Cartesian coordinates share homology, that is, an inherent identity corresponding across all objects in the sample. This allows their subsequent comparison in terms of position, reflecting shape differences between the analyzed objects (Dryden and Mardia, 1998). While for biological objects corresponding landmarks are placed following functional and phylogenetic considerations, for man-made artifacts the homology of landmarks stems from a consistent and explicit geometric orientation and positioning of both the studied item and of the landmarks on it (Lycett and Chauhan 2010; Lycett et al. 2006). Subsequently, the landmarks' coordinates are aggregated in a dataset that is subjected to a series of multivariate statistical procedures and analyses in order to express quantitatively the degree and nature of morphological variability in the sample and its various sub-groups (Dryden and Mardia 1998).

In the current study, all analyzed artifacts were scanned using a structured light scanner and a turntable to achieve high-resolution (>500k polygons) 3D digital models, consisting of the raw input for the analysis. Subsequently, these models were consistently positioned, fitted with landmarks, and statistically analyzed using the AGMT3-D (version 3.1) software for morphometric analysis of ar-

chaeological artifacts (Herzlinger and Grosman 2018) and SAS JMP (version 14.0). The positioning of the models was conducted using the following geometric protocol. First, the models were translated in space so that their centroid would be placed at the origin of a Cartesian coordinate system. Then, they were rotated about the X- and Y-axes so that the plane roughly intersecting the two faces of the artifact would be placed in parallel to the XY plane. Next, the items were rotated about the Z-axis so that the axis maximizing their bilateral mirror symmetry would be placed parallel to the Y-axis. Lastly, and in contrast to the previous steps that were carried out automatically, all items were manually flipped in 90 degree intervals so that their distal ends would point towards the positive side of the Y-axis and their ventral faces (when identifiable) towards the negative side of the Z-axis.

Following this positioning protocol each model was fitted with 5000 3D homologous landmarks placed on its surface as a deformed 3D grid using the following protocol. First, the maximum length of each artifact was identified and used as the prime meridian of the grid. It should be noted that this axis is not necessarily the axis maximizing bilateral symmetry and hence is not necessarily parallel to the Y-axis. Then, 48 parallel latitudes were placed equidistantly along and perpendicular to the length of the prime meridian. Thus, the length of each of these latitudes reflects the width of the artifact at that specific length interval. Two additional upper and lowermost latitudes are not actually latitudes as they are not parallel to the others, rather they capture the precise morphology of the distal and proximal tips below and above their adjacent latitudes. Next, 50 equidistant points were placed on each latitude amounting in total to 2500 points. It should be noted that their equidistance is only two-dimensional. Each of these points was then projected onto the two opposing surfaces (faces) of the artifact, providing two points with identical X- and Y- but different Z-coordinates, so that each set of two points captured the thickness of the artifact at their given XY coordinates. This amounted to a total of 5000 indexed 3D landmarks that drew their homology from their own consistent positioning and that of the model, capturing in high resolution the volumetric configuration of each artifact.

Following the standard methodology, the coordinates of all the artifacts were combined to form a comprehensive morphological dataset. This dataset was then subjected to two main multivariate statistical procedures—generalized Procrustes analysis (GPA) and principal component analysis (PCA) (Dryden and Mardia 1998). The first is used as a superimposition procedure that translates, rotates, and scales the coordinates of all artifacts to minimize their variability. Thus, it removes variability stemming from differences in position and orientation in space, as well as from differences in scale. It should be noted that, in contrast to previous publications using version 3.0 of the AGMT3-D software (Herzlinger and Goren-Inbar 2019, 2020; Herzlinger and Grosman 2018), this analysis was conducted using a newer version in which the landmarks of all artifacts in the sample are scaled to centroid size 1 and not to

the mean centroid size of the sample. This change affects the measurement of shape variability within- and between-sub-samples (see below) so that the absolute values now obtained are different from the ones that would have been obtained using the previous version. However, the new values are perfectly correlated with the ones obtained by the old version, so that the relative differences between groups remain constant. In addition, the values obtained by the new version are absolute, rather than sample-specific in the previous version, and hence variability comparisons between groups can now be made even if they were not processed together in a single analysis. Following this procedure all the variability between the landmarks' coordinates can be attributed exclusively to differences in shape. Next, the GPA-modified dataset was subjected to a PCA, which is the main analytical procedure in the shape analysis. It is used to reduce data dimensionality and detect the main axes of variability in the sample. Thus, it provides a number of components (i.e., non-correlated perpendicular axes in the shape space) equal to the number of items in the sample minus one, sorted in descending order according to the proportion of variability that they explain. Each principal component (PC) reflects a specific shape trend, a mutual change in the values of a number of homologous landmarks. Each item receives a value for each PC, which is based on the values of its relevant landmarks' coordinates in relation to the shape trend described by that particular PC. Hence, each tool is defined by a series of PC scores that describe its relative position in relation to other items in the sample for each specific shape trend. It should be noted that this study applies high-density morphometric analysis with an extremely high variable to observation ratio (p/n ratio) (Goswami et al. 2019; Rohlf 2021). While it is aimed at providing high-resolution morphological analysis, it naturally also incorporates high levels of 'noise' resulting in a more homogeneously distributed proportion of variability across the principal component. Accordingly, the first principal components explain a lesser fraction of the overall variability measured in the sample. This limitation is dealt with in this study by eliminating all principal components explaining less than 5% of the observed variability from all subsequent statistical analyses, thus avoiding the inclusion of redundant noise and mitigating the risk of overfitting.

Following the PCA, the complete sample consisting of all the analyzed artifacts was divided into discrete sub-groups according to the provenance of the artifacts and various technological attributes. The PC scores provided by the PCA were used to calculate the mean shape (central tendency) of each subgroup as the multidimensional centroid in the shape space of all the items in the group. This made it possible to calculate the within group shape variability, expressed by the mean multidimensional Euclidean distance of all items in the group from the centroid. The comparison between the different groups was conducted on several levels. First, the equivalence of the within-group shape variability between different groups, as well as the equivalence of their mean shapes were tested using a non-parametric Wilcoxon rank-sum test conducted on different

datasets of multidimensional inter-point distances. This method was chosen as it was found to circumvent many assumptions required for classic parametric statistical tests, as well as problems of high dimensionality with respect to sample size (Herzlinger and Grosman 2018; Marozzi 2016). In all subsequent tests, the significance level was set to 0.05. Furthermore, the multidimensional distances between the centroids of different groups were used to outline the overall similarity and differences in the shapes of artifacts classified to different groups. Lastly, the spatial and dimensional distribution of shape variability was compared between the groups using quantitative results and graphic visualization allowing a better understanding of the nature of variability within the different groups.

Additional results of the 3DGM method focused on specific shape aspects, consisting of artifact volume, symmetries and curvature and regularity of the lateral edges. The volume of each artifact was measured directly from the high-resolution 3D model and is presented in mm<sup>3</sup>. The deviation from perfect 3D bilateral and bifacial symmetries was calculated for each artifact. For bilateral symmetry, this value is expressed by the mean 3D Euclidean distance between the landmarks placed on one lateral half of the artifact and the mirror reflection of the landmarks on the opposite half (Figure 2a). A similar calculation was performed for bifacial symmetry with the exception that the landmarks were divided along the two opposing faces instead of along their prime meridian (Figure 2b).

The next morphometric measurements focused on the lateral edges and capture their degree of curvature, and the planform and section irregularities. While these measurements were conducted separately on the left and right lateral edges, the results were averaged for each artifact to provide a general value for each of these attributes. The curvature of each lateral edge was calculated as the first term of a polynomial function of the 2nd degree fitted onto the landmarks at the extremities of the 48 mid-latitudes (excluding the distal and proximal tips) (Figure 3a). The size of this value reflects the degree of curvature, while its positive or negative sign reflects whether the general aspect of the edge is convex or concave respectively. A value of zero reflects a perfectly straight edge. The planform irregularity of each edge was calculated by the sum of 2D distances on the XY plain between the landmarks on the extremities of the 48 mid-latitudes and their position as predicted by the fitted polynomial function (Fig. 3a). This reflects the deviation of each lateral edge from a perfect planform regularity. Lastly, the section irregularity of each edge was calculated by the sum of 2D distances on the ZY plane between landmarks on the extremities of the 48 mid-latitudes and their position as predicted by a linear function fitted onto them (Figure 3b). This reflects the deviation from perfect regularity of each edge when observed from a side-view.

### Analysis of Technological Attributes

The technological attribute analysis reflects observations that characterize the production and modification procedures used in the production of the artifacts. The analysis is

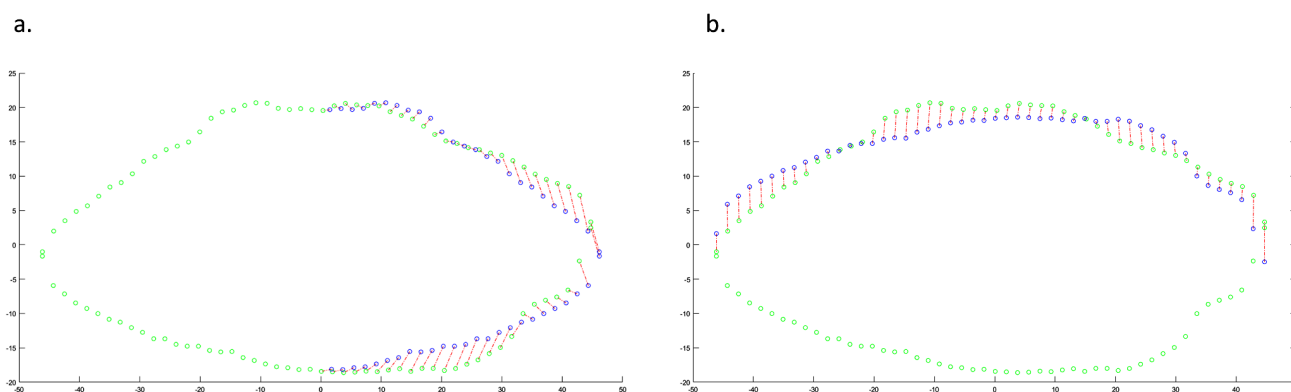


Figure 2. Visualization of deviation from perfect 3D bilateral and bifacial symmetries. Green points represent the landmarks placed along a single latitude (longitudinal section) of a handaxe. Red lines represent the degree of deviation from perfect 3D symmetry of each individual landmark. (a) Blue points represent a bilateral mirror reflection of the left side landmarks. (b) Blue points represent a bifacial mirror reflection of the lower (ventral) face landmarks.

constructed as a set of attributes, each describing a different technological trait. Each attribute can be assigned one of several standard attribute-states reflecting the specific trait on any individual artifact. In this study, the recorded attributes and their states were modified according to standard attribute lists that are widely applied in the technological analysis of Acheulian assemblages (Bar-Yosef and Goren-Inbar 1993; Goren-Inbar et al. 2018). Some of the attributes are relevant only to specifically defined subsets of the full sample, such as by period, site, or production technology. Due to the varied nature of the sample, only very general yet technologically indicative attributes were selected. The

specific details of each attribute used in the analysis are provided in Appendix 3.

The technological observations for the entire sample were combined to form a comprehensive dataset along with the morphological observations. Each attribute was subjected to common summary statistics in order to describe aspects of distribution, central tendencies and variability in samples, and relevant subsets. In order to assess the effect of the technological attributes on the morphological ones, each technological attribute was statistically tested against the following morphological attributes—shape variability (as described by each artifact's multidimensional Euclid-

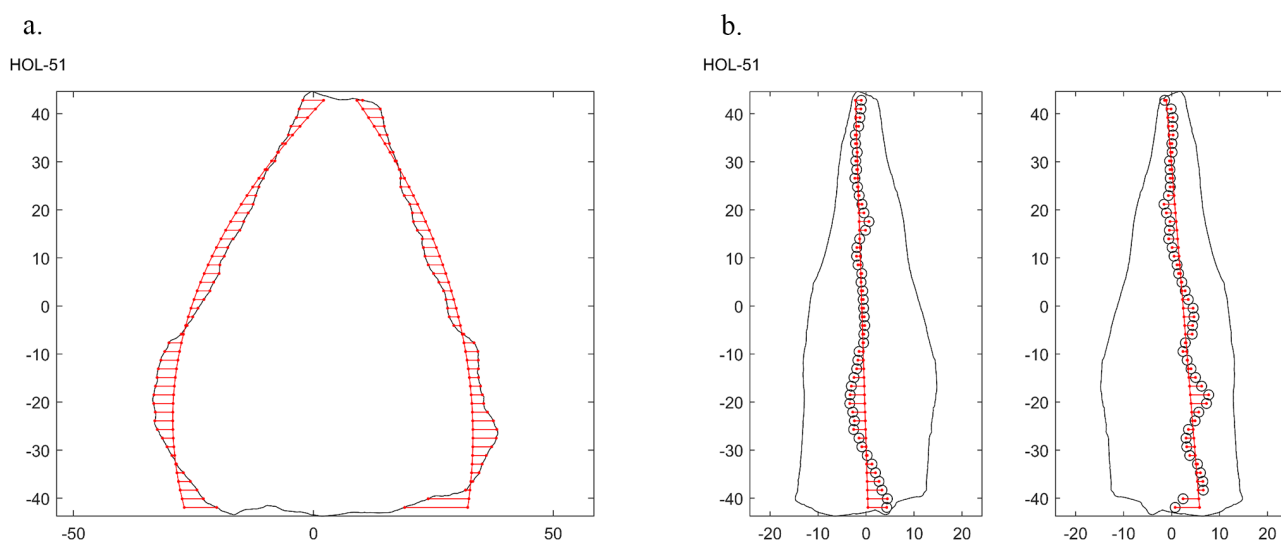


Figure 3. Visualization of lateral edges curvatures, and planform and section irregularities. (a) Black line represents the planform contour of a handaxe. X and Y axes correspond to the X and Y dimensions respectively. Curved red lines represent the polynomial function fitted to the landmarks placed at the left and right extremities of the latitudes, outlining the two lateral edges. The first term of these functions reflects the curvature of the edges. Horizontal red lines represent the planform irregularity of each edge landmark. (b) Black lines represent the section contours of the same handaxe when viewed from left and right. X and Y axes correspond to Z and Y dimensions respectively. Vertical red lines represent the linear function fitted to the landmarks placed at the left and right extremities of the latitudes, represented by the circled red points. Horizontal red lines represent the section irregularity of each edge landmark.

ean distance from its respective group's centroid), volume, deviation from bilateral and bifacial symmetries, total edge curvature, planform and section irregularities, and the scores on PC1 to 5 (each explaining more than 5% of shape variability in the sample). In cases where the technological attribute was nominal, a non-parametric Wilcoxon rank-sum test was conducted between the results of each pair of attribute-states to determine statistical significance. In cases where the technological attribute was continuous, linear-fit models were used to test the amount of variation explained by the attribute using the  $R^2$  statistic, and ANOVA and student's t-test were used to test the validity of the model and the parameters' estimates. All statistical modeling and testing were conducted using SAS JMP 14.0. Significance level for each of the tests was set to 0.05. In light of the large extent of data, only significant results are described in the following results section.

### Diacritic Diagrams

The technological attribute analysis is complemented by diacritic diagrams (Dauvois 1976; Soressi and Hays 2003; Tixier et al. 1980) produced from a sample that included material from all three late Acheulian assemblages. The sample consists of ten (11%) artifacts from Holon, eleven (14%) from MB and five (26%) from NH, and the handaxes were selected so as to reflect the entire range of morphological variability. For each object in the selected sample, views of both surfaces and sections of the 3D models were used to draw its contours and all the ridges (boundaries) of the scars. In addition, the direction of each scar was represented by an arrow.

The sequential removal order between every two adjacent scars or groups of scars was then identified in order to assess the sequence of steps taken in the production of each biface. Repetitions of sequential steps observed on the analyzed handaxes allowed the proposal of a schematic reconstruction of the *chaîne opératoire* for handaxe production at the assemblage scale. Comparisons between assemblages allowed highlighting of the similarities and differences between the studied assemblages. It should be noted that the diacritic diagrams of this study are interpretative and qualitative due to the fact that they are reconstructions based on interpretations of the intentions of the knappers during production and do not consist of objective measurable variables. However, these interpretations were made in accordance with the recorded technological attributes. In addition, this analytical method was applied in this study only to the three Late Acheulian assemblages that are entirely made on flint.

## RESULTS

This section presents the results obtained for the morphological and technological analyses and the statistical testing of the effect the latter have on the former. It begins with a description of the results obtained for the examination whose purpose was to ascertain whether to include broken artifacts in the sample. It continues with a detailed description of the morphological and technological results and

their significant associations. Finally, it provides a detailed description of the results obtained from the analysis of the diacritic diagrams.

### INCLUSION OF BROKEN ARTIFACTS

The morphometric variables compared between a sample of exclusively complete items and one which also includes tools with minor breakages consist of within-site shape variability, mean volume, mean deviation from perfect bilateral and bifacial 3D symmetry, mean curvatures, and planform and section irregularities for the left and right lateral edges. The results obtained for each subsample were statistically tested using the non-parametric Wilcoxon rank-sum tests. The results indicate that differences in all variables for all sites are negligible and are not statistically significant (see Appendix 2). The only exception is the within-site shape variability of Nahal Hesi, which is significantly lower in the small, exclusively complete sample. Nevertheless, as this sample comprises only five artifacts, and in light of the dominant pattern observed in all other samples, it was decided to conduct the study on the whole sample, including the broken artifacts.

### MORPHOLOGICAL ATTRIBUTES

The two main shape trends that characterize the morphological variability of the entire sample are seen in Figure 4. Together, these explain 37% of that variability. Despite this relatively low proportion, the figure reflects the general patterns observed regarding the within- and between-assemblage shape variability. Principal component (PC) 1 reflects a shape trend ranging from elongated, narrow, and pointed artifacts at the negative extremity, to wide and rounded items at the positive one. PC2, accounting for a very similar proportion of variability, reflects a shape trend ranging from artifacts with a low surface area to thickness ratio at the negative extremity to items with a high ratio at the positive one. When considering the shape space occupied by each of the assemblages and their centroids, 'Ubeidiya is clearly skewed towards the negative extremity on the two shape trends represented by PC1 and PC2. Holon and NH are both centrally located and similarly distributed across PC1, with Holon slightly tending towards the positive extremity of PC2. MB and GBY both show a more positive position on PC2 with the difference being that GBY is negatively positioned on PC1, whereas MB is more positively positioned. It should be noted that for both the general sample and for each specific assemblage no clustering of the artifacts, reflecting specific sub-types, is observed.

With regard to the within-assemblage shape variability, substantial differences are observed (Table 2). The 'Ubeidiya collection is by far the most variable with a shape variability value that is some 15% higher than the next highest assemblage of Holon. Concurrently, it is some 70% higher than the least variable assemblage of GBY. The distribution of the shape variability values indicates that both GBY and MB are relatively homogenous, while Holon and NH have similar intermediate values, with 'Ubeidiya standing out as an outlier with a substantially higher shape variability.

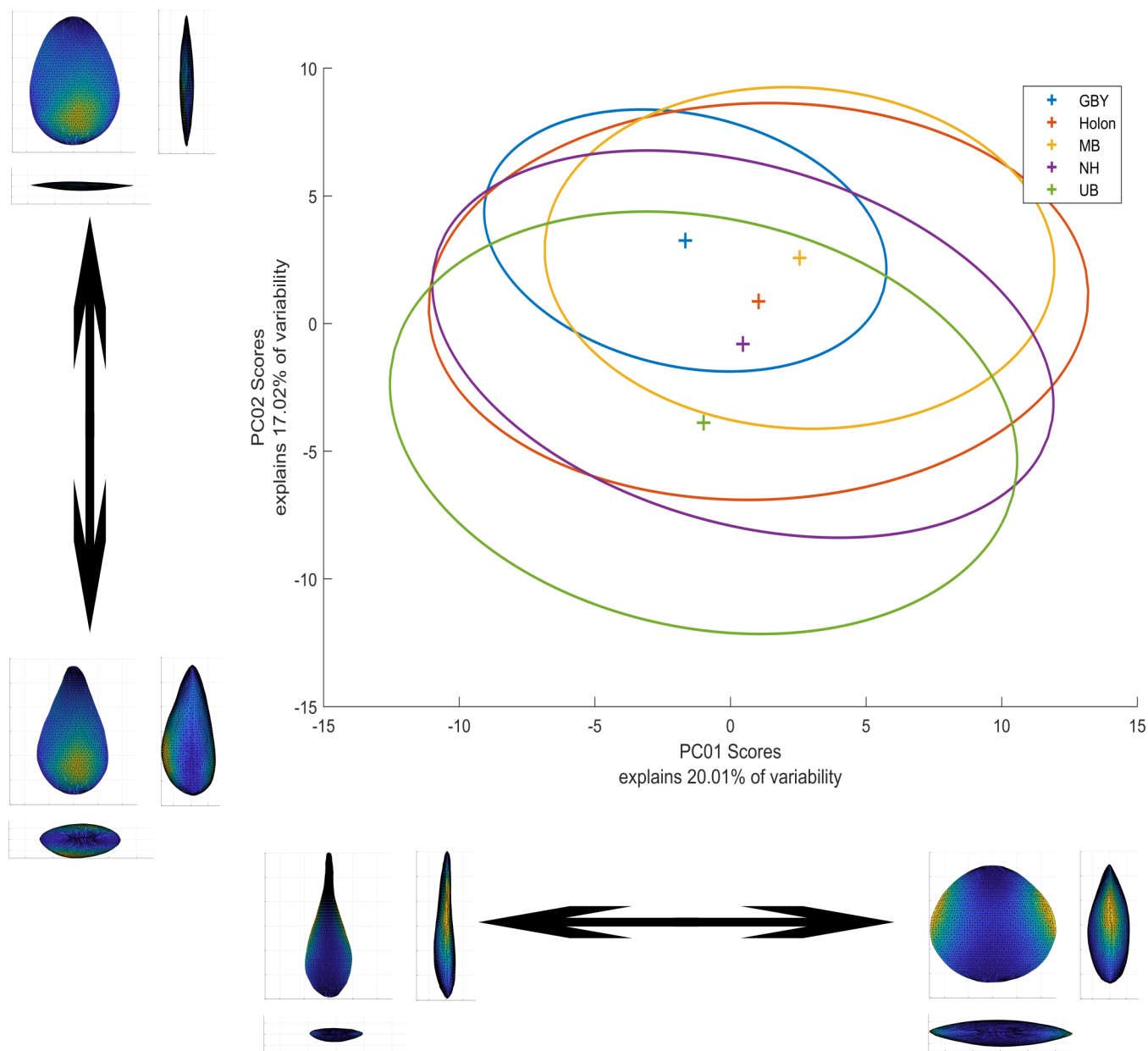


Figure 4. Principal components scatterplot. The X and Y axes correspond to the first two main principal components (PC1 and 2) respectively. The illustrated items represent hypothetical objects situated at the extremities of each principal component, reflecting the shape trend it represents. Their color-coding indicates the distribution of variability across all landmarks for the specific principal component. + signs represent the mean shapes (centroids) of each group. Ellipses represent 90% normal confidence ellipses.

Statistical testing confirms that the shape variability at GBY is significantly lower than that measured in MB, which in turn is significantly lower than that of NH. The differences between NH and Holon are insignificant, and the shape variability of 'Ubeidiya is significantly higher than that of all the other sites.

When considering the between-group variability, reflected in the differences between the assemblages' mean shapes, a pattern similar to that observed in Figure 4 emerges (Figure 5; Table 3). Thus, the distances between the sites of Holon, NH, and MB are the smallest as they are clustered together. The mean shape of Holon, which is

the most centrally located of the three, is not significantly different from either NH or MB, which in turn are significantly different from one another. These are the only two cases in which the mean shapes are not significantly different. The highest differences are observed between the mean shapes of 'Ubeidiya and those of MB and GBY.

The mean shapes of the different assemblages correspond to their positions on the shape trends described above (see Figure 4). Namely, if all mean shapes are to be located within a triangle in two-dimensional shape space (defined by PC1 and PC2), its vertices would be 'Ubeidiya, GBY, and MB. While the mean shape of 'Ubeidiya is the

**TABLE 2. SUMMARY STATISTICS OF SHAPE VARIABILITY FOR EACH SITE AS DESCRIBED BY EACH ARTIFACT'S MULTIDIMENSIONAL EUCLIDEAN DISTANCE FROM ITS RESPECTIVE GROUP'S MEAN SHAPE.**

	UB	GBY	Holon	MB	NH
<b>N</b>	150	96	93	80	19
<b>Max</b>	23.83	14.57	15.29	14.82	13.81
<b>Median</b>	10.52	6.03	9.37	7.36	9.01
<b>Min</b>	6.76	3.62	5.96	3.84	5.59
<b>Mean</b>	<b>11.07</b>	<b>6.52</b>	<b>9.58</b>	<b>7.69</b>	<b>9.47</b>
<b>Std Dev</b>	2.70	2.21	2.14	2.30	2.00
<b>Std Err</b>	0.22	0.23	0.22	0.26	0.46

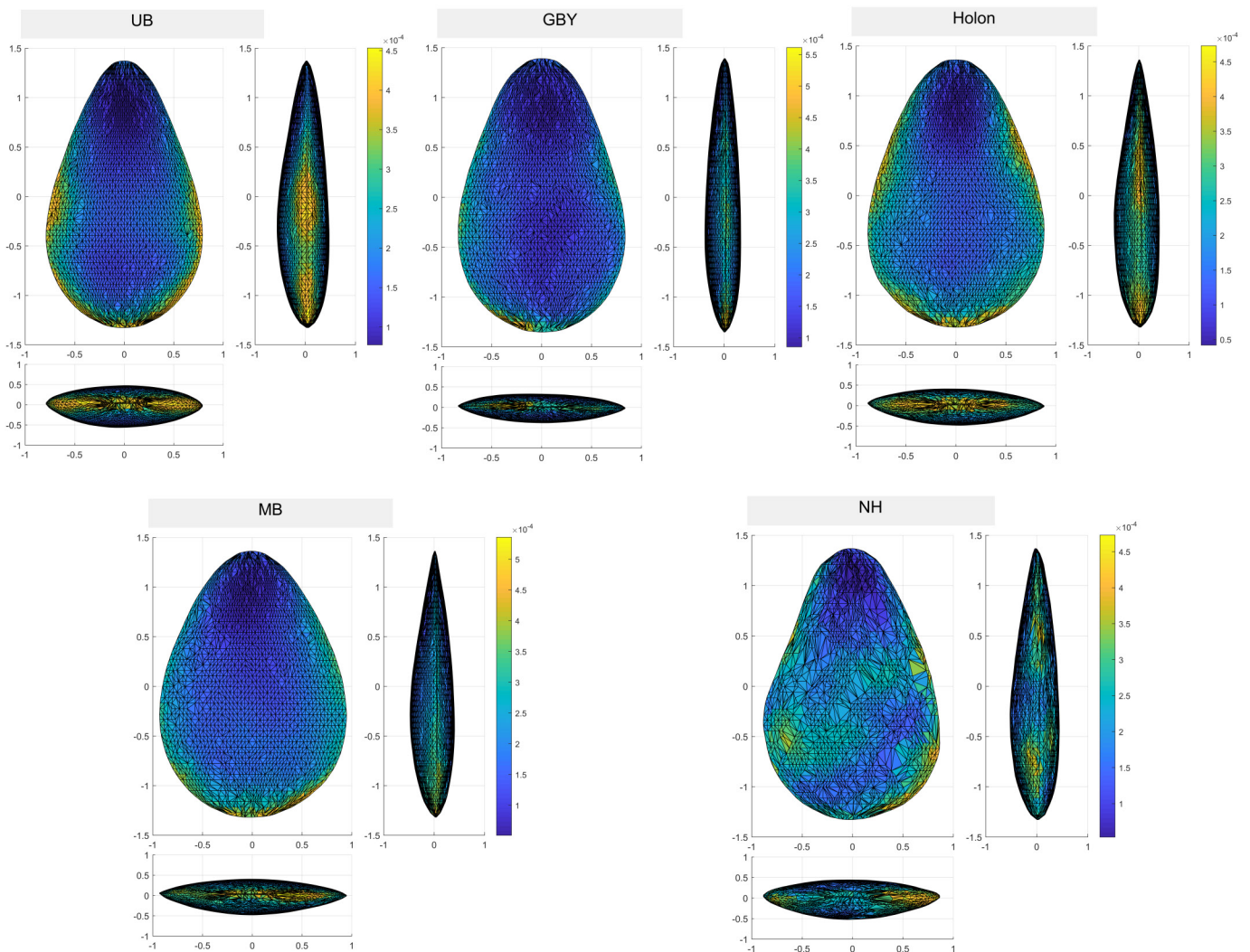


Figure 5. Mean handaxe-shape and spatial distribution of variability in each assemblage. The position of each landmark for each mean shape is determined as the mean coordinates of all corresponding landmarks of items in that group. Color-coding represents the proportion of variability of each individual landmark, reflecting the spatial distribution of variability across the tools in each group.

**TABLE 3: DISTANCE MATRIX OF MULTIDIMENSIONAL MATRIX EUCLIDEAN DISTANCES BETWEEN EACH PAIR OF GROUPS MEAN SHAPES.\***

	UB	GBY	Holon	MB	NH
UB	0.00	7.24	5.45	7.56	4.10
GBY		0.00	3.90	4.64	5.04
Holon			0.00	<b>2.54</b>	<b>2.65</b>
MB				0.00	4.43
NH					0.00

\*Bold blue numbers indicate mean shapes that are not significantly different.

thickest and very pointed, GBY is also pointed but with a much higher surface area to thickness ratio. MB is similar to GBY in its surface to thickness ratio, but more rounded and less elongated. The mean shapes of Holon and NH fall within this range of morphological variability.

Differences are also observed in the spatial distribution of shape variability between the assemblages (see Figure 5). In general, much of the variability in all the assemblages stems from differences in the lateral and proximal peripheral areas of the tools. However, while in 'Ubeidiya and Holon higher relative variability is found in these areas, GBY and MB present a much more homogenous distribution across the tools. The pattern emerging for NH is very patchy and irregular, and is probably affected by the low sample size. In addition, differences exist in the nature of the variability in terms of its spatial distribution (Table 4). 'Ubeidiya, GBY, and MB show a fairly similar pattern in which a little over 50% of the variability originates from differences in the Z dimension, corresponding to relative thickness, with less than 45% stemming from differences in the X dimension, corresponding to relative width. Different patterns are seen at Holon, where the proportions of variability stemming from differences in the X and Z dimensions are almost equal, and at NH, where over 60% stems from differences in relative thickness. However, for the latter, this again may stem from the small sample size.

Other morphometric indices in addition to shape variability were documented and used to compare the assemblages (Table 5). In terms of volume, the artifacts from

'Ubeidiya are by far the largest, with a mean volume value almost double than that of GBY. The mean volume value in the latter, in turn, is significantly larger than that of the assemblages from MB and Holon, which present very similar values. The assemblage composed of the smallest artifacts is NH, which is significantly smaller than Holon. GBY and MB are the most homogeneous assemblages in terms of artifact size, with 'Ubeidiya being the most variable. When considering the deviations from perfect symmetry, a somewhat different pattern than described above emerges. 'Ubeidiya is the least symmetrical and also significantly more variable in this respect in comparison with all the other assemblages. It is followed by the assemblages of Holon, GBY, NH, and MB, with GBY and MB again being the most homogeneous. This pattern is similar for both bilateral and bifacial symmetries, although the differences in deviation from bifacial symmetries between the assemblages are smaller.

With respect to edge curvature, it is in accordance with the mean shape scores on PC1. Namely, the artifacts from 'Ubeidiya and GBY are significantly more pointed than the ones from the other three assemblages, which are more rounded, with the roundest lateral edges found in MB. The irregularity indices show a relatively similar pattern to that observed for the symmetries, with the only difference being that the GBY assemblage is less regular than that of Holon. The 'Ubeidiya assemblage is again significantly less regular than all the others. In the Late Acheulian assemblages, the order remains constant, beginning with Holon as the

**TABLE 4. DIMENSIONAL DISTRIBUTIONS OF SHAPE VARIABILITY (across the X, Y, and Z dimensions) OF EACH GROUP.**

Site	N	Shape variability	% caused by X	% caused by Y	% caused by Z
UB	150	11.07	41.65	3.65	54.70
GBY	96	6.52	42.32	2.59	55.09
Holon	93	9.58	48.24	3.86	47.91
MB	80	7.69	43.48	4.26	52.26
NH	19	9.47	35.30	3.25	61.45

**TABLE 5. SUMMARY STATISTICS FOR THE MAIN MORPHOLOGICAL ATTRIBUTES FOR EACH SITE (red is the highest, green the lowest, and intermediate values are in shades of yellow, with darker hues showing higher intensity).**

		UB	GBY	Holon	MB	NH
		N=150	N=96	N=93	N=80	N=19
<b>Volume</b>	Max	984896	362160	340775	315650	337814
	Median	262814	150814	113826	112313	58794
	Min	35080	40984	9500	17628	17060
	<b>Mean</b>	<b>303715</b>	<b>160905</b>	<b>120678</b>	<b>122386</b>	<b>77997</b>
	Std Dev	191252	63354	77155	65757	72653
	Std Err	15616	6466	8001	7352	16668
<b>Deviation from bilateral symmetry</b>	Max	33.62	12.93	14.26	13.74	13.24
	Median	9.50	5.00	5.65	4.47	4.33
	Min	3.42	2.65	1.79	1.83	2.17
	<b>Mean</b>	<b>10.58</b>	<b>5.55</b>	<b>6.07</b>	<b>5.03</b>	<b>5.29</b>
	Std Dev	5.11	2.06	2.62	2.28	2.86
	Std Err	0.42	0.21	0.27	0.26	0.66
<b>Deviation from bifacial symmetry</b>	Max	31.72	10.83	17.43	12.66	12.24
	Median	9.18	4.80	4.58	4.06	4.48
	Min	2.88	2.19	1.51	1.32	1.77
	<b>Mean</b>	<b>9.77</b>	<b>5.18</b>	<b>5.43</b>	<b>4.74</b>	<b>4.84</b>
	Std Dev	4.57	2.01	2.89	2.39	2.68
	Std Err	0.37	0.21	0.30	0.27	0.61
<b>Total Curvature</b>	Max	1.50	1.50	2.34	2.05	1.92
	Median	0.59	0.61	0.82	0.93	0.92
	Min	0.15	0.27	0.22	0.39	0.58
	<b>Mean</b>	<b>0.59</b>	<b>0.62</b>	<b>0.94</b>	<b>1.01</b>	<b>0.99</b>
	Std Dev	0.26	0.20	0.48	0.36	0.32
	Std Err	0.02	0.02	0.05	0.04	0.07
<b>Total Planform Irregularity</b>	Max	292.08	188.84	211.72	169.11	233.57
	Median	133.07	106.86	94.12	81.08	75.87
	Min	44.71	49.62	28.68	30.47	43.40
	<b>Mean</b>	<b>141.31</b>	<b>112.05</b>	<b>100.68</b>	<b>82.65</b>	<b>91.61</b>
	Std Dev	54.72	32.12	42.28	28.72	46.84
	Std Err	4.47	3.28	4.38	3.21	10.75
<b>Total Section Irregularity</b>	Max	448.93	216.66	223.42	277.35	182.65
	Median	190.31	95.45	90.57	72.74	82.00
	Min	73.96	45.33	37.04	37.30	47.53
	<b>Mean</b>	<b>206.33</b>	<b>99.31</b>	<b>96.68</b>	<b>82.33</b>	<b>90.97</b>
	Std Dev	76.65	30.66	39.97	41.12	35.92
	Std Err	6.26	3.13	4.14	4.60	8.24

least regular and MB being the most regular. It is noteworthy that for these indices too, GBY is the most homogenous except for the planform irregularity index, where MB is slightly (albeit significantly) more regular.

The fact that the edge-curvature and irregularities indices are recorded for each edge separately allows explora-

tion of the differences between the two lateral sides of the handaxes in each assemblage. In general, all assemblages present fairly similar results for the left and right edges in all indices. The most prominent observations are that, on average, the right edge in MB is more curved than the left one, at NH the left edge has higher planform irregularity

TABLE 6. RAW MATERIAL DISTRIBUTIONS FOR EACH SITE.

Site	Flint		Limestone		Basalt		Total	
	N	%	N	%	N	%	N	%
UB	18	13.04	5	3.62	115	83.33	138	100.00
GBY	-	-	-	-	96	100.00	96	100.00
Holon	90	97.83	2	2.17	-	-	92	100.00
MB	80	100.00	-	-	-	-	80	100.00
NH	6	31.58	13	68.42	-	-	19	100.00
<b>Total</b>	194	45.65	20	4.71	211	49.65	425	100.00

than the right, and at GBY the left edge has higher section irregularity than the right one. The last difference is the only one that is statistically significant.

### TECHNOLOGICAL ATTRIBUTES

The differences in morphological aspects described above are underlain by substantial differences in production technologies and modifications recorded in the different assemblages. One of the most prominent technological aspects is the raw materials on which the handaxes were modified (Table 6). The samples from GBY and MB were made of a single raw material—basalt in the former and flint in the latter. The Holon sample was almost exclusively produced on flint with a negligible proportion of the bifaces produced on limestone. At NH, handaxes were produced on both flint and limestone, yet the small sample size prevents a more in-depth analysis. Thus, an analysis of the effect that raw material has on various morphological aspects must be restricted to the site of 'Ubeidiya, in which all three raw materials were used (albeit only five artifacts were modified on limestone). Different raw materials seem to have a significant effect on the size of the artifact, so that those produced on flint are significantly smaller than those made on basalt. Similarly, flint handaxes are significantly more bilaterally and bifacially symmetrical than basalt ones. Lastly, the edges of flint handaxes are significantly less irregular on both the planform and section aspects with respect to basalt ones. It should be noted though, that these observations are not deterministic—at least for symmetry—as the GBY assemblage, which is made only of basalt, is more symmetrical on average than that of Holon which is produced on flint.

Three other very important technological traits that have significant effects on various morphological aspects are the blank type, the number of scars created during the knapping process, and the extent of cortical coverage of the finished handaxe. In order to examine these effects in detail, and due to the influence of the raw material on them, these technological attributes were analyzed independently for each raw material type. The first technological attribute to be examined was the blank type on which the handaxes were modified. In this respect GBY is the best understood site due to its highly specific Large Flake Acheulian (LFA) technological tradition, allowing an easy identification of

flake blanks. In contrast, in all other assemblages the proportion of artifacts whose blank could not be determined surpasses 50% of the sample (Table 7). This situation stems from the fact that the amount and nature of flaking masks the original morphology of the blank type. Aside from this major part of the sample, the most commonly identified blank type is flake, accounting for about 30% of all observations. As mentioned above, these are mostly basalt flake blanks from the site of GBY. The 'Ubeidiya assemblage is the next most abundant in basalt flake blanks with 30 handaxes (some 22% of the entire sample). At Holon and MB, a small proportion of the samples could be definitely classified as made on flake blanks, all of them flint. At NH only a single artifact, a limestone one, is made on a flake. Chunks are a less common blank type, adding up to 61 handaxes (some 15%) of the entire sample. While GBY is completely devoid of this type, at 'Ubeidiya they account for 28 handaxes (some 20%). These are mostly made of basalt, although flint and limestone were also identified in this category. At Holon almost 20% of the tools are made on flint chunks, with a single limestone one, while at MB only six flint handaxes (7.5% of the sample) could definitely be identified as made on chunks. NH shows the highest proportion of items produced on chunk blanks (some 42%), the majority of them limestone. However, in absolute terms the numbers are too low to make significant inferences.

When considering the effect that the blank type has on the morphological aspects of flint, a statistically significant effect was observed in the bifacial symmetry, and PCs 2 and 4. Handaxes made on flakes are significantly less bifacially symmetrical than those produced on chunks and score significantly higher on PC2 (i.e., have higher surface area to thickness ratio) and PC4 (i.e., are more plano-convex in section, in contrast to convex-concave). When considering the effect this trait has in basalt, it seems to affect significantly more morphological attributes. These include the shape variability, volume, bilateral and bifacial symmetries, edge curvature, section irregularity, and the shape trends described by PCs 2 and 4. Thus, tools made on basalt flakes are significantly more homogenous, smaller, more bilaterally and bifacially symmetrical, have more curved and regular lateral edges, and score higher on PCs 2 and 4 than those made on basalt chunks. It is important to note, however, that due to the specific distributions of raw materials

TABLE 7. BLANK TYPE DISTRIBUTION ACCORDING TO RAW MATERIALS FOR EACH SITE.

Site	Flake							
	Flint		Limestone		Basalt		Total	
	N	%	N	%	N	%	N	%
UB	-	-	2	1.45	30	21.74	32	23.19
GBY	-	-	-	-	80	83.33	80	83.33
Holon	3	3.26	-	-	-	-	3	3.26
MB	9	11.25	-	-	-	-	9	11.25
NH	-	-	1	5.26	-	-	1	5.26
<b>Total</b>	12	2.82	3	0.71	110	25.88	125	29.41

Site	Chunk							
	Flint		Limestone		Basalt		Total	
	N	%	N	%	N	%	N	%
UB	8	5.80	2	1.45	18	13.04	28	20.29
GBY	-	-	-	-	-	-	-	-
Holon	18	19.57	1	1.09	-	-	19	20.65
MB	6	7.50	-	-	-	-	6	7.50
NH	3	15.79	5	26.32	-	-	8	42.11
<b>Total</b>	35	8.24	8	1.88	18	4.24	61	14.35

Site	Indeterminate								Total	
	Flint		Limestone		Basalt		Total		N	%
	N	%	N	%	N	%	N	%		
UB	10	7.25	1	0.72	67	48.55	78	56.52	138	100.00
GBY	-	-	-	-	16	16.67	16	16.67	96	100.00
Holon	69	75.00	1	1.09	-	-	70	76.09	92	100.00
MB	65	81.25	-	-	-	-	65	81.25	80	100.00
NH	3	15.79	7	36.84	-	-	10	52.63	19	100.00
<b>Total</b>	147	34.59	9	2.12	83	19.53	239	56.24	425	100.00

**TABLE 8. PREDICTED BLANK TYPE DISTRIBUTION ACCORDING TO RAW MATERIALS FOR EACH SITE.**

Site	Flake						Chunk						Total	
	Flint		Basalt		Total		Flint		Basalt		Total		N	%
	N	%	N	%	N	%	N	%	N	%	N	%		
<b>UB</b>	0	-	72	54.14	72	54.14	18	13.53	43	32.33	<b>61</b>	<b>45.86</b>	133	100.00
<b>GBY</b>	0	-	95	98.96	95	98.96	-	-	1	1.04	<b>1</b>	<b>1.04</b>	96	100.00
<b>Holon</b>	11	12.22	-	-	11	12.22	79	87.78	-	-	<b>79</b>	<b>87.78</b>	90	100.00
<b>MB</b>	17	21.25	-	-	17	21.25	63	78.75	-	-	<b>63</b>	<b>78.75</b>	80	100.00
<b>NH</b>	0	-	-	-	-	-	6	100.00	-	-	<b>6</b>	<b>100.00</b>	6	100.00
<b>Total</b>	<b>28</b>	<b>6.91</b>	<b>167</b>	<b>41.23</b>	<b>195</b>	<b>48.15</b>	<b>166</b>	<b>40.99</b>	<b>44</b>	<b>10.86</b>	<b>210</b>	<b>51.85</b>	<b>405</b>	

and blank types across sites, these significant differences actually reflect to a large extent the differences between the sites of GBY and 'Ubeidiya. These two sites are the main contributors to the respective categories of basalt flakes and chunks, and indeed these significant differences are in agreement with those described above for the morphological attributes at each site. For the limestone artifacts, no statistically valid differences could be determined due to the small sample size of artifacts with definitely identified blanks amounting to only eight artifacts made on chunks and three made on flakes.

Given the significant effect that this technological selection has on the morphological aspects specified above, they were integrated in nominal logistic fit model in order to assess the blank distribution in each site (Appendix 4). The model was applied only to basalt and flint artifacts of indeterminate blank due to the meager sample size of limestone artifacts of known blank type. The model provided a misclassification rate of 11.76% on a validation sample consisting of some 29% of the known observations. The model predictions suggest that the proportions of chunk blanks would range from as low as 1% at GBY to as high as 100% at NH (Table 8). Handaxes in Holon and MB are predicted to be predominantly produced on chunks. 'Ubeidiya is predicted to have a somewhat more dominant component

of flakes, reaching some 54%, which is entirely produced on basalt. The 'Ubeidiya artifacts predicted to be made on chunks are also mostly basalt, but include the entire flint component from the site.

Another technological procedure that affects morphological aspects of the handaxes is the total number of scars on the tool. This attribute reflects the intensity of blank modification into a finished tool. Like blank types, this attribute too is highly influenced by the raw material of the tool (Table 9). On average, the 'Ubeidiya handaxes have the lowest number of scars, with limestone ones having the lowest number (11.8) and flint the highest (19.1). The number of scars for basalt items at this site is much closer to the low one of limestone than to flint. At GBY, the basalt items show a significantly higher value than those observed on basalt at 'Ubeidiya, and it is even higher than 'Ubeidiya's flint items. Holon and NH show a similar trend in which the flint artifacts have significantly higher values than the limestone ones, but while the flint artifacts have more scars in Holon, at NH the limestone artifacts are more flaked. The sample of MB, which is made only on flint, shows significantly higher values than all other assemblages. Thus, flint artifacts are always more flaked than basalt and limestone ones. The GBY basalt assemblage is also on average more flaked than all limestone samples. When considering

**TABLE 9. SUMMARY STATISTICS OF THE NUMBER OF SCARS FOR EACH SITE.**

	UB			GBY	Holon		MB	NH	
	Flint	Limestone	Basalt	Basalt	Flint	Limestone	Flint	Flint	Limestone
N	17	5	115	90	89	2	78	5	12
Max	40	14	28	54	93	13	123	38	29
Median	18	13	12	21.5	39	12.5	64	33	16
Min	10	7	5	9	9	12	13	9	7
<b>Mean</b>	<b>19.06</b>	<b>11.80</b>	<b>12.82</b>	<b>23.32</b>	<b>41.56</b>	<b>12.50</b>	<b>63.46</b>	<b>29.20</b>	<b>16.75</b>
Std Dev	7.30	2.77	4.38	9.09	17.16	0.71	19.35	11.84	6.40
Std Err	1.77	1.24	0.41	0.96	1.82	0.50	2.19	5.30	1.85

**TABLE 10. SUMMARY STATISTICS OF THE NUMBER OF SCARS FOR EACH PREDICTED BLANK TYPE.**

	Flint		Basalt	
	Flake	Chunk	Flake	Chunk
<b>N</b>	28	161	161	44
<b>Max</b>	123	113	54	28
<b>Median</b>	63	45	16	13
<b>Min</b>	10	9	6	5
<b>Mean</b>	<b>62.82</b>	<b>45.71</b>	<b>18.65</b>	<b>12.95</b>
<b>Std Dev</b>	25.20	20.97	9.13	3.96
<b>Std Err</b>	4.76	1.65	0.72	0.60

the number of scars in light of the blank type predictions provided by the model, it is evident that flint artifacts are significantly more flaked than basalt ones, in accordance with the previous observations and regardless of blank type (Table 10). In addition, for both raw materials subjected to the model, tools produced on flake blanks are always significantly more flaked than those produced on chunks.

The number of scars recorded for each raw material shows significant and strong correlations with some morphological aspects. For flint artifacts, the number of scars is significantly and negatively correlated with shape variability ( $R^2=0.2$ ) so that items with more scars are more homogenous. A significant, albeit weaker, negative correlation also exists with the deviation from bilateral and bifacial symmetries ( $R^2=0.06$  and  $R^2=0.04$ ), so that items with higher scar counts are more symmetrical on both these aspects. It is also significantly correlated with edge section irregularity ( $R^2=0.14$ ), so that the edges of handaxes with more scars are more regular when observed from the side. Finally, a strong and positive correlation was observed with PC2 ( $R^2=0.3$ ), so that artifacts with more scars have a higher surface area to thickness ratios. In limestone artifacts, generally similar correlations were found between the number of scars and the morphological attributes. These include a negative correlation with shape variability ( $R^2=0.36$ ), deviation from bilateral and bifacial symmetries ( $R^2=0.29$  and  $R^2=0.15$ ), and edge planform and section irregularities ( $R^2=0.26$  and  $R^2=0.16$ ). In basalt artifacts the significant correlations between number of scars and morphological aspects include shape variability ( $R^2=0.25$ ), deviation from bilateral and bifacial symmetries ( $R^2=0.19$  and  $R^2=0.13$ ), edge planform and section irregularities ( $R^2=0.03$  and  $R^2=0.19$ ), and PC2 ( $R^2=0.24$ ).

Lastly, the technological attribute of the extent of cortical coverage was examined. As with previous attributes, this one too was divided following the raw-material distribution. It is important to note that for basalt and limestone a definite identification of the cortex is not always possible and hence not all artifacts have an observation for this attribute. The flint component, which has the most observations for this attribute is also the most varied (Table 11).

At 'Ubeidiya there is a fairly homogenous distribution of items ranging from non-cortical to items with 51–75% of their overall surface covered with cortex. GBY lacks any flint artifacts and the sample from NH is too small to be indicative. At Holon the most common state (39%) is that of artifacts with up to 25% cortical coverage, with lower proportions of non-cortical items (31%) and even less with 26–50% coverage (23%). Item with more than 50% coverage are extremely rare. A very similar pattern was observed for MB, with higher proportions of less cortical artifacts and fewer artifacts with more than 50% coverage. For the Limestone component, NH is the only site with a sufficiently large sample to discuss the distribution. Here, more than 40% of the artifacts have 26–50% coverage, and negligible proportions of other categories. For the basalt component, GBY shows a pattern in which the vast majority of the sample is entirely non-cortical and only very few items were classified to the next two categories. At 'Ubeidiya, on the other hand, almost half of the artifacts (47%) have up to 25% cortical coverage and an additional prominent component (22%) of items have 26–50%. In contrast, items with no-cortical coverage are very rare at this site, amounting to less than 5%.

When considering the way in which cortical coverage of flint artifacts affects the morphological attributes, only the section irregularity of the edges and the PC2 scores are significantly affected, so that artifacts that are less cortical are more regular and have higher surface area to thickness ratios. In the basalt component cortical coverage has significant effects on general shape variability, volume, bifacial and bilateral symmetries, the section aspect of edge irregularity and the scores of PC2. However, due to the specific composition of the sample and its distribution, these differences in fact reflect the morphological differences between 'Ubeidiya and GBY.

Some technological attributes were recorded only for the assemblages of Holon, MB and NH, thus allowing an in-depth analysis of the specific differences between the Late Acheulian sites. As the vast majority of artifacts in these sites are produced on flint, the analysis of these results was not conducted separately for each raw material. One

**TABLE 11. CORTICAL-COVERAGE DISTRIBUTION ACCORDING TO RAW MATERIALS FOR EACH SITE.**

Flint												
Site	0%		1–25%		26–50%		51–75%		76–100%		Total	
	N	%	N	%	N	%	N	%	N	%	N	%
UB	4	3.77	5	4.72	5	4.72	3	2.83	1	0.94	18	16.98
GBY	-	-	-	-	-	-	-	-	-	-	-	-
Holon	28	31.11	35	38.89	21	23.33	4	4.44	-	-	88	97.78
MB	31	38.75	39	48.75	8	10	2	2.5	-	-	80	100
NH	1	5.88	2	11.76	1	5.88	1	5.88	-	-	5	29.41
All	64	17.07	81	21.6	35	9.33	10	2.67	1	0.27	191	50.93

Limestone												
Site	0%		1–25%		26–50%		51–75%		76–100%		Total	
	N	%	N	%	N	%	N	%	N	%	N	%
UB	-	-	1	0.94	2	1.89	-	-	1	0.94	4	3.77
GBY	-	-	-	-	-	-	-	-	-	-	-	-
Holon	-	-	-	-	2	2.22	-	-	-	-	2	2.22
MB	-	-	-	-	-	-	-	-	-	-	-	-
NH	1	5.88	3	17.65	7	41.18	1	5.88	-	-	12	70.59
All	1	0.27	4	1.07	11	2.93	1	0.27	1	0.27	18	4.8

Basalt												
Site	0%		1–25%		26–50%		51–75%		76–100%		Total	
	N	%	N	%	N	%	N	%	N	%	N	%
UB	5	4.72	50	47.17	23	21.7	5	4.72	1	0.94	84	79.25
GBY	74	90.24	5	6.1	3	3.66	-	-	-	-	82	100
Holon	-	-	-	-	-	-	-	-	-	-	-	-
MB	-	-	-	-	-	-	-	-	-	-	-	-
NH	-	-	-	-	-	-	-	-	-	-	-	-
All	79	21.07	55	14.67	26	6.93	5	1.33	1	0.27	166	44.27

of these attributes is the proximal retouch, which displays differences between the assemblage of NH, where there are mainly artifacts with none of this retouch, and Holon and MB, where the majority of artifacts are retouched on both faces (Table 12).

This attribute has a significant effect on the artifact's distance from the mean shape of its respective group, on the section aspect of edge irregularity, and on the scores of artifacts on PC2 and 4. Thus artifacts with proximal retouch on both faces are significantly more similar to their respective group's mean shape, have significantly higher edge regularity in section and score significantly higher on PC2 and PC4 than artifacts with no such retouch.

The percussive technique used in the production and

modification of the handaxes also differs among the three assemblages, showing a somewhat similar pattern to that observed for the last attribute (Table 13). The MB handaxes present the highest frequency of production using a soft percussor, either exclusively, or in combination with a hard one. In contrast, the handaxes from NH are predominantly produced only by a hard percussor.

This attribute has a significant effect on the shape variability, so that artifact produced using only hard hammers are significantly less similar to their group's mean shape, have a less regular edge in planform and section aspects, and score lower on PC2 than those produced using only soft percussor or a combination of both types. Furthermore, artifacts that were produced using a soft percussor also

**TABLE 12. PROXIMAL RETOUCH DISTRIBUTION FOR THE LATE ACHEULIAN SITES.**

Site	No Retouch		Only Ventral		Only Dorsal		Both Faces		Total	
	N	%	N	%	N	%	N	%	N	%
Holon	24	26.67	4	4.44	12	13.33	50	55.56	90	100.00
MB	11	13.75	6	7.50	4	5.00	59	73.75	80	100.00
NH	10	62.50	1	6.25	2	12.50	3	18.75	16	100.00
<b>Total</b>	45	24.19	11	5.91	18	9.68	112	60.22	186	100.00

**TABLE 13. PERCUSSIVE TECHNIQUE DISTRIBUTION FOR THE LATE ACHEULIAN SITES.**

Site	Hard		Soft		Combined		Total	
	N	%	N	%	N	%	N	%
Holon	42	46.67	13	14.44	35	38.89	90	100.00
MB	5	6.41	19	24.36	54	69.23	78	100.00
NH	12	75.00	1	6.25	3	18.75	16	100.00
<b>Total</b>	59	32.07	33	17.93	92	50.00	184	100.00

score significantly higher on PC1 than those produced by using only a hard hammer.

Another technological attribute is the total number of hinge scars on both faces of the artifact (Table 14). The assemblage of NH shows on average the lowest number of such scars, which is quite similar to that of MB. The assemblage of Holon shows significantly higher frequencies of hinges. While this attribute does not seem to have a significant effect on any morphological aspect, it is directly related to the type of percussor which was used in tool production, as artifacts produced using only a hard percussor have significantly more hinge scars than those produced using only a soft hammer or a combination of the two types.

### DIACRITIC DIAGRAMS

In this section we present the general reduction sequence of each site as interpreted by samples of specific diacritic diagrams which are provided in Appendix 5. At Holon, the selected blanks are mainly chunks, in accordance with the model prediction. The *chaîne opératoire* at Holon follows five main production steps (Figure 6):

- Step 1: General shaping of the item by large bifacial thinning flakes for which only residual surfaces of the scars in the central area of the handaxes are observable.
- Step 2: Removal of bifacial thinning flakes from the edges in order to create the general morphology of the cutting edges.
- Step 3: Shaping of the proximal part by bifacial flakes in order to regularize and eventually thin it by the removal of residual cortical zones.
- Step 4 and 4': Retouching the cutting edges, mainly in an alternate manner. This means that one lateral edge is retouched on one face (Step 4), then the same edge is retouched on the other face (Step 4'). The same retouch

**TABLE 14. SUMMARY STATISTICS FOR THE NUMBER OF HINGE SCARS FOR THE LATE ACHEULIAN SITES.**

	Total Hinges		
	Holon	MB	NH
<b>N</b>	92	80	17
<b>Max</b>	6	4	2
<b>Median</b>	0.5	0	1
<b>Min</b>	0	0	0
<b>Mean</b>	1.08	0.63	0.59
<b>Std Dev</b>	1.44	0.96	0.62
<b>Std Err</b>	0.15	0.11	0.15

process, but in reverse order, is followed for the opposite lateral edge. Namely, the face that is retouched first on the first edge will be second on the opposite edge.

- Step 5: Retouching the distal pointed part, generally on only one of the two faces.
- Step 5.1: Removal of large scars on one of the two surfaces of the proximal part, removing in the process parts of the previous retouch scars on one of the edges. The knapping is usually done with a hard percussor and may be the expression of a recycling phase of the handaxe into a core. Another possibility is that the intention is to thin the proximal area.

At MB, blank types could be definitely determined for less than 20% of the sample. Of these, 60% were modified on flakes. In contrast, the predictive model suggests that the vast majority of the handaxes in this sample were pro-

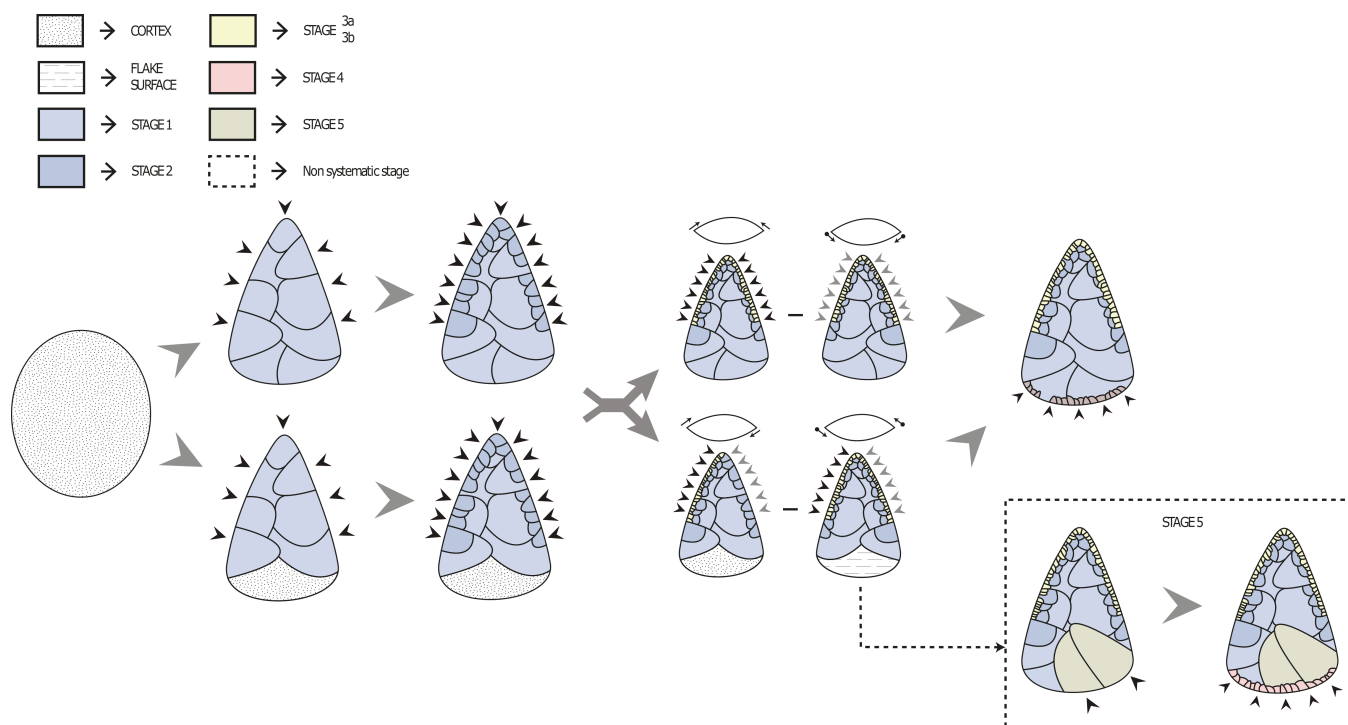


Figure 6. Schematic chaîne opératoire used for production of Holon handaxes.

duced on chunks. Regardless of the actual blank type used, the diacritic analysis provides details of the production sequence (Figure 7).

- Step 1: General shaping of the item by large bifacial thinning flakes for which only residual surfaces of the scars in the central area of the handaxes are observable.
- Step 2: Removal of bifacial thinning flakes from the edges in order to produce their general morphology.
- Step 3: From this step on, it is possible to distinguish two different parallel sequences—an alternate one, characterizing 58% of the sample, and a successive one observed on the rest.
- Step 3a: Similarly to Holon, cutting edges are retouched by an alternate sequence. One edge is retouched first on one face, then on the other. The same retouch process, but in reverse order is followed for the opposite lateral edge.
- Step 3b: The two cutting edges are retouched sequentially so that both edges are first retouched on the same face and only then on the opposite one. The last retouch phase is generally more intensive. In some cases, the retouch is observed only on a single face.
- Step 4: The proximal part is retouched during this step. Usually only on a single face, but retouch on both faces is also present.
- Step 5: Removal of large scars on one of the two surfaces of the proximal part, removing in the process parts of the previous retouch scars on one of the edges. This is performed with a hard percussor and, similarly to Holon, may be the expression either of a recycling phase of the handaxe into a core, or of an additional thinning of the proximal area. However, the first pos-

sibility may be questioned, as the edges are regularized after the removals of these large flakes. It should also be noted that this step is far from being systematic, as it appears on only two artifacts in the sample.

Concerning NH, the *chaîne opératoire* is simpler than that observed in the other two assemblages (Figure 8). It was probably affected by the size of the available raw material. Indeed, the selected blanks are mostly small and flat pebbles of flint or limestone. Thus, the shaping sequence is indeed shorter than in the previous assemblages.

- Step 1/1': Shaping the first edge on one face (Step 1), followed by the other face (Step 1').
- Step 2/2': Shaping the second edge on one face (Step 2), followed by the other face (Step 2').
- Step 3: Regularization of the distal pointed area and the adjacent edge area by retouch on a single face.

Alternating retouch of the two cutting edges, similarly to Holon and MB, was observed only on a single artifact.

## DISCUSSION

While Gilead's work clearly asserts a progressive evolution in hominins' craftsmanship levels, beginning from large and crude handaxes in its oldest manifestation to small refined ones in the later phase, it does not provide any description of the nature or rate of this trend (Gilead 1970a, b). The distinctiveness of the two oldest sites—'Ubeidiya and GBY—had been previously recognized by Gilead. The difference between them was expressed by classifying each assemblage as a separate group within a chronological order, with 'Ubeidiya representing the Early Acheulian of the Levant and GBY the Middle Acheulian. In addition, Gilead clearly recognized the high variability in the Late

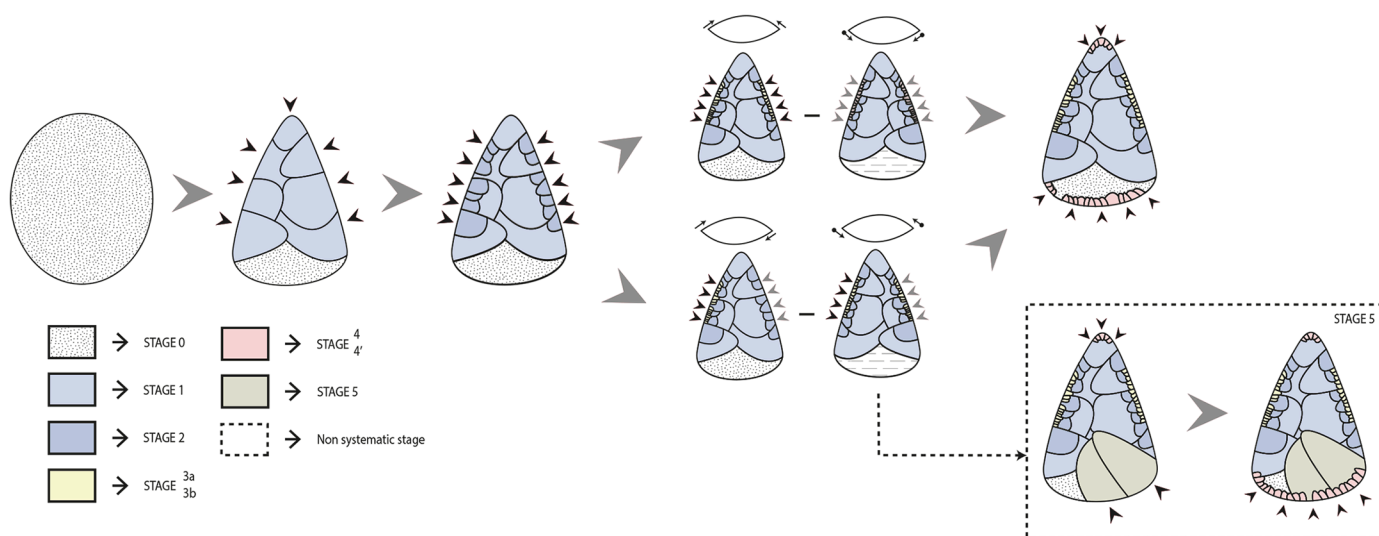


Figure 7. Schematic chaîne opératoire used for production of Ma'ayan Barukh handaxes.

Acheulian, and hence introduced an additional division for assemblages of this phase into several possibly contemporaneous and typologically characterized groups (Gilead 1970a, b). The relative increase in the number of well excavated and well dated Acheulian assemblages contributed almost entirely to the later part of the Technocomplex. Thus, the three main chrono-cultural units stemming from the tripartite division persist in interpretation of various phenomena associated with handaxe variability. In the current study, the scheme developed by Gilead is tested using novel methodological tools in order to validate or refute it. In addition, handaxe properties associated with craftsmanship are objectively measured and tested against various technological factors to provide a description of the nature

of change along the three phases.

The 'Ubeidiya handaxes studied in this sample are indeed the most distinct and furthest set apart from all other assemblages, in accordance with their substantially older chronology, predating GBY by some 800–400 Ky. Furthermore, with regards to all the morpho-technological characteristics that are associated with craftsmanship, they consistently present the lowest scores. These characteristics include general shape homogeneity, symmetry, and edge regularity. Many of the handaxes display shapes that are beyond the ranges of all other sampled sites in terms on narrowness, elongation, and low surface area to thickness ratio. Hence the mean handaxe-shape of the 'Ubeidiya sample is the least similar to any of the other assemblages. This

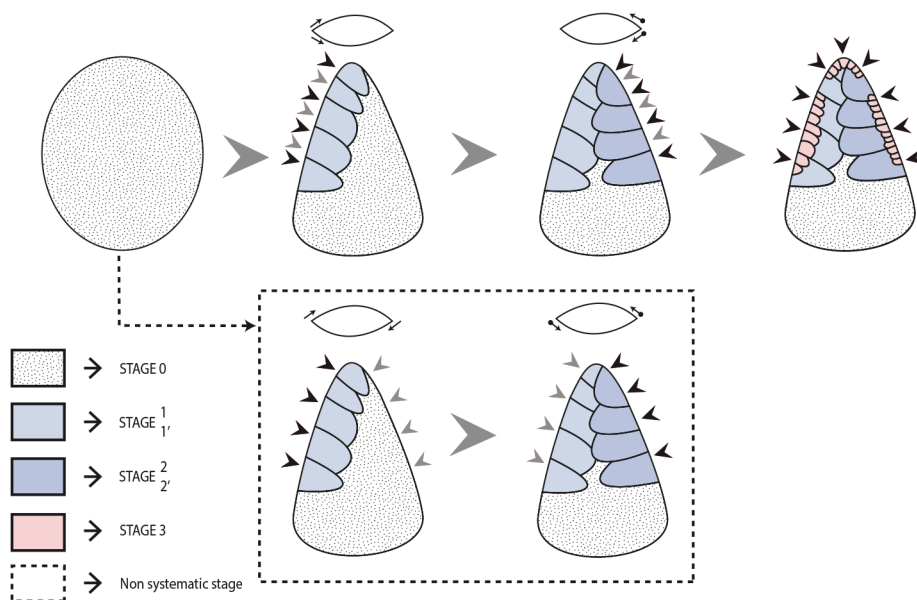


Figure 8. Schematic chaîne opératoire used for production of Nahal Hesi handaxes.

is true not only for the shapes but also for the size range of the artifacts, which greatly exceeds that of all other assemblages. These morphological patterns are in turn underlain both by the highly variable technological procedures and by low investment in shaping and modification. The former is expressed in the varied raw material selection and blank types used, the latter by the significantly lower number of scars observed on handaxes of all raw materials and blank types, as well as in the higher proportions of artifacts with extensive cortical coverage.

The GBY handaxes had been previously thoroughly described and analyzed in a series of studies describing their production technology and morphologies, and providing insights into their reduction sequence and *chaîne opératoire* (Goren-Inbar and Saragusti 1996; Goren-Inbar et al. 2018; Herzlinger and Goren-Inbar 2019, 2020). However, the current results allow their integration within the wider chrono-cultural scheme of the Acheulian in Israel and highlight their uniqueness. This is expressed not only by their relatively high mean scores in all morphological aspects and the unique technological tradition employed in their production, but mainly in their unparalleled homogeneity. This homogeneity is most prominent in terms of the general morphologies of the handaxes, for which GBY forms the most homogenous group in the sample. The general handaxe shapes observed at GBY have, on average, higher surface area to thickness ratio than any other sample and are less curved in their lateral edges than those observed in the Late Acheulian samples. Thus, based mainly on surface area to thickness ratio, the mean shape is substantially closer to those of the Late Acheulian samples than to that of 'Ubeidiya. The GBY sample also displays a high degree of symmetry, surpassing that of Holon, and although it is less regular than any of the Late Acheulian samples, it is almost always the most homogeneous in all these aspects. In terms of size, GBY is the second largest, although like in the case of morphology, it is closer to the values measured for the Late Acheulian assemblages.

These unique morphological patterns are directly derived from the unique technological tradition used for the production of the handaxes, conforming to the LFA. The specific LFA variant produced by the GBY hominins was thoroughly studied and described in detail in many publications (Goren-Inbar et al. 2018), and similarly to the morphological observations, is characterized by a high-degree of homogeneity. This is expressed in the raw material used for handaxes modification, which in this study is exclusively basalt. It is noteworthy, however, that while other raw materials such as flint and limestone were used for handaxe modification at GBY, they form only a very minor component of the assemblages. The technological homogeneity is also expressed in the blank selection, which in accordance with the fundamental principle of the LFA, is exclusively large flake blanks. The fact that the flake blanks were removed from modified giant cores is in turn reflected in the minimal representation of cortex on the artifacts. Another prominent characteristic of this technological tradition is its relatively low number of scars used

in the handaxes' modification. At GBY this number is on average higher than at 'Ubeidiya for all raw materials, and even higher than the number observed for the limestone component of Late Acheulian samples. However, it is significantly lower than that observed for flint artifacts in the assemblage from that phase. Thus, the highly specific LFA technological tradition, which is unique within the Middle Acheulian in Israel (i.e., to GBY), allowed the knappers to score higher than some of the Late Acheulian samples on morphological attributes associated with craftsmanship and refinement. Furthermore, it appears that for the GBY sample the homogeneity in morphological traits was of paramount importance to the knappers.

The fact that the Gilead's Late Acheulian group is represented in this study by three different samples allows exploration of its morpho-technological variability in a more detailed way. Firstly, this study confirms that all three assemblages are more similar to one another in terms of mean shape than to either of the two earlier ones. As Holon occupies the most central position of the three in shape space, its mean shape is not significantly different from either MB or NH, despite the fact that these two are significantly different from one another. The similarity is mainly based on their planform aspect, which is significantly more oval and less elongated than GBY or 'Ubeidiya. Despite the fact that this shape aspect, reflected by PC1 and the edge curvature index, is affected by blank type, this effect was found to be significant only for basalt, which is not represented in these assemblages. Thus, the pattern can be quite securely associated with intentional selection stemming from cultural or functional considerations rather than from technological constraints. In contrast, on the second main shape trend of surface area to thickness ratio, reflected by PC2, larger differences are observed. Thus, from this perspective the site of MB is more similar to GBY than to NH. Furthermore, substantial differences between the Late Acheulian sites are observed in other morphological traits such as within-group morphological homogeneity, artifact volume and deviation from perfect bilateral and bifacial symmetries. The assemblages of MB and NH are both highly symmetrical, while Holon is less symmetrical than GBY. A similar pattern is observed for the section and planform regularities, where Holon is not only the least regular, but it is more similar to GBY than to NH, while MB is significantly more regular than any of them.

In a similar manner to 'Ubeidiya (although to a substantially lesser degree), these differences in morphological attributes are associated with higher technological variability. This is especially pronounced when compared with the prominent technological homogeneity observed at GBY. At MB and Holon, a clear predominance of flint is observed, while at NH limestone is dominant. It is important to note that while the sample of MB used here only contains flint artifacts, a few basalt tools were reported from the site (Rosenberg et al. 2015), although they only form a negligible component. The technological attributes of the blank types posed a serious problem with regards to the Late Acheulian sites, as the high scar count on the flint com-

ponent prevented a clear classification in the vast majority of cases. However, thanks to the model used in this study, calculated predictions now allow a better understanding. These predictions also point towards higher variability than that observed at GBY as both flakes and chunks were concurrently used at Holon and MB. Despite the fact that in both sites chunks were predominantly preferred, their proportions differ, as the flake component in MB is almost twice as high as that in Holon. The fact that tools made on flint flake blanks have significantly higher cortical coverage, plano-convex section morphology, and lower bifacial symmetry than tools made on chunks of the same raw material is somewhat counter-intuitive. This is especially true in light of the fact that this trend is exactly opposite for tools made on basalt flakes, as they are more bifacially symmetrical and are less cortical than tools made on basalt chunks. This may suggest that the flint flake blanks have been produced using substantially different technological procedures than the ones observed at GBY, probably consisting of smaller, less modified, and standardized cores. The high variability of the Late Acheulian samples continues to be seen in other technological aspects such as the distribution of proximal retouch, the use of different flaking technique and the number of hinge scars, each with its own specific implications for handaxe morphology.

The use of diacritic diagrams to analyze the Late Acheulian assemblages allows obtaining of additional procedural differences both within and between the assemblages. These indicate that Holon and MB have in general a similar procedural sequence, consisting of a systematic alternating edge retouch. However, while at Holon this sequence appears in almost all analyzed artifacts, at MB it only appears on half of them, while the other half displays a successive sequence in which the alternation is applied to the faces rather than to the two lateral edges. The latter type of sequence has some similarities to the pattern observed at NH, where edges are almost always retouched on a single face. In addition, at both sites specific reduction stages suggest that handaxes may have been recycled to serve as cores for flakes. This kind of recycling process from handaxes to cores was indeed reported at the site of MB as well as at other Late Acheulean sites such as Revadim (DeBono and Goren-Inbar 2001; Marder et al. 2006).

The Acheulian technocomplex is chronologically and geographically one of the most extensive cultural entities in human prehistory (Lycett and Gowlett 2008). As such, it naturally displays immense differences in virtually all aspects of human behavior. The single common denominator of all Acheulian assemblages, regardless of age or region, is the handaxe, which in all respects still serves as the *fossil directeur* of this entity (Lepre et al. 2011; Moncel et al. 2013; Norton et al. 2006). In the Levant, this indicative tool appears in the archaeological record for well over a million years, a persistence that was used to describe the Acheulian as an unparalleled conservative phenomenon (Finkel and Barkai 2018). Nonetheless, over this prolonged time period substantial changes took place with regard to both production technologies of the handaxes and their mor-

phologies. Pronounced morpho-technological differences between Acheulian assemblages on a global-scale have made it possible to outline several distinct techno-cultural traditions pertaining to this technocomplex (Norton et al. 2006; Sharon 2010; Sharon and Barsky 2016). The Levant, being centrally located in the Acheulian world and serving as a land-bridge between Africa and Eurasia, displays several of these different traditions. Accordingly, it also plays a central role in most scenarios attempting to explain the globally observed patterns. Given the low archaeological and chronological resolutions of the earlier parts of the technocomplex, and the techno-morphological similarity of Acheulian assemblages from the Levant to ones from Africa and Europe, the chrono-cultural scheme devised by Gilead still serves as a benchmark with regards to understanding Acheulian morpho-technological variability in Israel and beyond.

The current study, with its novel methods and tools, generally confirms the validity of Gilead's observations. The morpho-technological analysis demonstrates that the Early, Middle, and Late Acheulian in Israel significantly differ in a general morpho-technological sense and can be regarded as different and discrete manifestations of this extensive cultural entity. The current analysis also provides a substantially more detailed description of the nature of the morpho-technological difference dividing them. Even more importantly, this description is objectively measured and quantitatively expressed, so that it can now truly serve as a yardstick, which can be updated or modified when necessary, and against which other assemblages can be evaluated.

The results also indicate that the development in aspects associated with craftsmanship and technological complexity from the Early to the Late Acheulian is non-uniform, intricate and more complex than previously assumed (Bar-Yosef 1994; Clark 1966, 1975; Hodgson 2015; McNabb and Cole 2015; Stout et al. 2011). This conclusion stems mainly from the observation demonstrating that the Middle Acheulian, as manifested at GBY, displays significantly higher scores of craftsmanship-associated aspects, and thus is by no means less developed or sophisticated than that observed in the substantially younger Late Acheulian assemblages. Furthermore, the morphological aspects similar to the later ones are reached via a very complex yet substantially different technological procedure. While these insights should be considered in any discussion about the nature and rate of hominin cognitive development, and their dispersion patterns in the Early and Middle Pleistocene, it is again stressed that this study is not intended to explore various factors underlying handaxe shape variability in the Acheulian. This is mainly due to the fact that, unfortunately, the fragmented nature of the archaeological record, especially in the older periods (Goren 1981), still prevents Paleolithic archaeology from clearly understanding the process and mechanisms responsible for this pattern. In contrast, this study does lay some foundations for better, more accurate, objective, and comprehensive comparisons between various Acheulian manifestations, and explora-

tion and testing hypotheses concerning the various factors associated with handaxe variability. All the raw data, observations, and results, as well as the analytical tools and methodological procedures are fully available to the entire research community. Accordingly, practitioners are eagerly encouraged to use them for describing and analyzing morpho-technological differences between assemblages from around the Acheulian world, while continuously adding their own data, making it publicly available. Among the most clearly required future venues of explorations are the notion that both 'Ubeidiya and GBY are more similar to African assemblages of comparable ages than to each other, and that there is a greater resemblance of the Late Acheulian assemblages to concurrent European assemblages. Reasons such as hominin anatomical and cognitive evolution, geographical expansions, population dynamics, and social complexity could all be considered plausible factors underlying these patterns and can be further explored through this approach (Hodgson 2015; Lycett and von Cramon-Taubadel 2008; Stout et al. 2014).

Finally, understanding chronological trends, such as the changes in craftsmanship-associated shape aspects, through modelling should optimally be conducted first on data from established chronological contexts. Unfortunately, such data are yet to be obtained outside of Africa for the older parts of the Acheulian Technocomplex. However, this type of data is relatively abundant in the Late Acheulian. Unfortunately, the data available to us were not optimal in this respect, and a better understanding of trends and patterns of handaxe variability in the Late Acheulian is still a challenge for future research. The Late Acheulian phase is represented here by only three sites (reflecting three of the four groups identified by Gilead), for which precise dating and context remain poorly controlled. Still, this study demonstrates the diverse nature of each assemblage and the extent of their within- and between-assemblage morpho-technological variability. The objective, quantitative, and reproducible nature of our results would allow future studies to integrate our data with additional observations in order to attain a better grasp of the possible chronological and geographical differences between sites assigned to later phases of the Acheulian Technocomplex. It is indeed the end of the Acheulian in the Levant, expressed by the Acheulo-Yabrudian Technocomplex, which may provide an unmatched research opportunity. This latest stage of the Acheulian is represented in different cave sites (Tabun, Misliya, Qesem) that provide modern data for large handaxe assemblages on the one hand, and an excellent record of stratigraphy and chronology on the other. Tabun (Gisis 2008; Ronen et al. 2011; Shimelmitz et al. 2017), Misliya (Zaidner and Weinstein-Evron 2016; Zaidner et al. 2006), and Qesem (Barkai et al. 2003; Gopher et al. 2010; Mercier et al. 2013), could contribute greatly to the issues discussed here. The extensive database from which our conclusions are derived will provide an additional source of reference for future studies.

## ACKNOWLEDGMENTS

This research was supported by the Ministry of Science and Technology, Israel, the Ministère de l'Enseignement Supérieur, de la Recherche et de l'Innovation, and Ministère de l'Europe et des Affaires Étrangères, France through the PHC Maimonide project (2018–2019). This research was made possible thanks to the generous scholarship granted to GH by the Israeli Planning and Budgeting Committee (VATAT) in memory of Nathan Rotenstreich, via the Hebrew University's Ph.D. honors program at The Jack, Joseph and Morton Mandel School for Advanced Studies in the Humanities. The authors are thankful for additional funding provided to GH by the Braginsky Center for the Interface between Science and the Humanities at the Weizmann Institute of Science and to Prof. Uzy Smilansky for his support. The authors thank Smadar Gabrieli for editing the manuscript and Ruhama Bonfil for the production of Figure 1. We kindly thank Erella Hovers and two anonymous reviewers for their constructive comments and suggestions, which undoubtedly improved this study.

## REFERENCES

- Apel, J. 2008. Knowledge, know-how and raw material - The production of Late Neolithic flint daggers in Scandinavia. *Journal of Archaeological Method and Theory* 15, 91–111.
- Bamforth, D.B., Finlay, N. 2008. Introduction: Archaeological approaches to lithic production skill and craft learning. *Journal of Archaeological Method and Theory* 15, 1–27.
- Barkai, R., Gopher, A., Lauritzen, S.E., Frumkin, A. 2003. Uranium series dates from Qesem Cave, Israel, and the end of the Lower Palaeolithic. *Nature* 423, 977–979.
- Barkai, R., Lemorini, C., Gopher, A. 2010. Palaeolithic cutlery 400 000–200 000 years ago: tiny meat-cutting tools from Qesem Cave, Israel. *Antiquity* 84, 2–6.
- Bar-Yosef, O. 1994. The lower Paleolithic of the Near East. *Journal of World Prehistory* 8, 211–265.
- Bar-Yosef, O., Goren-Inbar, N. 1993. *The lithic assemblage of Ubeidiya. A lower Paleolithic site in the Jordan Valley*. Qadim, Jerusalem.
- Barzilai, O., Aga, N., Crouvi, O. 2010. The prehistoric remains in Emeq Rephaim (Area C). In *New Studies in the Archaeology of Jerusalem and Its Region*, Amit, D., Peleg-Barkat, O., Stiebel, G. (eds.). Institute of Archaeology, The Hebrew University of Jerusalem, Jerusalem, pp. 31–39.
- Barzilai, O., Malinsky-Buller, A., Ackerman, O. 2006. Kefer Menachem West: A Lower Palaeolithic site in the Southern Shephela, Israel. *Journal of the Israel Prehistoric Society* 36, 7–38.
- Blasco, R., Rosell, J., Gopher, A., Barkai, R. 2014. Subsistence economy and social life: a zooarchaeological view from the 300 kya central hearth at Qesem Cave, Israel. *Journal of Anthropological Archaeology* 35, 248–268.
- Bookstein, F.L., Chernoff, B., Elder, R.L., Humphries, J., Smith, G.R., Strauss, R.E. 1985. *Morphometrics in Evolutionary Biology: The Geometry of Size and Shape Change, with Examples from Fishes*. Academy of Natural Sciences

- of Philadelphia Philadelphia, Philadelphia.
- Bordes, F. 1961. *Typologie du Paléolithique ancien et moyen*. Imprimeries Delmas, Bordeaux.
- Chazan, M. 2013. Butchering with small tools: the implications of the Evron Quarry assemblage for the behaviour of *Homo erectus*. *Antiquity* 87, 350–367.
- Clark, D.J. 1966. Acheulian occupation sites in the Middle East and Africa: a study in cultural variability. *American Anthropologist* 68, 202–229.
- Clark, D.J. 1975. A comparison of the Late Acheulian industries of Africa and the Middle East. In *After the Australopithecines: Stratigraphy, Ecology and Culture Change in the Middle Pleistocene*, Isaac, G.L., Butzer, K.W. (eds.). Aldine, Chicago, pp. 605–659.
- Dauvois, M. 1976. *Précis de dessin dynamique et structural des industries lithiques préhistoriques*. Pierre Fanlac, Perigueux.
- DeBono, H., Goren-Inbar, N. 2001. Note on a link between Acheulian handaxes and the Levallois method. *Journal of the Israel Prehistoric Society* 31, 9–23.
- Dryden, I.L., Mardia, K.V. 1998. *Statistical Shape Analysis*. John Wiley & Sons, Chichester.
- Enzel, Y., Bar-Yosef, O. (Eds.). 2017. *Quaternary of the Levant: Environments, Climate Change, and Humans*. Cambridge University Press, Cambridge.
- Eren, M.I., Roos, C.I., Story, B.A., von Cramon-Taubadel, N., Lycett, S.J. 2014. The role of raw material differences in stone tool shape variation: an experimental assessment. *Journal of Archaeological Science* 49, 472–487.
- Finkel, M., Barkai, R. 2018. The Acheulean handaxe technological persistence: a case of preferred cultural conservatism? *Proceedings of the Prehistoric Society* 84, 1–19.
- Fornai, C., Benazzi, S., Gopher, A., Barkai, R., Sarig, R., Bookstein, F.L., Hershkovitz, I., Weber, G.W. 2016. The Qesem Cave hominin material (Part 2): a morphometric analysis of dm2-QC2 deciduous lower second molar. *Quaternary International* 398, 175–189.
- Frumkin, A., Karkanas, P., Bar-Matthews, M., Barkai, R., Gopher, A., Shahack-Gross, R., Vaks, A. 2009. Gravitational deformations and fillings of aging caves: the example of Qesem karst system, Israel. *Geomorphology* 106, 154–164.
- Garrod, D., Bate, D. 1937. *The Stone Age of Mount Carmel I: Excavations in the Wady el-Mughara*. Clarendon, Oxford.
- Gilead, D. 1970a. Handaxe industries in Israel and the Near East. *World Archaeology* 2, 1–11.
- Gilead, D. 1970b. *Early Paleolithic cultures in Israel and the Near East*. Ph.D. thesis. The Hebrew University of Jerusalem, Jerusalem.
- Gilead, D., Ronen, A. 1977. Acheulian industries from Evron on the Western Galilee coastal plain. *Eretz-Israel: Archaeological, Historical and Geographical Studies* 13, 56–86.
- Ginat, H., Zilberman, E., Saragusti, I. 2003. Early Pleistocene lake deposits and Lower Paleolithic finds in Nahal (Wadi) Zihor, Southern Negev desert, Israel. *Quaternary Research* 59, 445–458.
- Gisis, I. 2008. *The Lower Paleolithic Industries of Tabun Cave*. Ph.D. thesis. University of Haifa, Haifa.
- Gopher, A., Ayalon, A., Bar-Matthews, M., Barkai, R., Frumkin, A., Karkanas, P., Shahack-Gross, R. 2010. The chronology of the late Lower Paleolithic in the Levant based on U–Th ages of speleothems from Qesem Cave, Israel. *Quaternary Geochronology* 5, 644–656.
- Goren, N. 1981. The Lower Palaeolithic in Israel and adjacent countries. In *Préhistoire du Levant*, Cauvin, J. (Ed.). C.N.R.S., Lyon, pp. 193–205.
- Goren-Inbar, N., Alperson-Afil, N., Sharon, G., Herzlinger, G. 2018. *The Acheulian Site of Gesher Benot Ya'aqov*. Volume IV: *The Lithic Assemblages*. Vertebrate Paleobiology and Paleoanthropology. Springer International Publishing, Cham.
- Goren-Inbar, N., Saragusti, I. 1996. An Acheulian biface assemblage from Gesher Benot Ya'aqov, Israel: indications of African affinities. *Journal of Field Archaeology* 23, 15–30.
- Goren-Inbar, N., Speth, J.D. (eds.). 2004. *Human Paleocology in the Levantine Corridor*. Oxbow Books Limited, Oxford.
- Goswami, A., Watanabe, A., Felice, R.N., Bardua, C., Fabre, A.-C., Polly, P.D. 2019. High-density morphometric analysis of shape and integration: the good, the bad, and the not-really-a-problem. *Integrative and Comparative Biology* 59, 669–683.
- Grosman, L., Goldsmith, Y., Smilansky, U. 2011. Morphological analysis of Nahal Zihor handaxes: a chronological perspective. *PaleoAnthropology* 2011, 203–15.
- Gvirtzman, G., Wieder, M., Marder, O., Khalaily, H., Rabinovich, R., Ron, H. 1999. Geological and pedological aspects of an Early-Paleolithic site: Revadim, Central Coastal Plain, Israel. *Geoarchaeology* 14, 101–126.
- Herzlinger, G., Deschamps, M., Brenet, M., Varanda, A., López-Tascón, C., Goren-Inbar, N. 2020. Reevaluation of the Classification scheme of the Acheulian in the Levant – 50 years later: a morpho-technological analysis of handaxe variability. *Open Science Framework Online Repository*. <https://doi.org/10.17605/OSF.IO/YZTK>
- Herzlinger, G., Goren-Inbar, N. 2019. Do a few tools necessarily mean a few people? A techno-morphological approach to the question of group size at Gesher Benot Ya'aqov, Israel. *Journal of Human Evolution* 128, 45–58.
- Herzlinger, G., Goren-Inbar, N. 2020. Beyond a cutting edge: a morpho-technological analysis of Acheulian handaxes and cleavers from Gesher Benot Ya'aqov, Israel. *Journal of Paleolithic Archaeology* 3, 33–58.
- Herzlinger, G., Goren-Inbar, N., Grosman, L. 2017. A new method for 3D geometric morphometric shape analysis: the case study of handaxe knapping skill. *Journal of Archaeological Science: Reports* 14, 163–173.
- Herzlinger, G., Grosman, L. 2018. AGMT3-D: a software for 3-D landmarks-based geometric morphometric shape analysis of archaeological artifacts. *PLoS One* 13, e0207890.
- Hodgson, D. 2015. The symmetry of Acheulean handaxes and cognitive evolution. *Journal of Archaeological Science: Reports* 2, 204–208.
- Horowitz, A. 2001. *The Jordan Rift Valley*. Balkema, Lisse.

- Isaac, G.L., Isaac, B. 1977. *Ologresailie: Archeological Studies of a Middle Pleistocene Lake Basin in Kenya*. University of Chicago Press, Chicago.
- Jelinek, A.J. 1982. The Tabun Cave and Paleolithic man in the Levant. *Science* 216, 1369–1375.
- Kohn, M., Mithen, S. 1999. Handaxes: products of sexual selection? *Antiquity* 73, 518–526.
- Lepre, C.J., Roche, H., Kent, D.V., Harmand, S., Quinn, R.L., Brugal, J.-P., Texier, P.-J., Lenoble, A., Feibel, C.S. 2011. An earlier origin for the Acheulian. *Nature* 477, 82–85.
- Lycett, S.J., Chauhan, P.R. 2010. Analytical approaches to Palaeolithic technologies: an introduction. In *New Perspectives on Old Stones*, Lycett, S.J., Chauhan, P.R. (eds.). Springer, New York, pp. 1–22.
- Lycett, S.J., Gowlett, J.A.J. 2008. On questions surrounding the Acheulean 'tradition.' *World Archaeology* 40, 295–315.
- Lycett, S.J., von Cramon-Taubadel, N. 2008. Acheulean variability and hominin dispersals: a model-bound approach. *Journal of Archaeological Science* 35, 553–562.
- Lycett, S.J., von Cramon-Taubadel, N., Foley, R.A. 2006. A crossbeam co-ordinate caliper for the morphometric analysis of lithic nuclei: a description, test and empirical examples of application. *Journal of Archaeological Science* 33, 847–861.
- Machin, A. 2009. The role of the individual agent in Acheulean biface variability: a multi-factorial model. *Journal of Social Archaeology* 9, 35–58.
- MacLeod, N. 2001. Landmarks, localization, and the use of morphometrics in phylogenetic analysis. In *Fossils, Phylogeny, and Form*, Adrain, J.M., Edgecombe, G.D., Lieberman, B.S. (eds.). Topics in Geobiology. Springer US, Boston, MA, pp. 197–233.
- Malinsky-Buller, A. 2014. Contextualizing curatorial strategies at the late lower Paleolithic site of Holon, Israel. *PaleoAnthropology* 2014, 483–504.
- Malinsky-Buller, A. 2016. The muddle in the Middle Pleistocene: the Lower–Middle Paleolithic transition from the Levantine perspective. *Journal of World Prehistory* 29, 1–78.
- Malinsky-Buller, A., Barzilai, O., Ayalon, A., Bar-Matthews, M., Birkenfeld, M., Porat, N., Ron, H., Roskin, J., Ackermann, O. 2016. The age of the Lower Paleolithic site of Kefar Menachem West, Israel—Another facet of Acheulean variability. *Journal of Archaeological Science: Reports* 10, 350–362.
- Malinsky-Buller, A., Hovers, E., Marder, O. 2011. Making time: 'living floors', 'palimpsests' and site formation processes – A perspective from the open-air Lower Paleolithic site of Revadim Quarry, Israel. *Journal of Anthropological Archaeology* 30, 89–101.
- Marder, O., Malinsky-Buller, A., Shahack-Gross, R., Ackermann, O., Ayalon, A., Bar-Matthews, M., Goldsmith, Y., Inbar, M., Rabinovich, R., Hovers, E. 2011. Archaeological horizons and fluvial processes at the Lower Paleolithic open-air site of Revadim (Israel). *Journal of Human Evolution* 60, 508–522.
- Marder, O., Milevski, I., Matskevich, Z. 2006. The handaxes of Revadim Quarry: typo-technological considerations and aspects of intra-site variability. In *Axe Age: Acheulian Tool-Making From Quarry to Discard*, Goren-Inbar, N., Sharon, G. (eds.). Equinox, London, pp. 223–242.
- Marozzi, M. 2016. Multivariate tests based on interpoint distances with application to magnetic resonance imaging. *Statistical Methods in Medical Research* 25, 2593–2610.
- McNabb, J., Cole, J. 2015. The mirror cracked: symmetry and refinement in the Acheulean handaxe. *Journal of Archaeological Science: Reports* 3, 100–111.
- McPherron, S.P. 1999. Ovate and pointed handaxe assemblages: two points make a line. *Préhistoire Européenne* 14, 9–32.
- Mercier, N., Valladas, H., Falguères, C., Shao, Q., Gopher, A., Barkai, R., Bahain, J.-J., Vialettes, L., Joron, J.-L., Reyss, J.-L. 2013. New datings of Amudian layers at Qesem Cave (Israel): results of TL applied to burnt flints and ESR/U-series to teeth. *Journal of Archaeological Science* 40, 3011–3020.
- Mercier, N., Valladas, H., Froget, L., Joron, J.-L., Ronen, A. 2000. Datation par thermoluminescence de la base du gisement paléolithique de Tabun (mont Carmel, Israël). *Comptes Rendus de l'Académie des Sciences - Series IIA - Earth and Planetary Science* 330, 731–738.
- Moncel, M.-H., Despriée, J., Voinchet, P., Tissoux, H., Moreno, D., Bahain, J.-J., Courcimault, G., Falguères, C. 2013. Early evidence of Acheulean settlement in North-western Europe - La Noira Site, a 700 000 Year-Old Occupation in the center of France. *PLoS One* 8, e75529.
- Neuville, R. 1931. L'acheuléen supérieur de la grotte d'Oumm-Qatafa (Palestine). *L'Anthropologie* 41, 253–263.
- Neuville, R. 1951. *Le Paléolithique et le Mésolithique du Désert de Judée*. Archives de l'institut de Paleontologie humaine, Paris.
- Nonaka, T., Bril, B., Rein, R. 2010. How do stone knappers predict and control the outcome of flaking? Implications for understanding early stone tool technology. *Journal of Human Evolution* 59, 155–167.
- Norton, C.J., Bae, K., Harris, J.W.K., Lee, H. 2006. Middle Pleistocene handaxes from the Korean Peninsula. *Journal of Human Evolution* 51, 527–536.
- O'Brien, E.M. 1981. The projectile capabilities of an Acheulean handaxe from Ologresailie. *Current Anthropology* 76–79.
- Olausson, D. 2017. Knapping skill and craft specialization in Late Neolithic flint daggers. *Lithic Technology* 42, 127–139.
- Roe, D.A. 1964. The British Lower and Middle Palaeolithic: some problems, methods of study and preliminary results. *Proceedings of the Prehistoric Society* 30, 245–267.
- Rohlf, F.J. 2021. Why clusters and other patterns can seem to be found in analyses of high-dimensional data. *Evolutionary Biology* 48, 1–16.
- Ronen, A. 1991. The Lower Palaeolithic site Evron-Quarry in western Galilee, Israel. *Sonderveröffentlichungen Geologisches Institut der Universität zu Köln* 82, 187–212.
- Ronen, A. 2003. The small tools of Evron-Quarry, western

- Galilee, Israel. In *Lower Palaeolithic Small Tools in Europe and the Levant*, Burdukiewicz, J.M., Ronen, A. (eds.). British Archaeological Reports 1115, Oxford, pp. 113–120.
- Ronen, A., Gisis, I., Tchernikov, I. 2011. The Mougharan Tradition reconsidered. In *The Lower and Middle Palaeolithic in the Middle East and Neighbouring Regions*, Le Tensorer, J.-M., Jagher, R., Otte, M. (eds.). Basel Symposium, Mai [i.e. May] 8 - 10 2008, Études et Recherches Archéologiques de l'Université de Liège. Presented at the Symposium, ERAUL, Liège, pp. 59–66.
- Ronen, A., Ohel, M.Y., Lamdan, M., Assaf, A. 1980. Acheulean artifacts from two trenches at Ma'ayan Barukh. *Israel Exploration Journal* 30, 17–33.
- Rosenberg, D., Shimelmitz, R., Gluhak, T.M., Assaf, A. 2015. The geochemistry of basalt handaxes from the Lower Palaeolithic site of Ma'ayan Baruch, Israel—A perspective on raw material selection: basalt handaxes from Ma'ayan Baruch, Israel. *Archaeometry* 57, 1–19.
- Saragusti, I., Ginat, H. 1996. Lower Paleolithic finds from the region of Nahal Zihor, Southern Negev. Presented at the The Geological Society Annual Meeting 1996, The Geological Society of Israel, Eilat.
- Schick, T., Stekelis, M. 1977. Mousterian assemblages in Kebara Cave. *Eretz-Israel: Archaeological, Historical and Geographical Studies* 13, 97–149.
- Schwarcz, H.P., Goldberg, P., Blackwell, B. 1980. Uranium series dating of archaeological sites in Israel. *Israel Journal of Earth Sciences* 29, 157–165.
- Sharon, G. 2008. The impact of raw material on Acheulian large flake production. *Journal of Archaeological Science* 35, 1329–1344.
- Sharon, G. 2010. Large flake Acheulian. *Quaternary International* 223–224, 226–233.
- Sharon, G. 2017. The Acheulian of the Levant. In *Quaternary of the Levant: Environments, Climate Change, and Humans*, Enzel, Y., Bar-Yosef, O. (Eds.). Cambridge University Press, Cambridge, pp. 539–548.
- Sharon, G., Barsky, D. 2016. The emergence of the Acheulian in Europe – A look from the east. *Quaternary International* 411, 25–33.
- Shemer, M., Crouvi, O., Shaar, R., Ebert, Y., Matmon, A., ASTER Team, Horwitz, L.K., Eisenmann, V., Enzel, Y., Barzilai, O. 2019. Geochronology, paleogeography, and archaeology of the Acheulian locality of 'Evron Landfill in the western Galilee, Israel. *Quaternary Research* 91, 729–750.
- Shimelmitz, R., Bisson, M., Weinstein-Evron, M., Kuhn, S.L. 2017. Handaxe manufacture and re-sharpening throughout the Lower Paleolithic sequence of Tabun Cave. *Quaternary International* 428, 118–131.
- Solodenko, N., Zupancich, A., Cesaro, S.N., Marder, O., Lemorini, C., Barkai, R. 2015. Fat residue and use-wear found on Acheulian biface and scraper associated with butchered elephant remains at the site of Revadim, Israel. *PLoS One* 10, e0118572.
- Soressi, M., Hays, M.A. 2003. Manufacture, transport, and use of Mousterian bifaces: a case study from the Périgord (France). In *Multiple Approaches to the Study of Bifacial Technologies*, Soressi, M., Dibble, H.L. (eds.). University of Pennsylvania Museum of Archaeology and Anthropology, Philadelphia, pp. 125–148.
- Stekelis, M. 1956. Nouvelles fouilles dans la Grotte de Kebara. In *Cronica Del IV Congres Internacional de Ciencias Prehistoricas y Protohistoricas Madrid 1954*, Beltrán-Martínez, A. (ed.). Zaragoza, pp. 385–389.
- Stekelis, M. 1960. The Palaeolithic deposits of Jisr Banat Yaquob. *Bulletin of the Research Council of Israel* 9, 61–89.
- Stekelis, M., Gilead, D. 1966. Ma'ayan Barukh: a Lower Paleolithic site in Upper Galilee. *Journal of the Israel Prehistoric Society* 8, 1–23.
- Stout, D., Apel, J., Commander, J., Roberts, M. 2014. Late Acheulean technology and cognition at Boxgrove, UK. *Journal of Archaeological Science* 41, 576–590.
- Stout, D., Passingham, R., Frith, C., Apel, J., Chaminade, T. 2011. Technology, expertise and social cognition in human evolution: technology and cognition in human evolution. *European Journal of Neuroscience* 33, 1328–1338.
- Tchernov, E. (ed.). 1986. *Les mammifères du Pleistocène inférieur de la vallée du Jourdain à Oubeidiyeh*. Association Paleorient, Paris.
- Tixier, J., Inizan, M.L., Roche, H. 1980. *Préhistoire de la pierre taillée, I: terminologie et technologie*. Cercle de recherches et d'études préhistoriques, Antibes.
- Turville-Petre, F.A.J. 1927. *Researches in Prehistoric Galilee, 1925-1926*. British School of Archaeology in Jerusalem, London.
- Valladas, H., Mercier, N., Hershkovitz, I., Zaidner, Y., Tsatskin, A., Yeshurun, R., Vialettes, L., Joron, J.-L., Reyss, J.-L., Weinstein-Evron, M. 2013a. Dating the Lower to Middle Paleolithic transition in the Levant: a view from Misliya Cave, Mount Carmel, Israel. *Journal of Human Evolution* 65, 585–593.
- Weinstein-Evron, M., Beck, A., Ezersky, M. 2003. Geophysical investigations in the service of Mount Carmel (Israel) prehistoric research. *Journal of Archaeological Science* 30, 1331–1341.
- Zaidner, Y., Druck, D., Weinstein-Evron, M. 2006. Acheulo-Yabrudian handaxes from Misliya Cave, Mount Carmel, Israel. In *Axe Age: Acheulian Tool-Making from Quarry to Discard*, Goren-Inbar, N., Sharon, G. (eds.). Equinox, London, pp. 243–266.
- Zaidner, Y., Porat, N., Zilberman, E., Herzlinger, G., Almogi-Labin, A., Roskin, J. 2018. Geo-chronological context of the open-air Acheulian site at Nahal Hesi, northwestern Negev, Israel. *Quaternary International* 464, 18–31.
- Zaidner, Y., Weinstein-Evron, M., 2016. The end of the Lower Paleolithic in the Levant: the Acheulo-Yabrudian lithic technology at Misliya Cave, Israel. *Quaternary International* 409, 9–22.
- Zupancich, A., Shemer, M., Barkai, R. 2021. Biface use in the Lower Paleolithic Levant: first insights from late Acheulean Revadim and Jaljulia (Israel). *Journal of Archaeological Science: Reports* 36, 102877.
- Zupancich, A., Solodenko, N., Rosenberg-Yefet, T., Barkai,

R. 2018. On the function of Late Acheulean stone tools: new data from three specific archaeological contexts

at the Lower Palaeolithic site of Revadim, Israel. *Lithic Technology* 43, 255–268.

## APPENDIX 1

### Detailed description of the archaeological sites sampled for this study.

#### ‘UBEIDIYA

The site of ‘Ubeidiya (UB), located in the central Jordan Valley (see Figure 1, Table 1), is bedded in the geological ‘Ubeidiya Formation. It is a small sedimentary anticline, which was only partially exposed and studied, providing an archive of the 190m thick sedimentological record (Picard and Baida 1966). Over 80 discrete archaeological horizons were identified and described at the site, forming the earliest and the most extensive faunal, lithic, and paleoenvironmental record of the Acheulian Technocomplex in Israel. All the archaeological horizons at the site were assigned to the Early Acheulian (Bar-Yosef and Goren-Inbar 1993). Stekelis, Bar-Yosef, and Tchernov excavated the site from 1960 to 1974; from 1988 to 1994 excavations were carried out in association with a French team (Guérin et al. 1996). This was followed by a cooperation with a German team (Gaudzinski 1997–1999) and, finally, excavations were conducted in association with an American team (Shea 1988–1994).

There are no radiometric dates from the site or from the formation of ‘Ubeidiya and thus, its chronological assignment is primarily based on bio-chronological markers that allow comparisons between the faunal assemblages of ‘Ubeidiya and other known paleontological localities (Martínez-Navarro et al. 2009, 2012; Tchernov 1986, 1988), on some geological field- relationship with other formations (Bar-Yosef and Goren-Inbar, 1993; Picard and Baida 1966), and on several attempts to obtain a paleomagnetic record (Braun et al. 1991; Verosub and Tchernov 1991). The ‘Ubeidiya Formation provides evidence for a remarkable paleoclimatic and environmental changes along its depositional archive, yet most of the archaeological horizons occur in its drier members, particularly in that of Member Fi (Bar-Yosef and Goren-Inbar 1993; Bar-Yosef and Tchernov 1972; Feibel, 2004).

Artifacts are made on flint, basalt, and limestone, and include chopping tools, polyhedrons, spheroids, and bifaces, a toolkit resembling known assemblages from East African sites and hence providing evidence for one of the earliest out-of-Africa hominin’s sorties (Bar-Yosef and Goren-Inbar 1993).

#### GESHER BENOT YA’AQOV

The open-air waterlogged site of GBY has been known since the 1930’s. It is located in the southern Hula Valley, the northern Jordan Valley (see Figure 1, Table 1). The site, estimated to be ca. 3.5km long, was surveyed, tested, and

excavated by Garrod, Gilead and Stekelis. Renewed excavations took place between 1989 and 1997 on the left bank of the River Jordan and produced a wealth of geological, sedimentological, paleoclimatic, faunal, and floral data pertaining to the Lower and Middle Pleistocene and to MIS 18–20 (Goren-Inbar et al. 2018). The site, bedded in the Benot Ya’akov Formation, overlies a sequence of basalt and basanite flows whose top is dated by  $^{40}\text{Ar}/^{39}\text{Ar}$  to  $1,195\pm 0.67$  and  $1.137\pm 0.69$  Ma. In addition, the Matuyama-Brunhes boundary (MBB) (0.79 Ma) was identified in the sedimentary sequence of the site, which also includes an inter-fingering basalt flow north of the bridge, dated to  $659\pm 85$  ka (Proborukmi et al. 2018). Based on other sedimentological considerations, it is assumed that the 34m thick depositional sequence exposed at the excavations and characterized by repeated human occupations lasted for about 100 ka (Feibel 2004). A wealth of floral and faunal remains were found and identified, providing the means for a detailed reconstruction of the environment, which consisted of trees, bushes, climbers, and over 50 edible plants that constituted the Early – Middle Pleistocene Mediterranean flora (Goren-Inbar et al. 2002a, 2002b, 2015; Melamed et al. 2016). The faunal remains include a large array of species with an emphasis on medium and large mammals (Rabinovich and Biton 2011; Rabinovich et al. 2008, 2012), and on other exploitable vertebrate species (Biton et al. 2019; Zohar and Biton 2011; Zohar et al. 2014). All the above illustrate the particular habitats of the lake and its environs, as well as hominin behavioral patterns in the paleo-Hula Valley.

The entire lithic record at the site is assigned to the Acheulian Technocomplex (Goren-Inbar et al. 2018) and to the ‘Large Flake Acheulian’ tradition (LFA) (Sharon 2007). Three types of raw materials were used for the production of the artifacts—flint, limestone, and basalt, with bifaces (handaxes and cleavers) produced primarily on the last (Goren-Inbar et al. 2018). Currently, the GBY site with all its technological and typological similarities to African Acheulian sites is the only one of its kind known in the Levant. Gilead (1970a) assigned this assemblage to the Middle Acheulian.

#### MA’AYAN BARUKH

Ma’ayan Barukh (MB) is an open-air Acheulian site located in the northern part of the Hula Valley, on the gentle slopes descending to the center of the Hula Basin (see Figure 1, Table 1). It has been known since the 1920’s and was mentioned by several researchers (Guy 1924; Neuville 1931;

Stekelis and Gilead 1966; Turville-Petre 1927). Clusters of Acheulian artifacts were found in a *terra rossa* soil in an area of ca. 0.3km<sup>2</sup> with a maximal thickness of 50cm at an elevation of 250–275m above msl (Stekelis and Gilead 1966). The artifact layer overlies a series of travertines (Kfar Yuval travertines) (Picard 1963), which in turn overlie the Hasbani basalt (Sneh and Weinberger 2003) that is dated by K/Ar to 1.62–0.89 Ma (Mor 1993). The late Amnon Assaf, a member of Ma'ayan Barukh kibbutz collected the lithic artifacts for many years. The major part of the collections have been curated and stored in the Upper Galilee Museum of Prehistory (Ma'ayan Barukh), and a part of this assemblage (ca. 300 artifacts) is stored in the Department of Prehistory, The Hebrew University of Jerusalem.

An additional collection was made in 1974 from two trenches (one natural, the other artificial) at the north-western fringes of the site. This collection resulted in a few additional artifacts (mainly bifaces, and a few bones [Ronen et al. 1980]).

Thousands of handaxes, very few cleavers, tools, and waste products characterize the assemblage (Ronen et al. 1980; Stekelis and Gilead 1966). Some 300 artifacts, mainly handaxes, were analyzed by Stekelis and Gilead (1966) and the sample analyzed here is a subset of this collection (see Table 1). Of the thousands of flint artifacts, only seven basalt handaxes were identified (Rosenberg et al. 2015). Several attempts were made to provide better stratigraphic and chronological indications for the assemblage (Horowitz 2001; Lister et al. 2013; Schwarcz et al. 1980). These include the cleaning and sampling of the two small trenches (Ronen et al. 1980) and an attempt to obtain radiometric dates from carbonates adhering to tools (Schwarcz et al. 1980). Following Gilad's (1970a) scheme, this assemblage was assigned to a sub-group of the Late Acheulian.

### HOLON

The Acheulian site of Holon, located in the central coastal plain (currently the city of Holon), was excavated during 1963–1964 and 1967 by Yizraeli (1963, 1967; Chazan and Horwitz 2007; Noy and Isaac 1971) (see Figure 1, Table 1). The artifacts and faunal remains were bedded in a layer of light gray clay (layer C), attaining a vertical dispersion of 60cm. The fauna includes fallow deer, red deer, aurochs, mountain gazelle, wild boar, straight-tusked elephant, hippopotamus, and marsh turtles (Davies and Lister 2007; Hartman and Horwitz 2007; Horwitz and Monchot 2007; Lister 2007; Monchot and Horwitz 2007). Several attempts to date the site include OSL dates, which were obtained from the excavations and from a nearby test pit whose stratigraphy was associated with the archaeological horizon excavated by Noy (Porat, 2007; Porat et al. 1999, 2002). The results produced ages around 200 ka. Malinsky-Buller (2014, 2016) doubts the validity of the correlation between the test pit and the excavation. He disputes the age obtained for the site using stratigraphic data from further trenching that was done in 2006. He also summarizes the opposition of others to the validity of the dates, which are considered to be too young for the Acheulian assemblage (Malinsky-

Buller 2014, 2016).

During two field seasons some 2948 flint artifacts were found, comprising among other tool types an abundant handaxe component (N=107) (Chazan and Horwitz, 2007; Malinsky-Buller, 2014, 2016; Noy and Isaac, 1971; Yizraeli 1963, 1967). These were assigned by Gilead (1970a) to the Late Acheulian.

### NAHAL HESI

The open-air site of Nahal Hesi (NH) is located in the southern coastal plain, on the eastern bank of Nahal Shikma (see Figure 1). It was excavated during 1971 and 1973 by D. Gilead, and later by Goren-Inbar and Zaidner as part of a field school conducted by the Institute of Archaeology of the Hebrew University (Zaidner et al. 2018) (see Figure 1, Table 1). Faunal remains include equids, *Bos*, and gazelle (Davis 1980; Yeshurun et al. 2011). Faunal remains and lithic artifacts were found in a grey clay unit some 35cm thick, which had a marshy character. The combined TT-OSL and pIR-IR290 methods provide an average of 430±35 ka for the Acheulian layer (Zaidner et al. 2018). During the field work of the later excavation, 129 flint and limestone artifacts were found, including 7 handaxes. The lithic assemblage was assigned by Gilead (1970a) to the Late Acheulian.

### REFERENCES

- Bar-Yosef, O., Goren-Inbar, N. 1993. *The Lithic Assemblage of Ubeidiya. A Lower Paleolithic Site in the Jordan Valley*. Qedem, Jerusalem.
- Bar-Yosef, O., Tchernov, E. 1972. *On the Paleo-Ecological History of the Site of 'Ubeidiya*. Israel Academy of Sciences and Humanities.
- Biton, R., Bailon, S., Goren-Inbar, N., Sharon, G., Rabinovich, R. 2019. Pleistocene amphibians and squamates from the Upper Jordan Rift Valley, Gesher Benot Ya'aqov and Nahal Mahanayem Outlet (MIS 20–18 and MIS 4/3). *Quaternary Research* 91, 345–366.
- Braun, D., Ron, H., Marco, S. 1991. Magnetostratigraphy of the hominid tool-bearing Erk el Ahmar Formation in the northern Dead Sea Rift. *Israel Journal of Earth-Sciences* 40, 191–197.
- Chazan, M., Horwitz, L.K. (eds.). 2007. *Holon: A Lower Paleolithic Site in Israel*. Bulletin / American School of Prehistoric Research. Peabody Museum of Archaeology and Ethnology, Harvard University, Cambridge.
- Davies, P., Lister, A. 2007. Palaeoecology. In *Holon: A Lower Paleolithic Site in Israel*, Chazan, M., Horwitz, L.K. (eds.). Bulletin / American School of Prehistoric Research. Peabody Museum of Archaeology and Ethnology, Harvard University, Cambridge, pp. 123–132.
- Davis, S.J. 1980. Late Pleistocene and Holocene equid remains from Israel. *Zoological Journal of the Linnean Society* 70, 289–312.
- Feibel, C.S. 2004. Quaternary lake margins of the Levant Rift Valley. In *Human Paleoecology in the Levantine Corridor*, Speth, J.D., Goren-Inbar, N. (eds.). Oxbow Books, Oxford, pp. 21–36.
- Gilead, D. 1970. Handaxe industries in Israel and the Near

- East. *World Archaeology* 2, 1–11.
- Goren-Inbar, N., Alpersen-Afil, N., Sharon, G., Herzlinger, G. 2018. *The Acheulian Site of Gesher Benot Ya'aqov* Volume IV: *The Lithic Assemblages*. Vertebrate Paleobiology and Paleoanthropology. Springer International Publishing, Cham.
- Goren-Inbar, N., Sharon, G., Alpersen-Afil, N., Herzlinger, G. 2015. A new type of anvil in the Acheulian of Gesher Benot Ya'aqov, Israel. *Philosophical Transactions of the Royal Society B: Biological Sciences* 370, 20140353.
- Goren-Inbar, N., Sharon, G., Melamed, Y., Kislev, M. 2002a. Nuts, nut cracking, and pitted stones at Gesher Benot Ya'aqov, Israel. *Proceedings of the National Academy of Sciences* 99, 2455–2460.
- Goren-Inbar, N., Werker, E., Feibel, C.S., 2002b. *The Acheulian Site of Gesher Benot Ya'aqov, Israel. The Wood Assemblage*. Oxbow Books, Oxford.
- Guérin, C., Bar-Yosef, O., Debard, E., Faure, M., Shea, J., Tchernov, E. 1996. Mission archéologique et paléontologique dans le Pléistocène ancien d'Oubéidiyeh (Israël) : résultats 1992-1994. *Comptes rendus de l'Académie des sciences, Série 2, Sciences de la terre et des planètes* 322, 709–712.
- Guy, P.L. 1924. Prehistoric and other remains in the Huleh Basin. *Bulletin of the British School of Archaeology in Jerusalem* 6, 77.
- Hartman, G., Horwitz, L.K. 2007. Remains of fresh-water turtles. In *Holon: A Lower Paleolithic Site in Israel*, Chazan, M., Horwitz, L.K. (eds.). Bulletin / American School of Prehistoric Research. Peabody Museum of Archaeology and Ethnology, Harvard University, Cambridge, pp. 89–91.
- Horowitz, A. 2001. *The Jordan Rift Valley*. Balkema, Lisse.
- Horwitz, L.K., Monchot, H. 2007. *Sus, Hippopotamus, Bos and Gazella*. In *Holon: A Lower Paleolithic Site in Israel*, Chazan, M., Horwitz, L.K. (eds.). Bulletin / American School of Prehistoric Research. Peabody Museum of Archaeology and Ethnology, Harvard University, Cambridge, pp. 91–110.
- Lister, A. 2007. Cervidae. In *Holon: A Lower Paleolithic Site in Israel*, Chazan, M., Horwitz, L.K. (eds.). Bulletin / American School of Prehistoric Research. Peabody Museum of Archaeology and Ethnology, Harvard University, Cambridge, pp. 111–122.
- Lister, A., Dirks, W., Assaf, A., Chazan, M., Goldberg, P., Applbaum, Y.H., Greenbaum, N., Horwitz, L.K. 2013. New fossil remains of *Elephas* from the southern Levant: implications for the evolutionary history of the Asian elephant. *Palaeogeography, Palaeoclimatology, Palaeoecology* 386, 119–130.
- Malinsky-Buller, A. 2014. Contextualizing curatorial strategies at the Late Lower Paleolithic site of Holon, Israel. *PaleoAnthropology* 2014, 483–504.
- Malinsky-Buller, A. 2016. The muddle in the Middle Pleistocene: the Lower–Middle Paleolithic transition from the Levantine perspective. *Journal of World Prehistory* 29, 1–78.
- Martínez-Navarro, B., Belmaker, M., Bar-Yosef, O. 2009. The large carnivores from 'Ubeidiya (early Pleistocene, Israel): biochronological and biogeographical implications. *Journal of Human Evolution* 56, 514–524.
- Martínez-Navarro, B., Belmaker, M., Bar-Yosef, O. 2012. The Bovid assemblage (Bovidae, Mammalia) from the Early Pleistocene site of 'Ubeidiya, Israel: biochronological and paleoecological implications for the fossil and lithic bearing strata. *Quaternary International* 267, 78–97.
- Melamed, Y., Kislev, M.E., Geffen, E., Lev-Yadun, S., Goren-Inbar, N. 2016. The plant component of an Acheulian diet at Gesher Benot Ya'aqov, Israel. *Proceedings of the National Academy of Sciences USA* 113, 14674–14679.
- Monchot, H., Horwitz, L.K. 2007. Taxon representation and age and sex distribution. In *Holon: A Lower Paleolithic Site in Israel*, Chazan, M., Horwitz, L.K. (eds.). Bulletin / American School of Prehistoric Research. Peabody Museum of Archaeology and Ethnology, Harvard University, Cambridge, pp. 85–88.
- Mor, D. 1993. A time-table for the Levant volcanic province, according to K-Ar dating in the Golan Heights, Israel. *Journal of African Earth Sciences (and the Middle East)* 16, 223–234.
- Neuville, R. 1931. L'Acheuléen supérieur de la grotte d'Oumm-Qatafa (Palestine). *L'Anthropologie* 41, 253–263.
- Noy, T., Isaac, A. 1971. Holon. *Revue Biblique* 78, 581–582.
- Picard, L. 1963. The Quaternary in the Northern Jordan Valley. *Proceedings of the Israel Academy of Science and Humanities* 1, 1–34.
- Picard, L., Baida, U. 1966. Stratigraphic position of the Ubeidiya Formation. *Proceedings of the Israel Academy of Science and Humanities* 4, 1–39.
- Porat, N. 2007. Luminescence and electron spin resonance dating. In *Holon: A Lower Paleolithic Site in Israel*, Chazan, M., Horwitz, L.K. (eds.). Bulletin / American School of Prehistoric Research. Peabody Museum of Archaeology and Ethnology, Harvard University, Cambridge, pp. 27–42.
- Porat, N., Chazan, M., Schwarcz, H., Horwitz, L.K. 2002. Timing of the Lower to Middle Paleolithic boundary: new dates from the Levant. *Journal of Human Evolution* 43, 107–122.
- Porat, N., Zhou, L.P., Chazan, M., Noy, T., Horwitz, L.K. 1999. Dating the Lower Paleolithic open-air site of Holon, Israel by luminescence and ESR techniques. *Quaternary Research* 51, 328–341.
- Proborukmi, M.S., Urban, B., Mischke, S., Mienis, H.K., Melamed, Y., Dupont-Nivet, G., Jourdan, F., Goren-Inbar, N. 2018. Evidence for climatic changes around the Matuyama-Brunhes Boundary (MBB) inferred from a multi-proxy palaeoenvironmental study of the GBY#2 core, Jordan River Valley, Israel. *Palaeogeography, Palaeoclimatology, Palaeoecology* 489, 166–185.
- Rabinovich, R., Biton, R. 2011. The Early–Middle Pleistocene faunal assemblages of Gesher Benot Ya'aqov: inter-site variability. *Journal of Human Evolution* 60, 357–374.

- Rabinovich, R., Gaudzinski-Windheuser, S., Goren-Inbar, N. 2008. Systematic butchering of fallow deer (*Dama*) at the early middle Pleistocene Acheulian site of Gesher Benot Ya'aqov (Israel). *Journal of Human Evolution* 54, 134–149.
- Rabinovich, R., Gaudzinski-Windheuser, S., Kindler, L., Goren-Inbar, N. 2012. *The Acheulian Site of Gesher Benot Ya'aqov*, Volume III: *Mammalian Taphonomy. The Assemblages of Layers V-5 and V-6*. Springer, Dordrecht.
- Ronen, A., Ohel, M.Y., Lamdan, M., Assaf, A. 1980. Acheulian artifacts from two trenches at Ma'ayan Barukh. *Israel Exploration Journal* 30, 17–33.
- Rosenberg, D., Shimelmitz, R., Gluhak, T.M., Assaf, A. 2015. The geochemistry of basalt handaxes from the Lower Palaeolithic Site of Ma'ayan Baruch, Israel—A perspective on raw material selection: basalt handaxes from Ma'ayan Baruch, Israel. *Archaeometry* 57, 1–19.
- Schwarcz, H.P., Goldberg, P., Blackwell, B. 1980. Uranium series dating of archaeological sites in Israel. *Israel Journal of Earth Sciences* 29, 157–165.
- Sharon, G. 2007. Acheulian Large Flake Industries: Technology, Chronology, and Significance. British Archaeological Reports International Series 1701, Oxford.
- Sneh, A., Weinberger, R. 2003. Geology of the Metulla quadrangle, northern Israel: implications for the offset along the Dead Sea Rift. *Israel Journal of Earth Sciences* 52, 123–138.
- Stekelis, M., Gilead, D. 1966. Ma'ayan Barukh: a Lower Palaeolithic Site in Upper Galilee. *Mitekufat Haeven: Journal of the Israel Prehistoric Society* 8, 1–23.
- Tchernov, E. (ed.). 1986. *Les mammifères du Pleistocène inférieur de la vallée du Jourdain à Oubeidiyeh*. Association Paléorient, Paris.
- Tchernov, E. 1988. La biochronologie du site de Ubeidiya (vallée du Jourdain) et les plus anciens hominidés du Levant. *L'Anthropologie* 92, 839–861.
- Turville-Petre, F.A.J. 1927. *Researches in Prehistoric Galilee, 1925-1926*. British School of Archaeology in Jerusalem, London.
- Verosub, K.L., Tchernov, E. 1991. Résultats préliminaires de l'étude magnétostratigraphique d'une séquence sédimentaire à industrie humaine en Israël. In *Les premiers Européens: actes du 114e Congrès National des Sociétés Savantes (Paris, 3-9 avril 1989)*, Bonifay, E., Vandermeersch, B., Frankreich, Congrès National des Sociétés Savantes (eds.). Editions du CTHS, Paris, pp. 237–242.
- Yeshurun, R., Zaidner, Y., Eisenmann, V., Martínez-Navarro, B., Bar-Oz, G. 2011. Lower Paleolithic hominin ecology at the fringe of the desert: faunal remains from Bizat Ruhama and Nahal Hesi, Northern Negev, Israel. *Journal of Human Evolution* 60, 492–507.
- Yizraeli, T. 1963. Holon. *Israel Exploration Journal* 13, 137.
- Yizraeli, T. 1967. A Lower Palaeolithic site at Holon: preliminary report. *Israel Exploration Journal* 17, 144–152.
- Zaidner, Y., Porat, N., Zilberman, E., Herzlinger, G., Almogi-Labin, A., Roskin, J., 2018. Geo-chronological context of the open-air Acheulian site at Nahal Hesi, northwestern Negev, Israel. *Quaternary International* 464, 18–31.
- Zohar, I., Biton, R. 2011. Land, lake, and fish: investigation of fish remains from Gesher Benot Ya'aqov (paleo-Lake Hula). *Journal of Human Evolution* 60, 343–356.
- Zohar, I., Goren, M., Goren-Inbar, N. 2014. Fish and ancient lakes in the Dead Sea Rift: the use of fish remains to reconstruct the ichthyofauna of paleo-Lake Hula. *Palaeogeography, Palaeoclimatology, Palaeoecology* 405, 28–41.

**APPENDIX 2**  
**Comparison of morphometric variables for samples including and excluding broken artifacts..**

**APPENDIX 2 TABLE 01.**

Site		Excluding broken	All artifacts	Difference	Wilcoxon Rank-sum p
<b>Holon</b>	N	69	93	24	
	Within-group shape variability	9.31	9.58	-0.27	0.48
	Volume	117460	120678	-3219	0.8
	Deviation form bilateral symmetry	6.01	6.07	-0.06	0.86
	Deviation from bifacial symmetry	5.61	5.43	0.18	0.83
	L curvature	1.01	0.96	0.05	0.77
	R curvature	0.92	0.93	-0.01	0.91
	L planform irregularity	99.09	100.43	-1.34	0.84
	R planform Irregularity	101.16	100.93	0.23	0.92
	L section irregularity	99.84	100.87	-1.03	0.94
	R section irregularity	88.99	92.48	-3.49	0.63
<b>MB</b>	N	61	80	19	
	Within-group shape variability	7.78	7.69	0.09	0.91
	Volume	114661	122386	-7725	0.51
	Deviation form bilateral symmetry	4.94	5.03	-0.09	0.77
	Deviation from bifacial symmetry	4.74	4.74	-0.01	0.87
	L curvature	1.00	0.96	0.03	0.64
	R curvature	1.08	1.05	0.03	0.7
	L planform irregularity	73.86	78.15	-4.29	0.49
	R planform Irregularity	83.68	87.15	-3.47	0.58
	L section irregularity	79.94	79.62	0.32	0.84
	R section irregularity	84.27	85.04	-0.76	0.96

APPENDIX 2 TABLE 01 (continued).

Site		Excluding broken	All artifacts	Difference	Wilcoxon Rank-sum p
NH	N	5	19	14	
	Within-group shape variability	7.13	9.47	-2.34	0.02
	Volume	63985	77997	-14012	0.75
	Deviation from bilateral symmetry	3.35	5.29	-1.95	0.14
	Deviation from bifacial symmetry	3.98	4.84	-0.86	0.64
	L curvature	1.04	0.96	0.07	0.48
	R curvature	0.84	1.02	-0.18	0.43
	L planform irregularity	76.41	99.85	-23.44	0.55
	R planform irregularity	58.21	83.37	-25.15	0.27
	L section irregularity	94.21	87.11	7.11	0.55
	R section irregularity	72.38	94.83	-22.45	0.3
UB	N	112	150	38	
	Within-group shape variability	11.09	11.07	0.02	0.99
	Volume	301272	303715	-2443	0.86
	Deviation from bilateral symmetry	10.50	10.58	-0.09	0.67
	Deviation from bifacial symmetry	9.72	9.77	-0.06	0.77
	L curvature	0.61	0.59	0.02	0.69
	R curvature	0.61	0.59	0.01	0.7
	L planform irregularity	143.47	139.29	4.18	0.62
	R planform Irregularity	139.01	143.34	-4.33	0.7
	L section irregularity	206.03	204.01	2.02	0.92
	R section irregularity	207.56	208.66	-1.10	0.91

### APPENDIX 3

#### Detailed description of technological attributes.

Below are the details regarding each technological attribute used in this study.

**Raw material** – A nominal qualitative variable that describes the raw material from which the artifacts are made. The attribute can be assigned the following values: flint, limestone, basalt.

**Blank type** – A nominal qualitative variable that describes the type of blank on which the handaxe was modified. The attribute can be assigned the following values: 1) flake – items with a clearly identifiable ventral face; 2) chunk – items which are not produced on flakes. That is, they do not have a clearly identifiable ventral face and may retain some of the original unmodified tabular or nodular morphology; 3) indeterminate – items whose blank type cannot be clearly identified.

**Cortex** – An ordinal qualitative variable that describes the proportion of the artifact's surface area that is covered by cortex. It ranges from no cortex to over 75% coverage in 25% intervals and also includes a value of indeterminate for cases in which cortex cannot be clearly identified.

**Total number of scars** – a continuous quantitative variable that describes the number of negative flake scars over 2mm in maximal dimension on both faces of the artifacts.

**Proximal retouch** – a nominal qualitative variable that describes whether retouch exists on the dorsal, ventral, or both faces of the proximal end of the handaxe. This attribute was recorded only for Late Acheulian assemblages.

**Percussive technique** – a nominal qualitative variable that describes the physical properties of the hammer used to modify the tool. The classification is based on morphological aspects of the scars consisting of their size, flatness, and concavity. The attribute can be assigned the following values: 1) hard hammer – items which were modified exclusively with a hammer made of hard stone such as basalt or flint; 2) soft hammer – items which were modified exclusively with a hammer made of soft stone such as limestone or organic material such as antler or wood; 3) combined – items which were modified using both hard and soft hammers. This attribute was recorded only for Late Acheulian assemblages.

**Total number of hinges** – a continuous quantitative variable that describes the number of negative flake scars over 2mm in maximal dimension that exhibit a hinge termination. This attribute was recorded only for Late Acheulian assemblages.

### APPENDIX 4

#### Nominal logistic fit model for blank type.

In light of the significant effects found between numerous morphological attributes and the type of blank a model was designed to predict blank types of artifacts with indeterminate blanks.

Given the nominal nature of the dependent variable and the continuous nature of most independent variables, a nominal logistic fit model was selected. Due to the strong effect of raw material differences on the morphological attributes and the low number of observations, limestone artifacts were not included in the model and no prediction was provided for them. The remaining sample, consisting of all artifacts of known blank, were randomly divided according to raw materials and blank types into a training and validation sets. The validation set consisted of 41 (37%) basalt flakes, 6 (33%) basalt chunks, 4 (33%) flint flakes, and 11 (31%) flint chunks.

The dependent variable was the blank type. The independent variables initially consisted of all morphological attributes that were found to be significantly affected by the blank type. These included the shape variability, volume, bilateral and bifacial symmetries, edge curvature and section irregularity, and the shape trends described by PCs 2 and 4. In addition, the raw material was also used as an independent variable. Next, variables were gradually removed in a stepwise manner with the intention of minimizing the misclassification rate in the validation set while maximizing the number of variables scoring significant results on their likelihood ratio test. The remaining variables consisted of raw material, PC2, bifacial symmetry, and section irregularity. The statistical details of the model are provided below.

**NOMINAL LOGISTIC FIT FOR BLANK TYPE 2.**

**Effect Summary**

Source	LogWorth	PValue
Raw material	10.089	0.00000
PC02	3.158	0.00070
Deviation from bifacial symmetry	1.370	0.04264
Total section irregularity	0.873	0.13389

Converged in Gradient, 21 iterations.

**WHOLE MODEL TEST**

Model	-LogLikelihood	DF	ChiSquare	Prob>ChiSq
Difference	44.629834	8	89.25967	<.0001*
Full	32.580819			
Reduced	77.210653			
RSquare (U)		0.5780		
AICc		87.1085		
BIC		113.364		
Observations (or Sum Wgts)		124		

**FIT DETAILS**

Measure	Training	Validation	Test	Definition
Entropy RSquare	0.5780	0.4889		. 1-Loglike(model)/Loglike(0)
Generalized RSquare	0.7206	0.6323		. (1-(L(0)/L(model))^(2/n))/(1-L(0)^(2/n))
Mean -Log p	0.2627	0.3003	22.530	$\sum -\text{Log}(q[j])/n$
RMSE	0.2924	0.3035	1.0000	$\sqrt{\sum (y[j]-q[j])^2/n}$
Mean Abs Dev	0.1665	0.1738	1.0000	$\sum  y[j]-q[j] /n$
Misclassification Rate	0.1210	0.1176	1.0000	$\sum (q[j] \neq q_{\text{Max}})/n$
N	124	51	230	n

**LACK OF FIT**

Source	DF	- LogLikelihood	ChiSquare	Prob>ChiSq
Lack Of Fit	238	32.580819	65.16164	
Saturated	246	0.000000		
Fitted	8	32.580819	1.0000	

## PARAMETER ESTIMATES

Term		Estimate	Std Error	ChiSquare	Prob>ChiSq
Intercept	Unstable	21.4691264	28263.772	0.00	0.9994
Raw material [flint]		-1.0397268	9959.7833	0.00	0.9999
Deviation from bifacial symmetry		0.11512218	2721.4737	0.00	1.0000
PC02		0.18363509	2990.4873	0.00	1.0000
Total section irregularity		-0.0057739	200.46384	0.00	1.0000
Intercept	Unstable	21.1206432	28263.772	0.00	0.9994
Raw material [flint]		1.36287593	9959.7833	0.00	0.9999
Deviation from bifacial symmetry		-0.1405856	2721.4737	0.00	1.0000
PC02		-0.2362279	2990.4873	0.00	0.9999
Total section irregularity		0.00876068	200.46384	0.00	1.0000

For log odds of Flake/Indeterminate, Chunk/Indeterminate

## EFFECT LIKELIHOOD RATIO TESTS

Source	Nparm	DF	L-R ChiSquare	Prob>ChiSq
Raw material	2	2	46.4635483	<.0001*
Deviation from bifacial symmetry	2	2	6.30996871	0.0426*
PC02	2	2	14.5418278	0.0007*
Total section irregularity	2	2	4.02148752	0.1339

## CONFUSION MATRIX

## Training

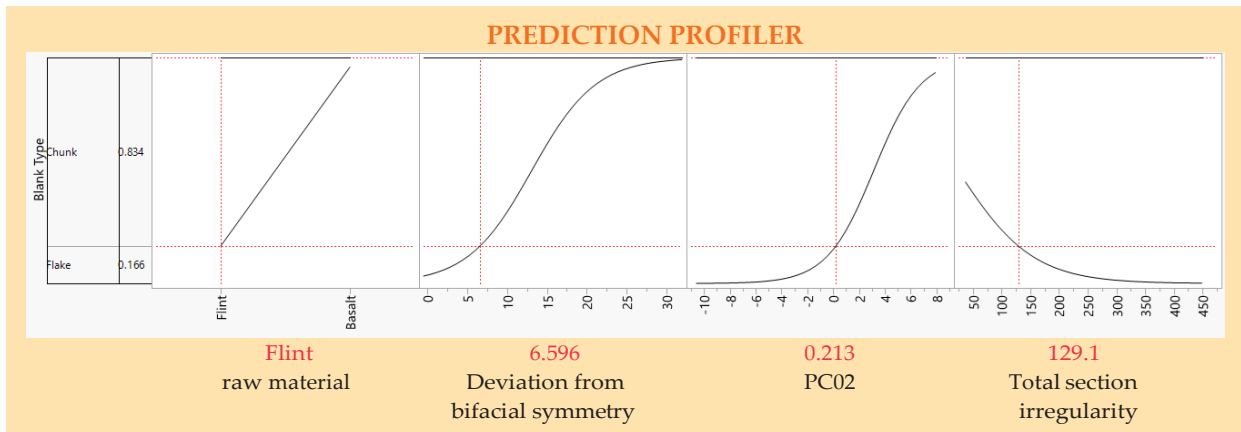
Actual	Predicted Count		
	Flake	Chunk	Indeterminate
Blank Type 2			
Flake	77	8	0
Chunk	7	32	0
Indeterminate	0	0	0

## Validation

Actual	Predicted Count		
	Flake	Chunk	Indeterminate
Blank Type 2			
Flake	33	4	0
Chunk	2	12	0
Indeterminate	0	0	0

## Test

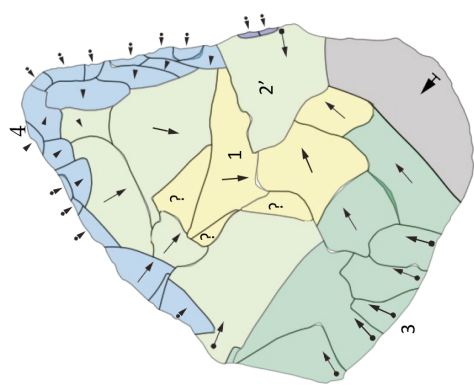
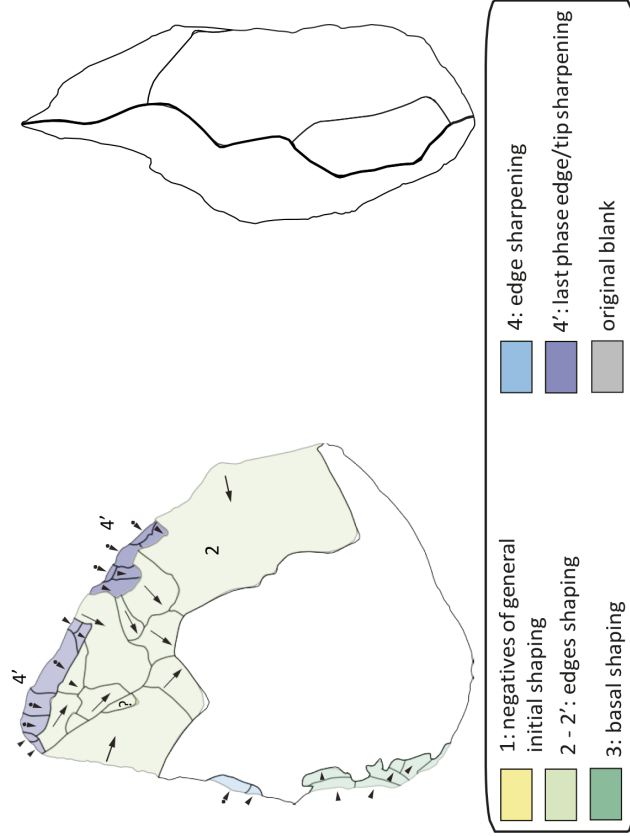
Actual	Predicted Count		
	Flake	Chunk	Indeterminate
Blank Type 2			
Flake	0	0	0
Chunk	0	0	0
Indeterminate	76	154	0



**APPENDIX 5**

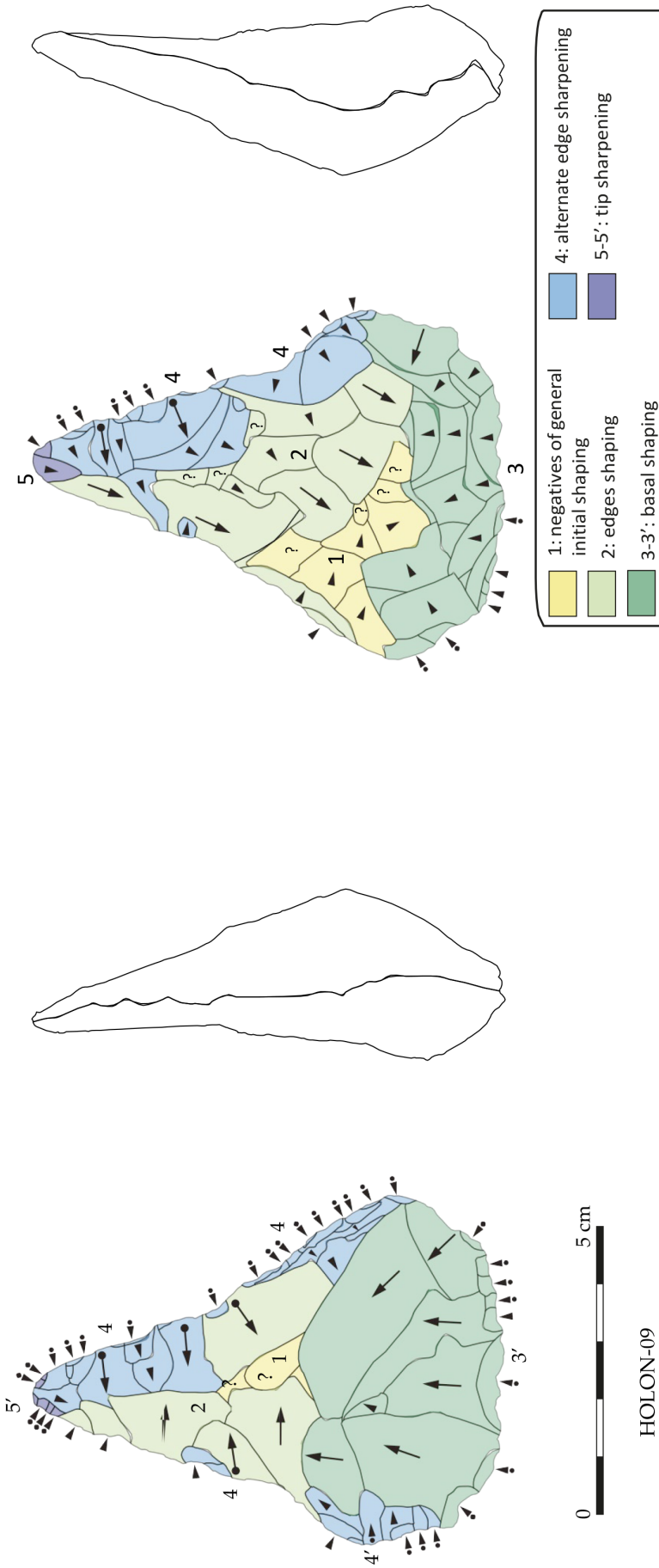
Diacritic diagrams of artifacts sampled from the assemblages of Holon, Ma'ayan Barukh, and Nahal Hesi.

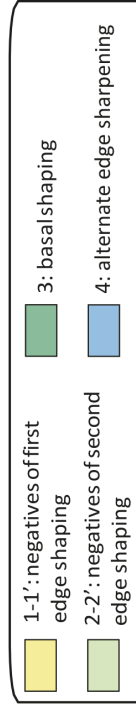
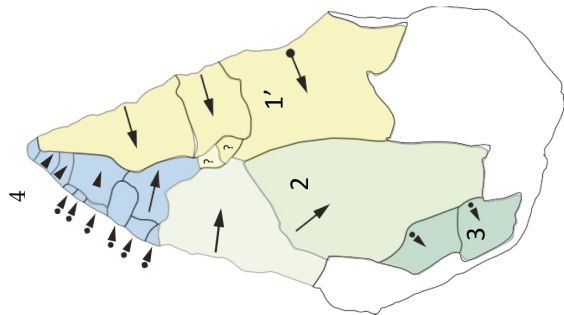
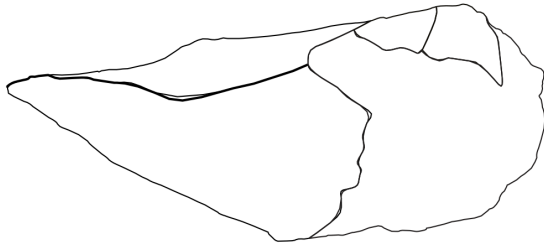
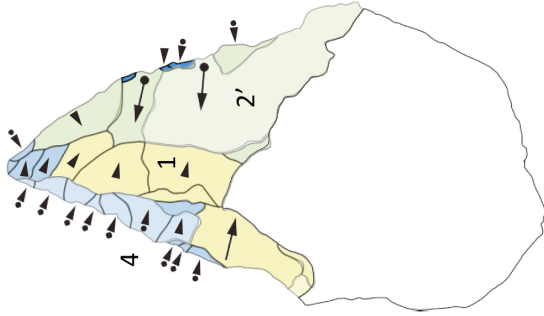
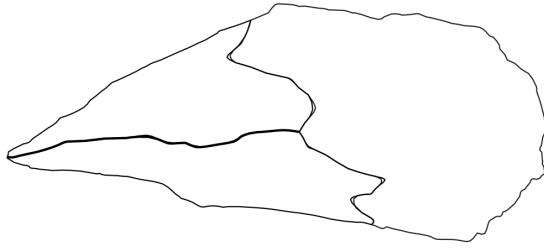
Item	Page
HOL-06	60
HOL-09	61
HOL-14	62
HOL-16	63
HOL-33	64
HOL-43	65
HOL-57	66
HOL-68	67
HOL-70	68
HOL-87	69
MB-35	70
MB-36	71
MB-56	72
MB-59	73
MB-61	74
MB-63	75
MB-67	76
MB-68	77
MB-70	78
MB-71	79
MB-80	80
NH-2-39-1	81
NH-2-39-5	82
NH-2-39-11	83
NH-2-40-2	84



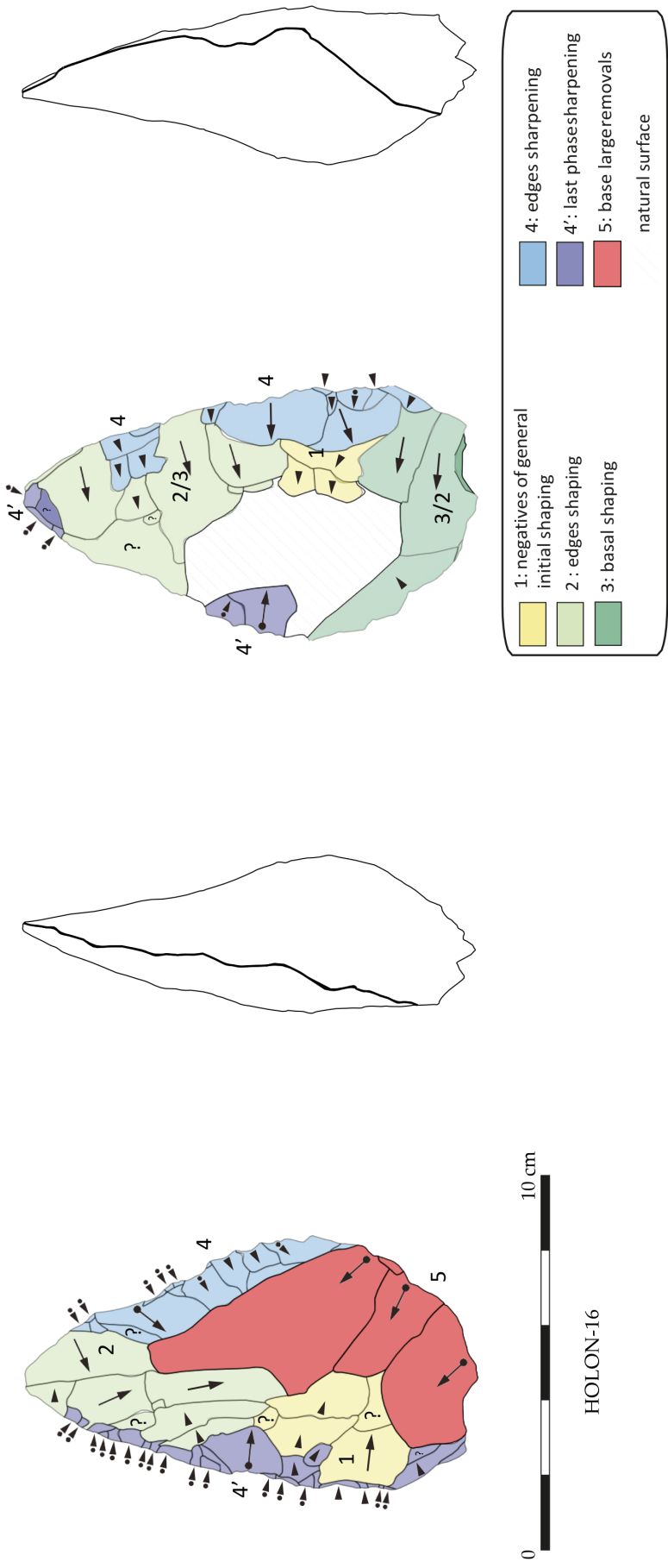
0 5 cm

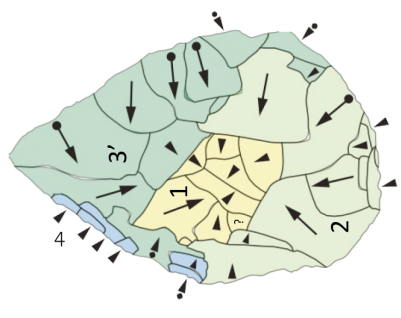
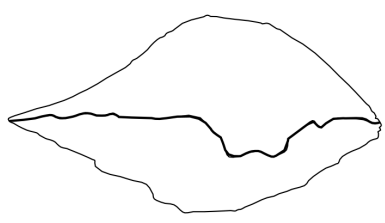
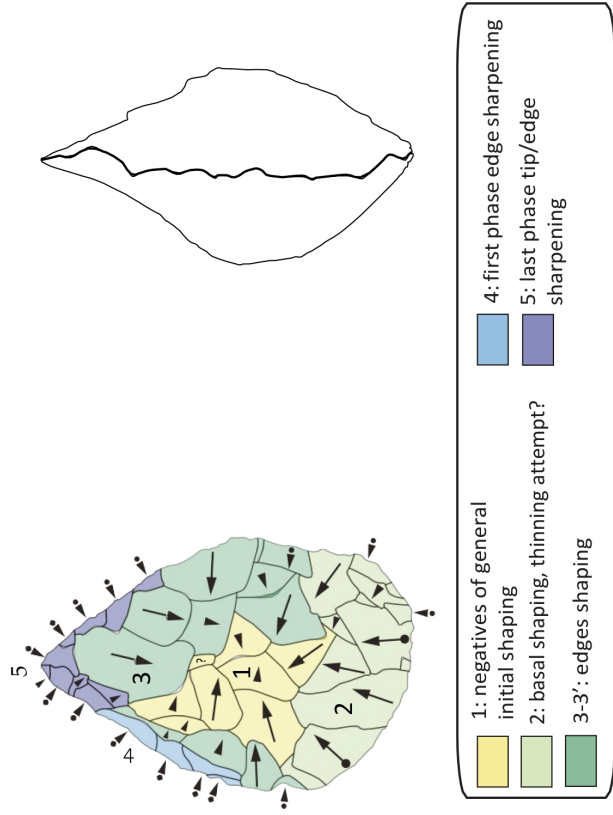
HOLON-06





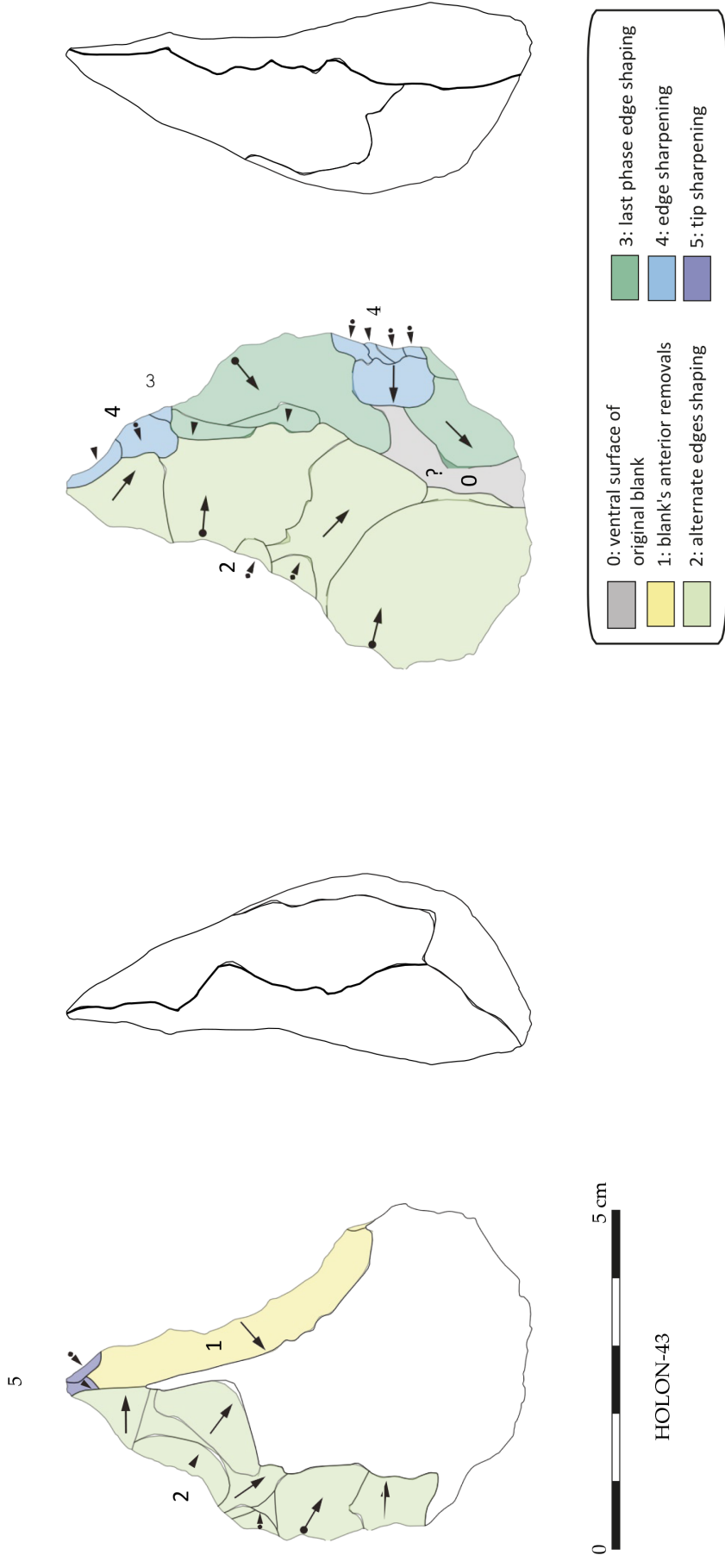
HOLON-14

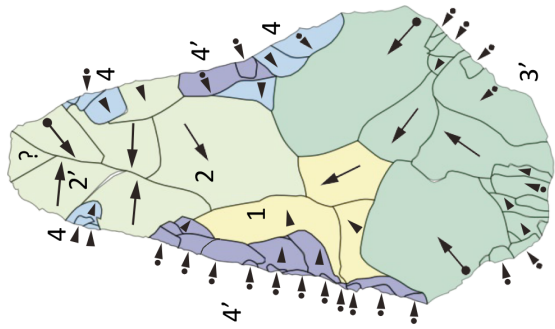
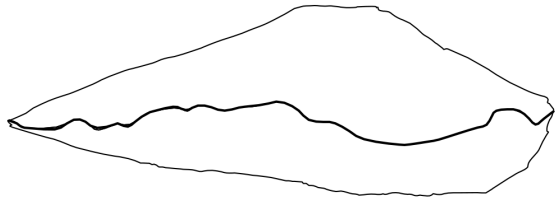
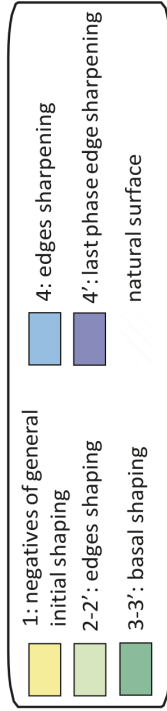
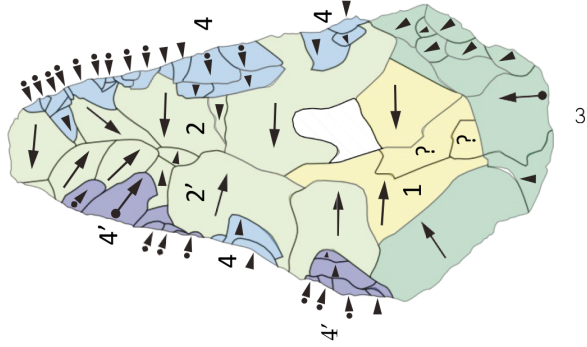
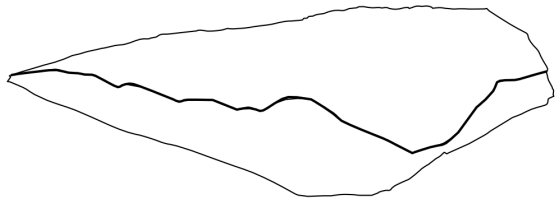




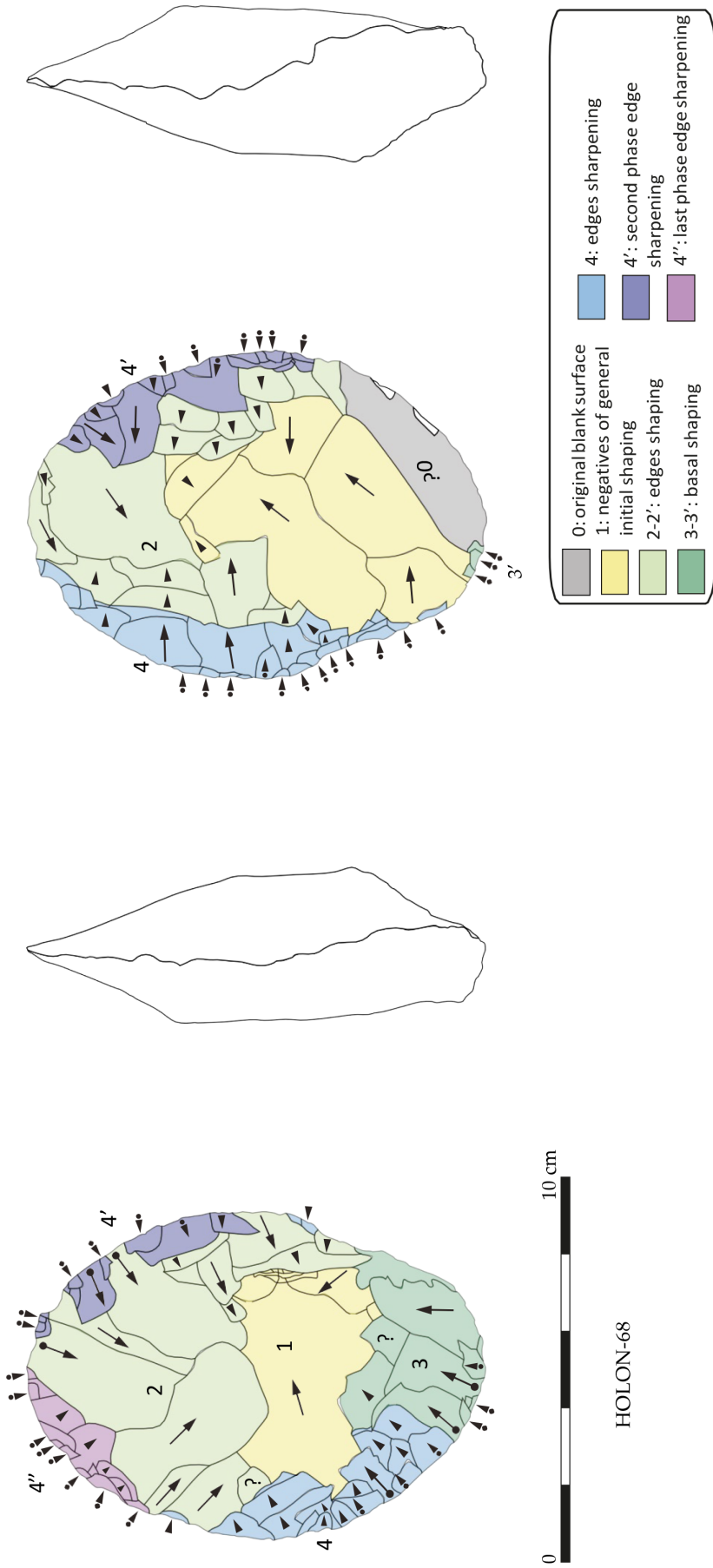
0 5 cm

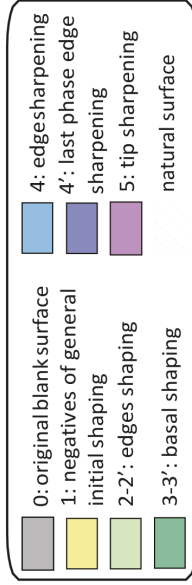
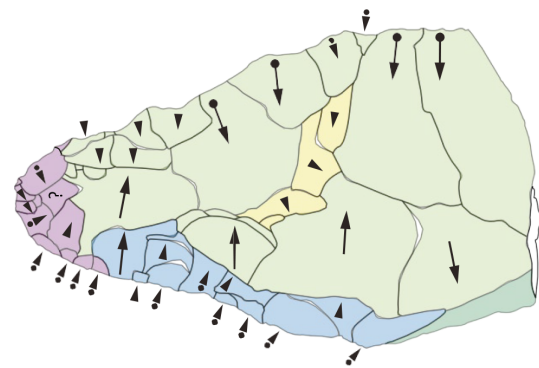
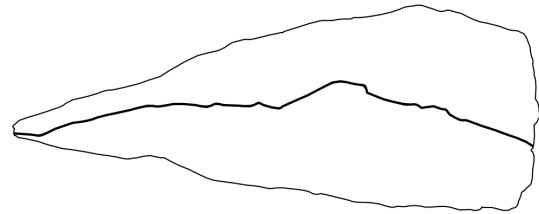
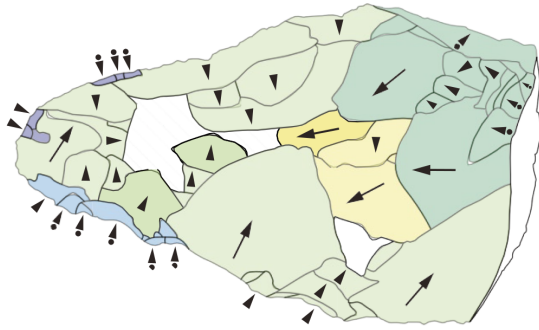
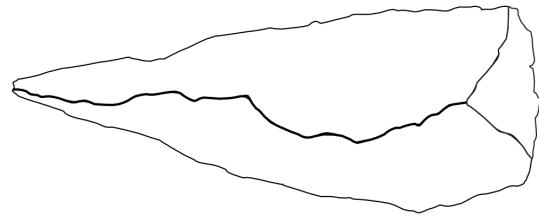
HOLON-33





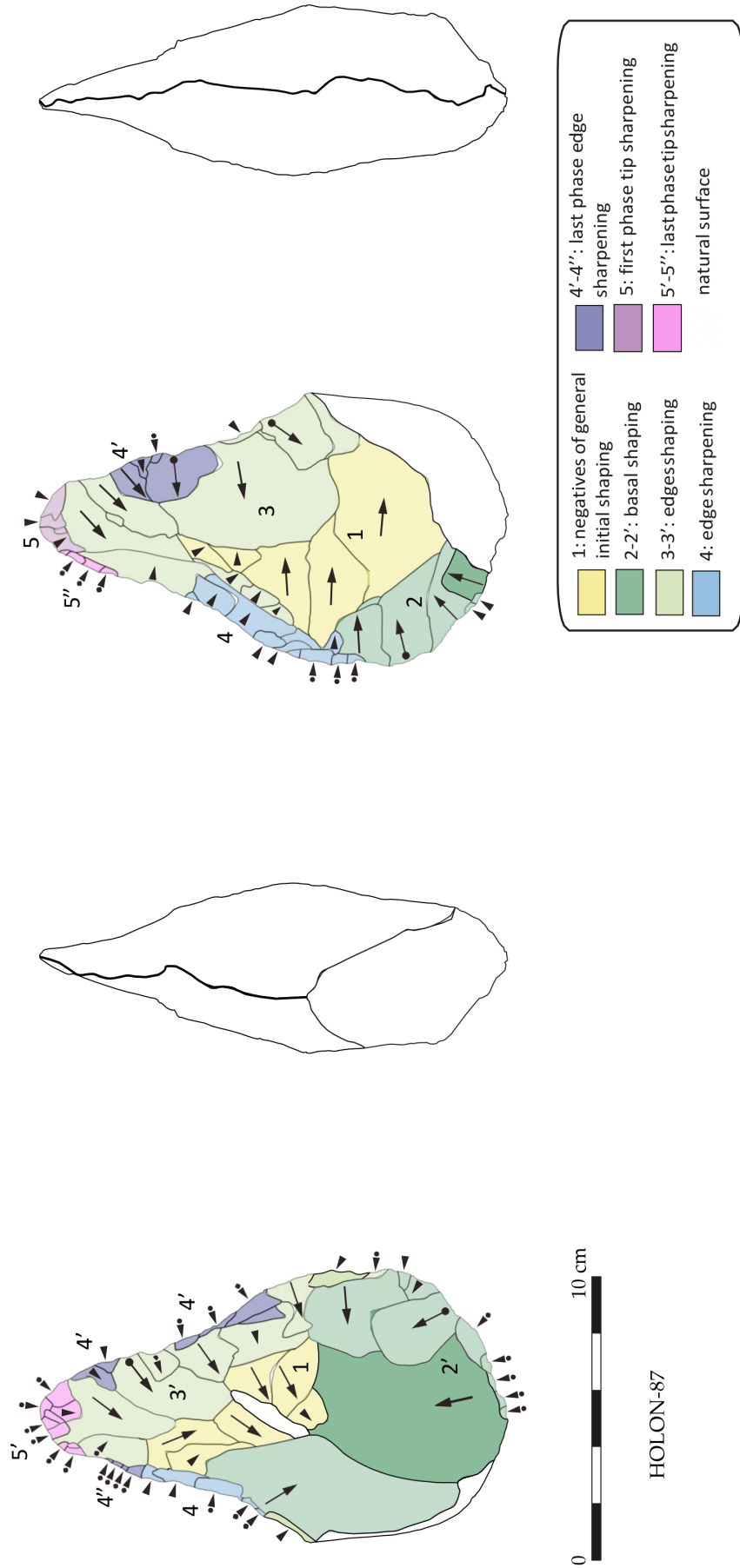
HOLON-57

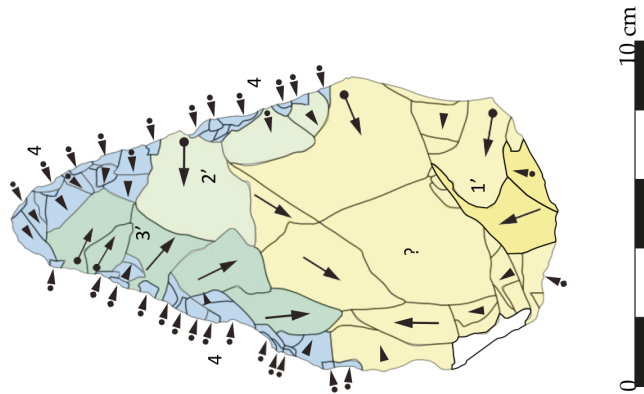
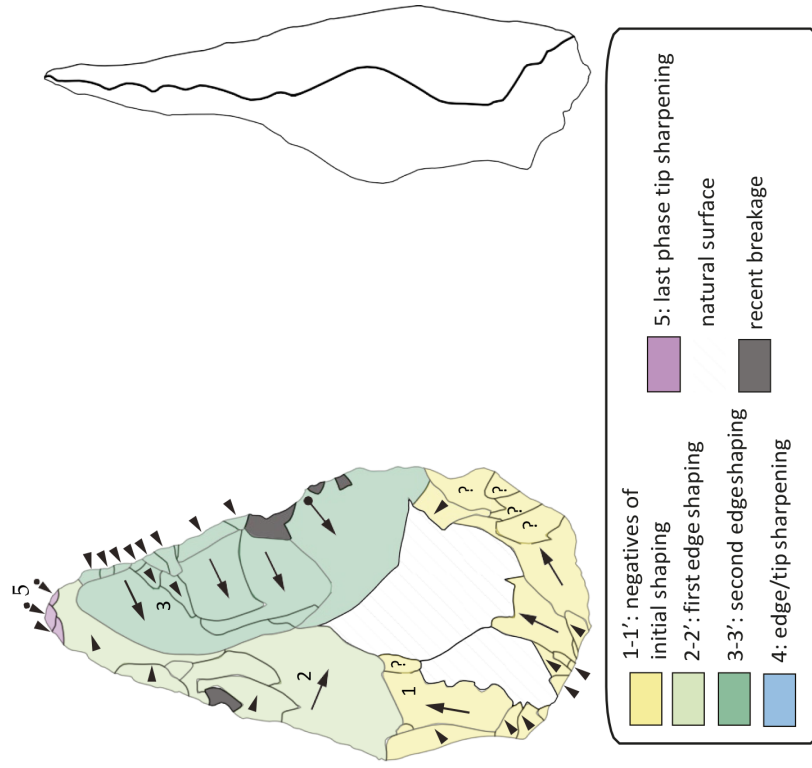


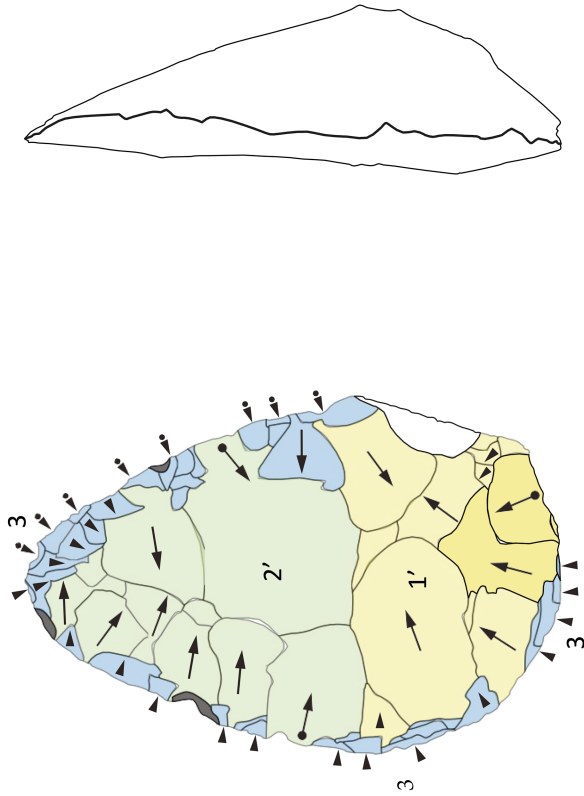
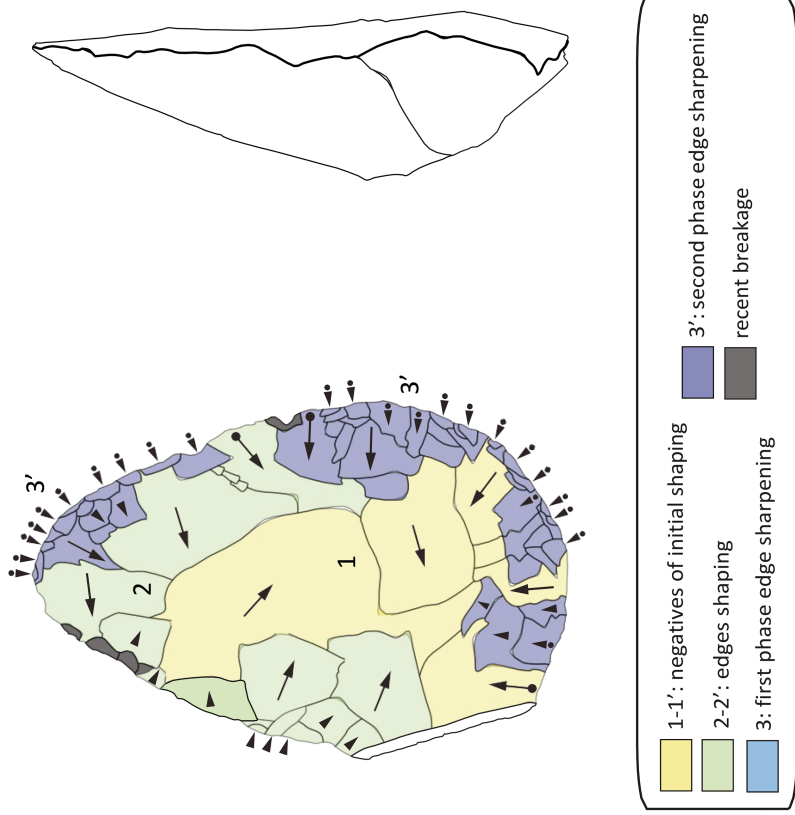


0 10 cm

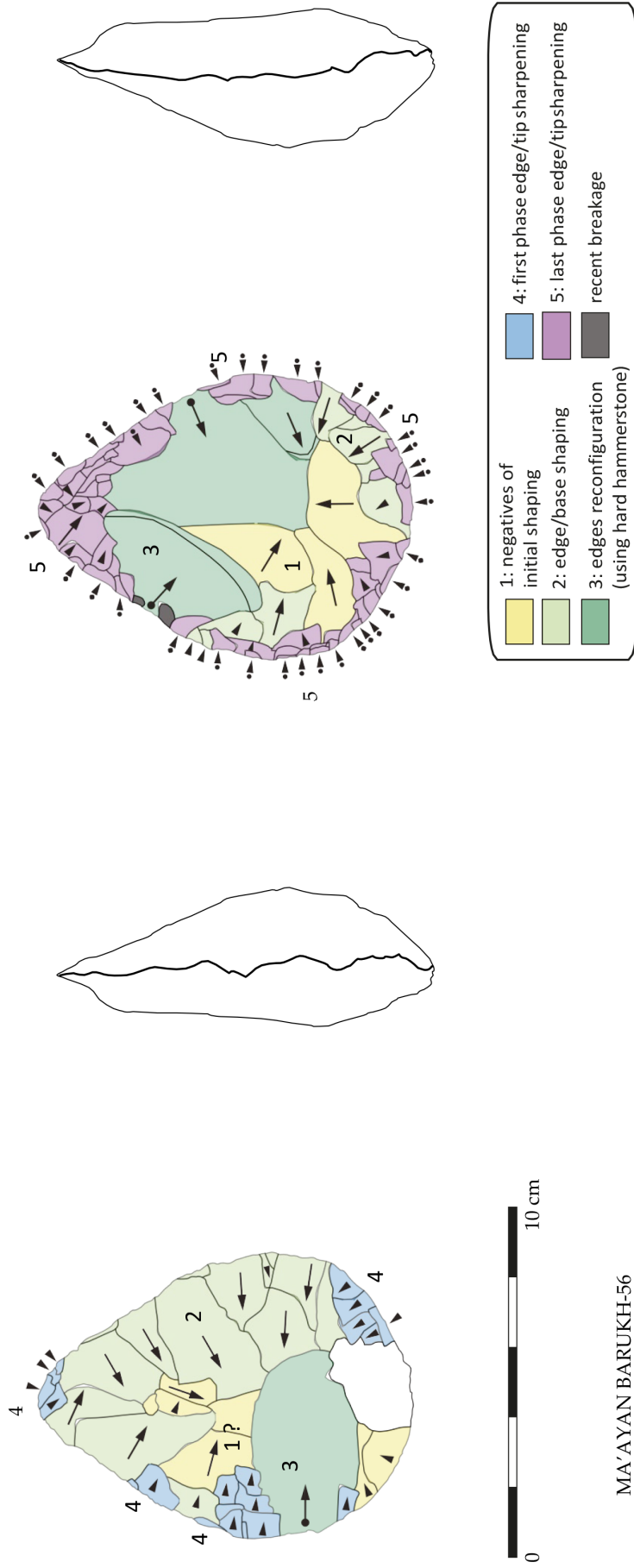
HOLON-70

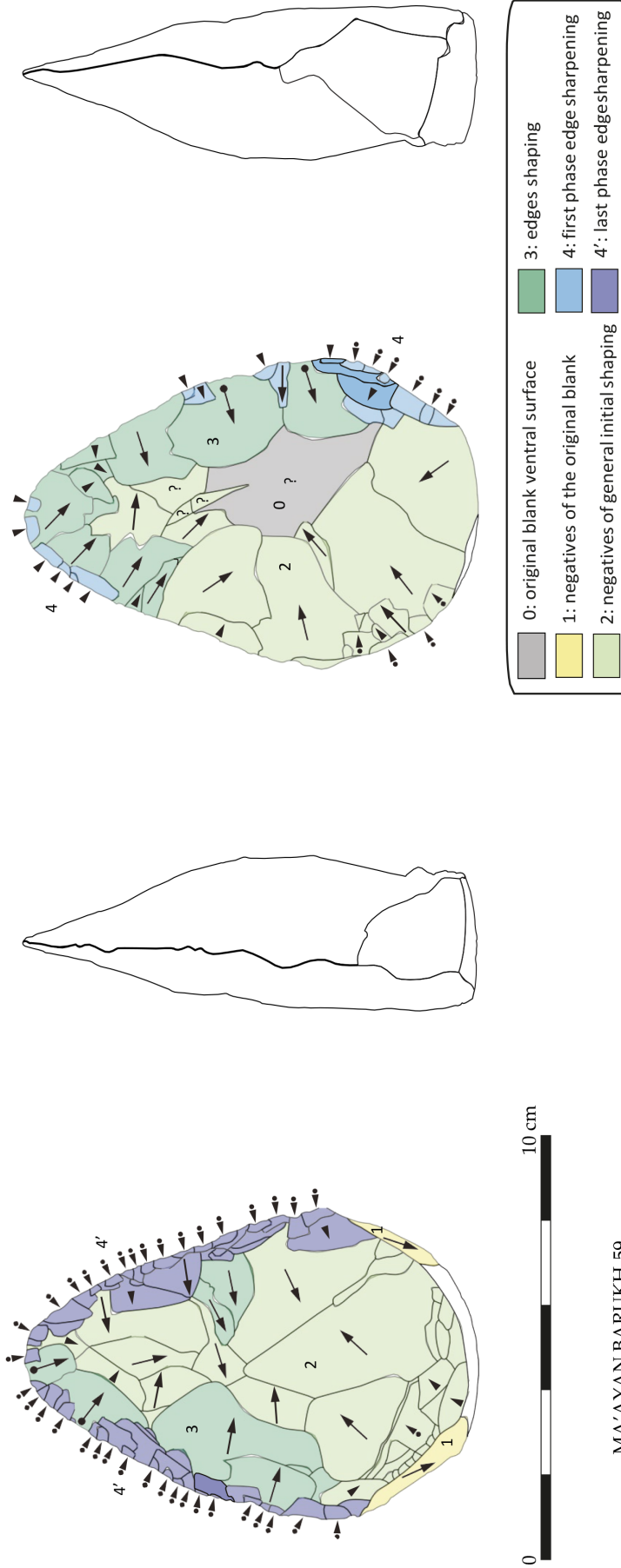


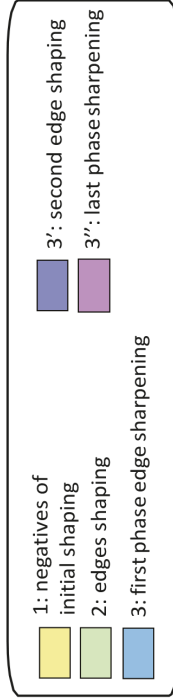
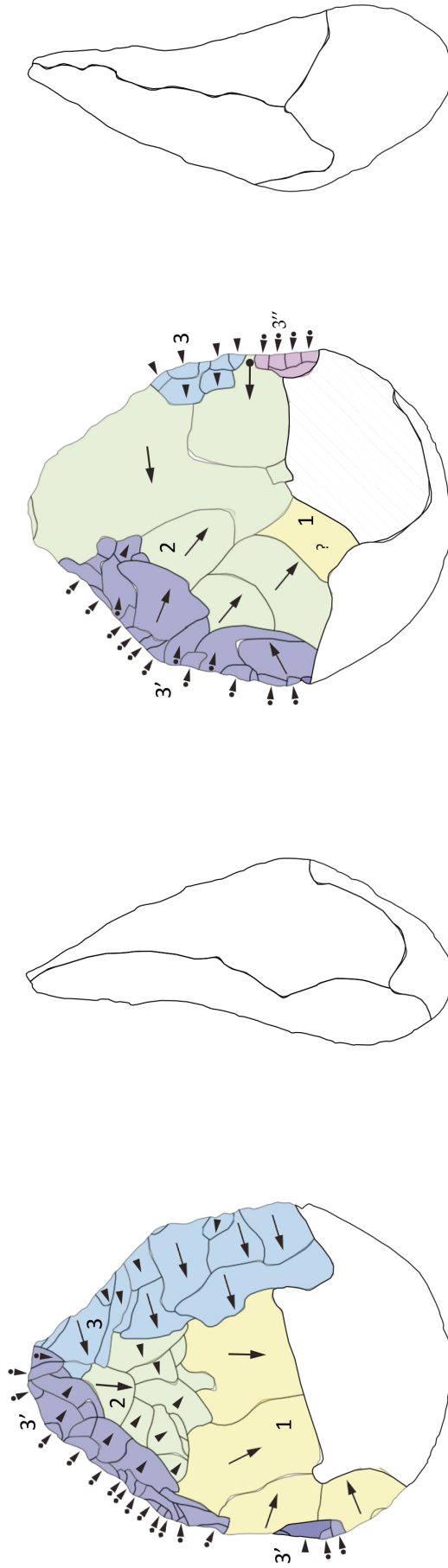




MA'AYAN BARUKH-36

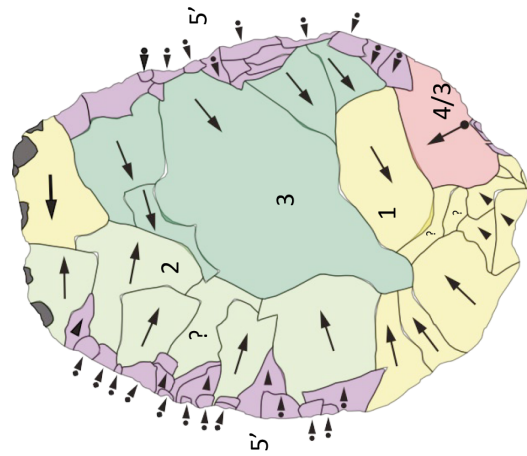
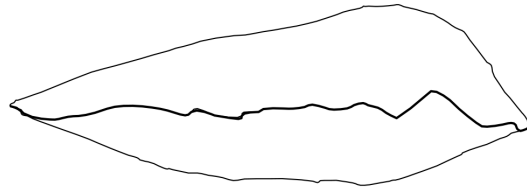
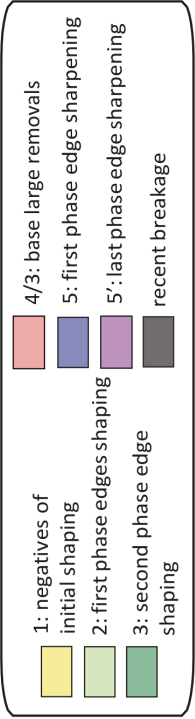
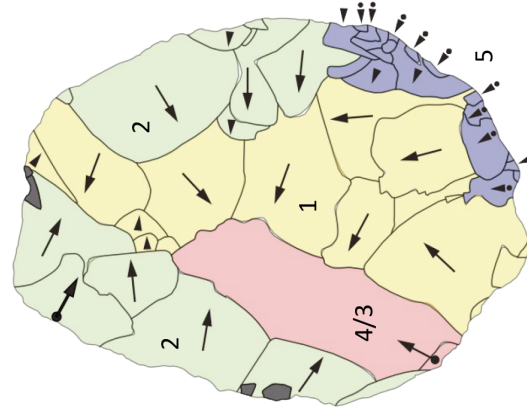
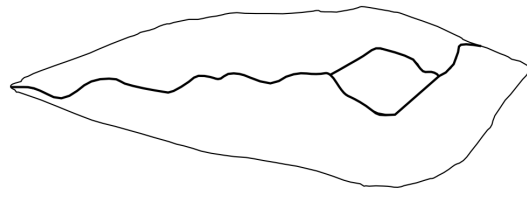




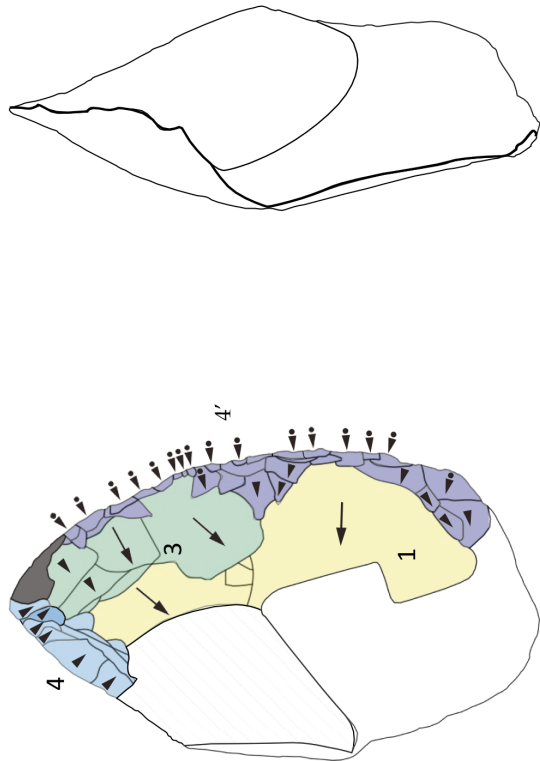
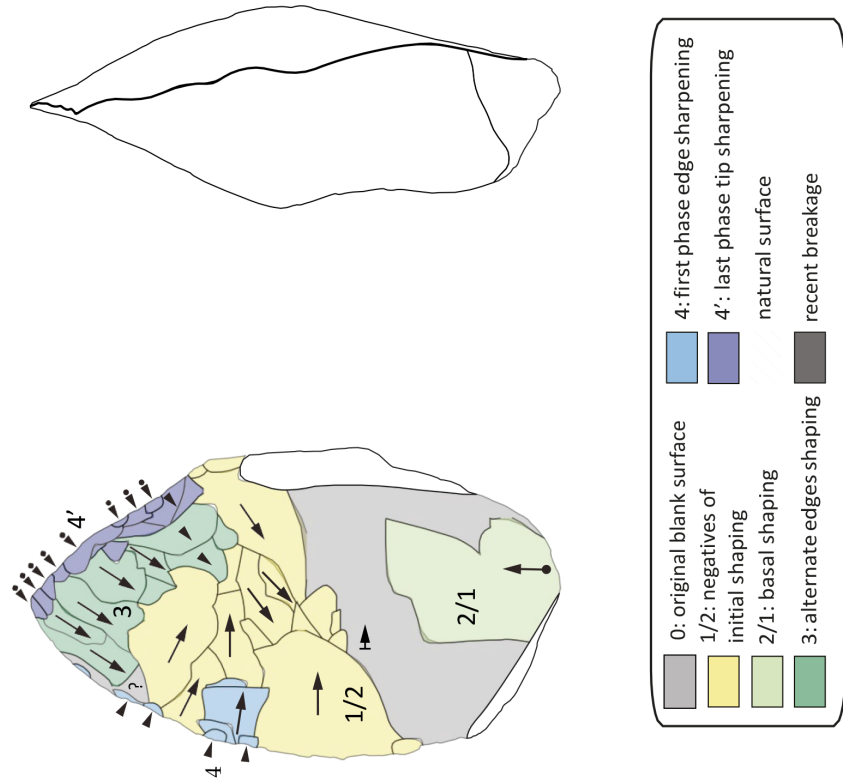


MA'AYAN BARUKH-61



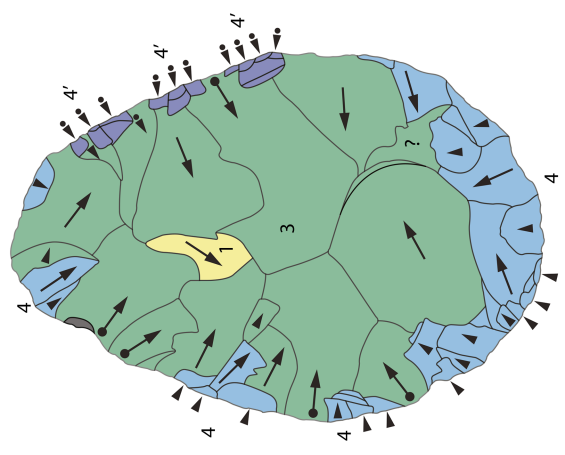
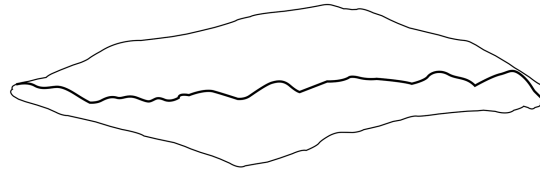
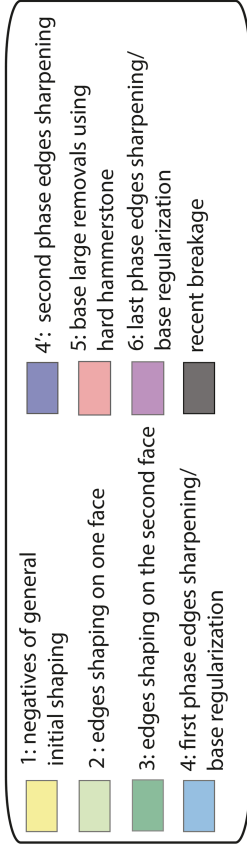
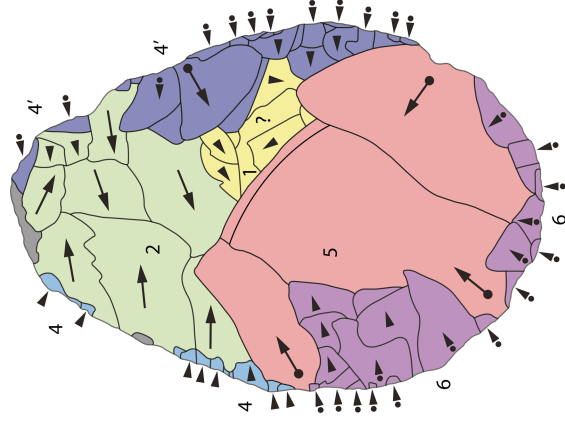
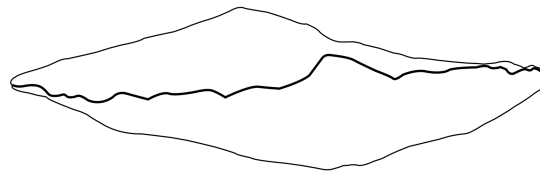


MA'AYAN BARUKH-63

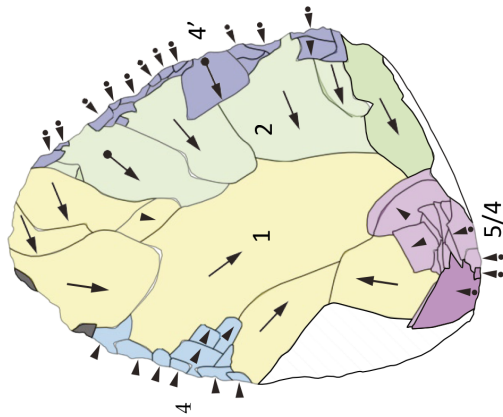
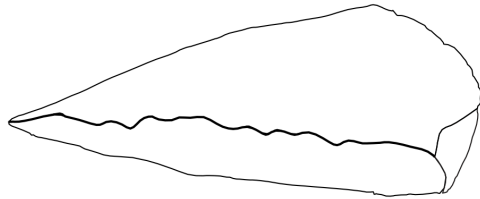
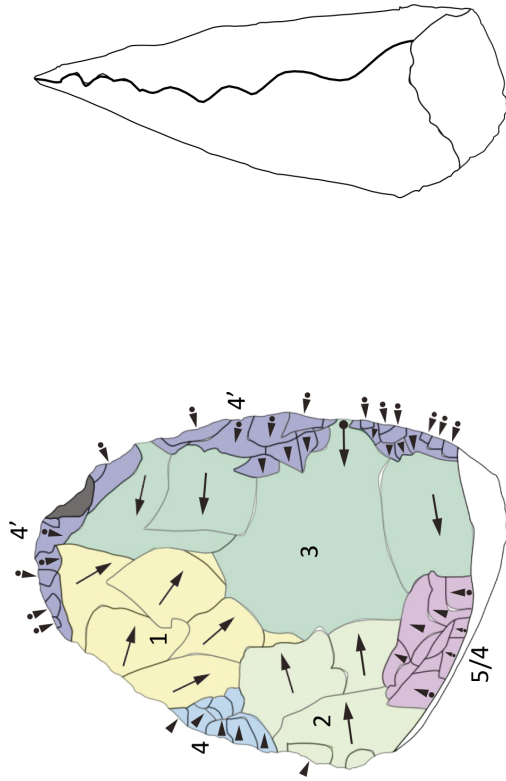


0 10 cm

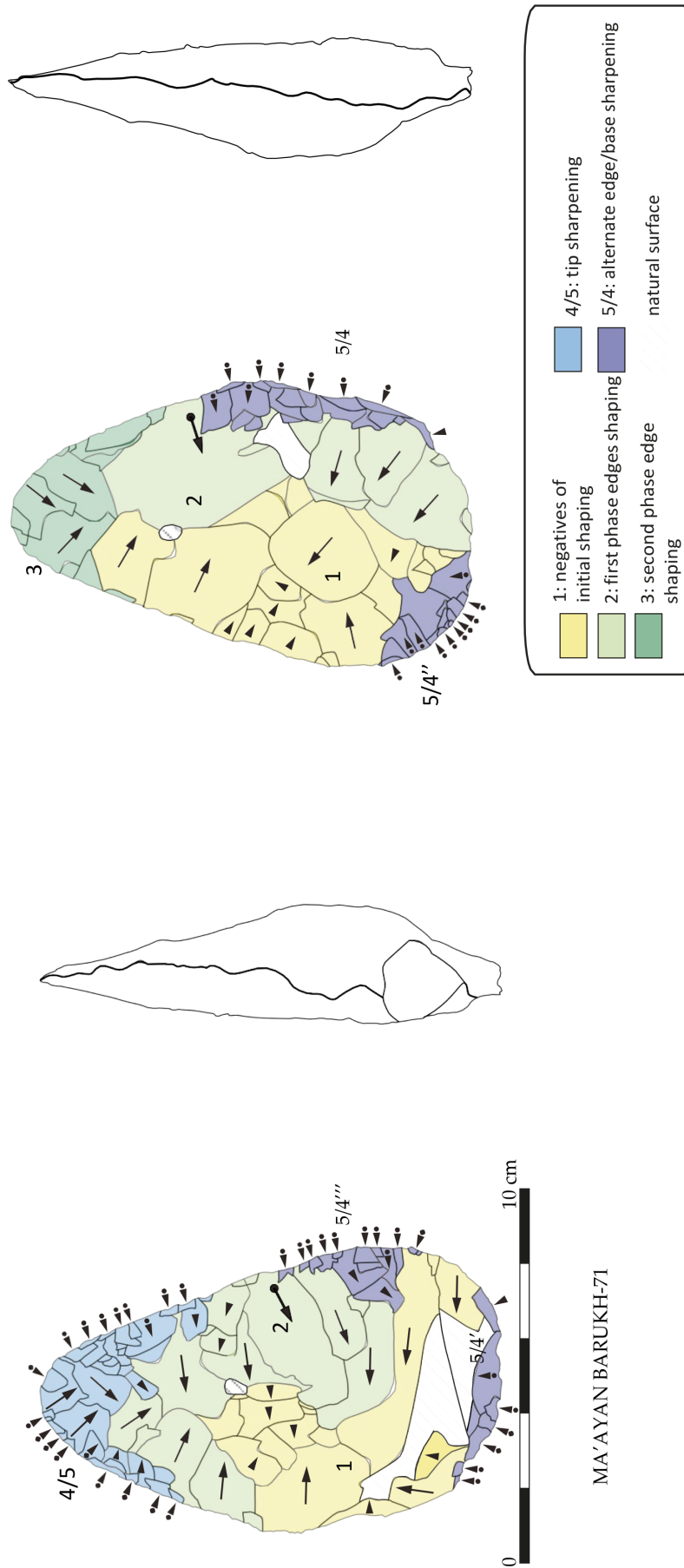
MA'AYAN BARUKH-67



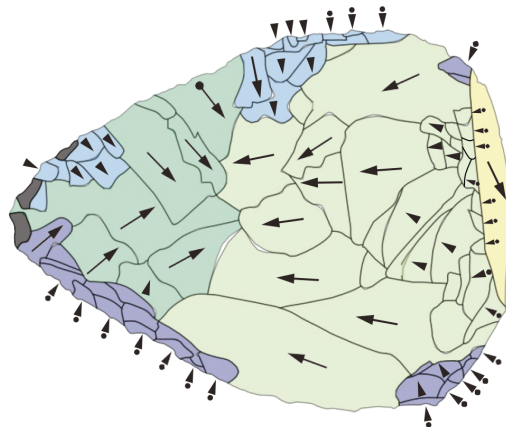
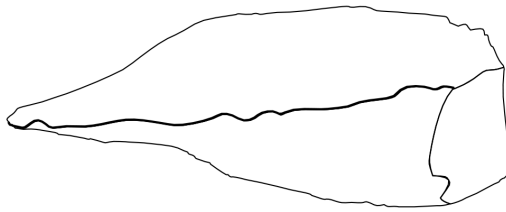
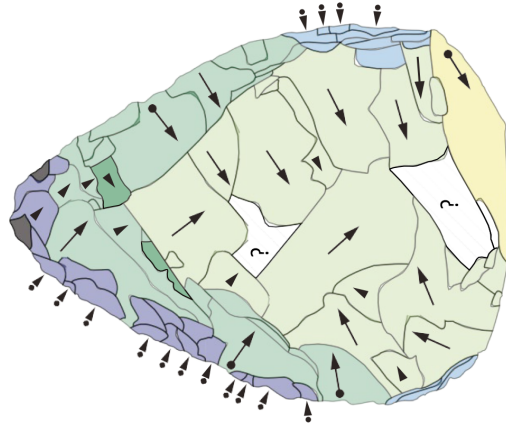
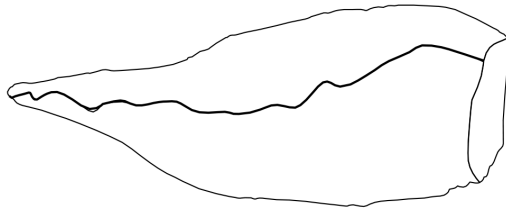
MAYAYAN BARUKH-68



MA'AYAN BARUKH-70



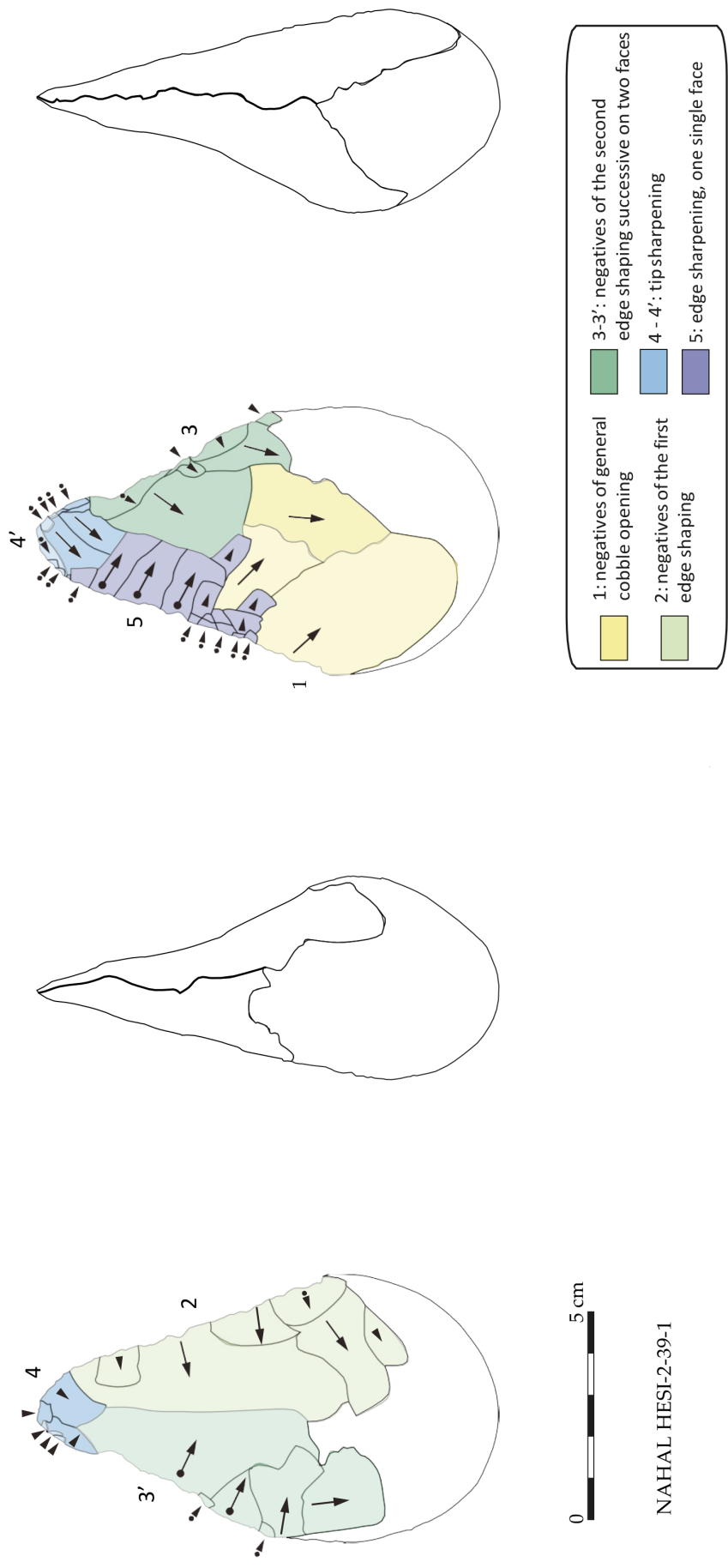
MA'AYAN BARUKH-71

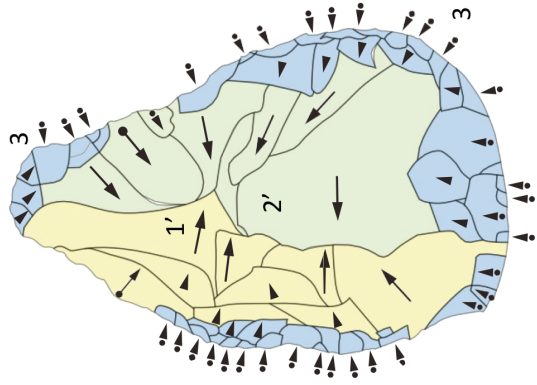
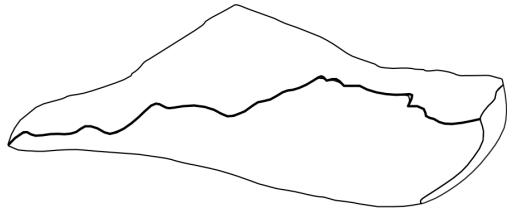


	1: blank's anterior removals		4': last phase edge sharpening
	2: negatives of initial shaping		recent breakage
	3: edges shaping		natural surface
	4: first phase edge sharpening		

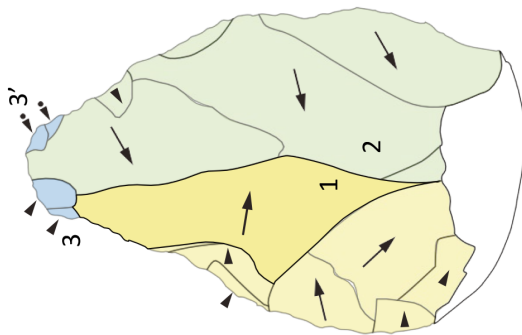
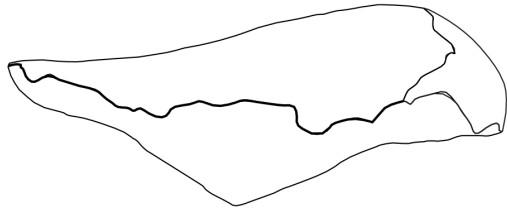


MA'AYAN BARUKH-80

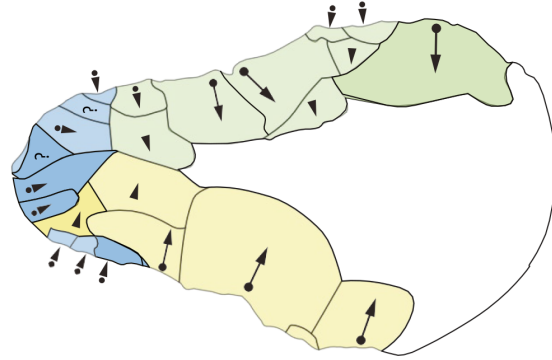




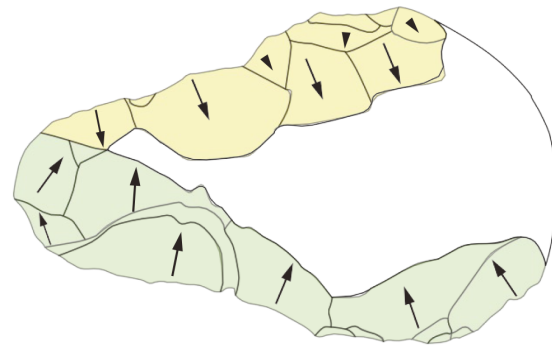
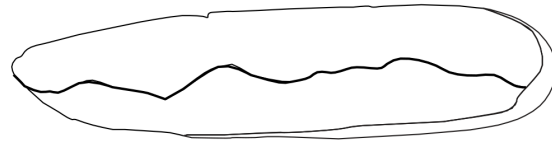
	1-1': first phase alternate edge shaping
	2-2': second phase alternate edge shaping
	3-3': edge/tip sharpening



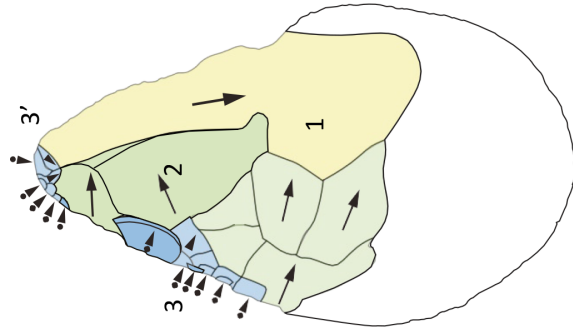
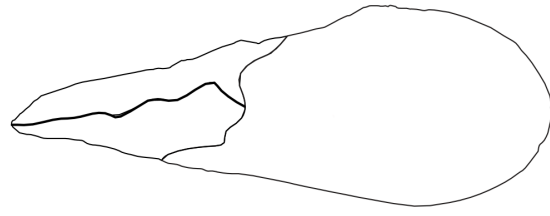
NAHAL HESI-2-39-5



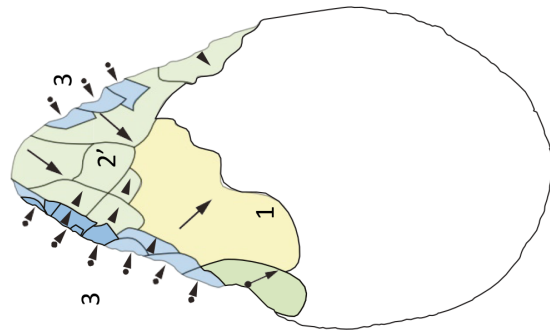
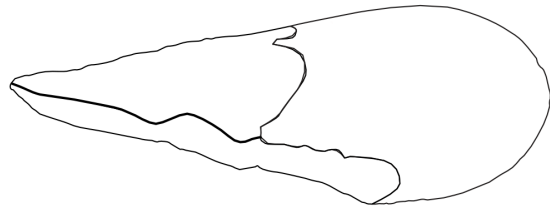
1-1': first edge shaping  
2-2': second edge shaping  
3: edge/tip sharpening

A legend box containing three colored squares corresponding to the morpho-technological analysis: a yellow square for '1-1': first edge shaping', a light green square for '2-2': second edge shaping', and a blue square for '3: edge/tip sharpening'.

NAHAL HESL-2-39-11



1: negatives of initial shaping  
2: edges shaping  
3-3': Alternate edge sharpening



NAHAL HESI-2-40-2